The detail formulation of SCALE-RM

Seiya Nishizawa, Hirofumi Tomita, and Team SCALE

July 6, 2016

Contents

Chapter 1

Introduction

Correnspoinding author : ???

Chapter 2

Governing equations

Correnspoinding author : Hirofumi Tomita

2.1 Continuity equations

The continuity equations for each material can be described as the flux form:

$$\frac{\partial \rho q_d}{\partial t} + \nabla \cdot (\rho q_d \mathbf{u}) = \mathrm{DIFF}\,[q_d] \tag{2.1}$$

$$\frac{\partial \rho q_v}{\partial t} + \nabla \cdot (\rho q_v \mathbf{u}) = S_v + \mathrm{DIFF}\,[q_v] \tag{2.2}$$

$$\frac{\partial \rho q_l}{\partial t} + \nabla \cdot (\rho q_l \mathbf{u}) + \frac{\partial \rho q_l w_l}{\partial z} = S_l + \mathrm{DIFF}\,[q_l] \tag{2.3}$$

$$\frac{\partial \rho q_s}{\partial t} + \nabla \cdot (\rho q_s \mathbf{u}) + \frac{\partial \rho q_s w_s}{\partial z} = S_s + \mathrm{DIFF}\,[q_s] \tag{2.4}$$

The summation of the mass concentrations should be unit:

$$q_d + q_v + q_l + q_s = 1. \tag{2.5}$$

The source terms of water substances should satisfy the following relation:

$$S_v + S_l + S_s = 0. \tag{2.6}$$

The summation of Eqs.(2.1)-(2.4) gives the continuity equation of total density:

$$\frac{\partial \rho}{\partial t} + \nabla \cdot (\rho \mathbf{u}) + \frac{\partial \rho q_l w_l}{\partial z} + \frac{\partial \rho q_s w_s}{\partial z} = 0, \tag{2.7}$$

For this derivation, we assume that the operator DIFF [] is distributive. Using Eq.(2.5),

$$\begin{aligned} & \mathrm{DIFF}\,[q_d] + \mathrm{DIFF}\,[q_v] + \mathrm{DIFF}\,[q_l] + \mathrm{DIFF}\,[q_s] \\ = \;& \mathrm{DIFF}\,[q_d + q_v + q_l + q_s] = \mathrm{DIFF}\,[1] = 0 \end{aligned} \tag{2.8}$$

2.2 Momentum equations

The momentum equations for the gas, liquid, and solid material are described as

$$\begin{aligned} & \frac{\partial \rho \left(q_d + q_v\right) \mathbf{u}}{\partial t} + \nabla \cdot \left[\rho \left(q_d + q_v\right) \mathbf{u} \otimes \mathbf{u}\right] && (2.9) \\ = \; & -\nabla p - \left[\rho \left(q_d + q_v\right) g + \left(f_l + f_s\right)\right] \mathbf{e_z} \\ & + \mathbf{u} S_v + \mathrm{DIFF}\left[(q_d + q_v)\mathbf{u}\right] && (2.10) \\ & \frac{\partial \rho q_l \mathbf{u}}{\partial t} + \nabla \cdot \left(\rho q_l \mathbf{u} \otimes \mathbf{u}\right) + \frac{\partial \rho q_l \mathbf{u} w_l}{\partial z} = -\left(\rho q_l g - f_l\right) \mathbf{e_z} \\ & + \mathbf{u} S_l + \mathrm{DIFF}\left[q_l \mathbf{u}\right] && (2.11) \\ & \frac{\partial \rho q_s \mathbf{u}}{\partial t} + \nabla \cdot \left(\rho q_s \mathbf{u} \otimes \mathbf{u}\right) + \frac{\partial \rho q_s \mathbf{u} w_s}{\partial z} = -\left(\rho q_s g - f_s\right) \mathbf{e_z} \\ & + \mathbf{u} S_s + \mathrm{DIFF}\left[q_s \mathbf{u}\right] && (2.12) \end{aligned}$$

The pressure is derived from the equation of state as

$$p = \rho \left(q_d R_d + q_v R_v\right) T. \tag{2.13}$$

The summation of Eqs.(2.10)-(2.12) gives the total momentum equation as

$$\begin{aligned} & \frac{\partial \rho \mathbf{u}}{\partial t} + \nabla \cdot \left(\rho \mathbf{u} \otimes \mathbf{u}\right) + \left(\frac{\partial \rho q_l w_l}{\partial z} + \frac{\partial \rho q_s w_s}{\partial z}\right) \mathbf{e_z} \\ = \; & -\nabla p - \rho g \mathbf{e_z} + \mathrm{DIFF}\left[\mathbf{u}\right] && (2.14) \end{aligned}$$

Note that the drag forces by water loading does not appear in Eq.(2.14), because those term are cancelled out through the summation.

2.3 Thermodynamics equations

The equations of the internal energies are described as

$$\begin{aligned} & \frac{\partial \rho (q_d e_d + q_v e_v)}{\partial t} + \nabla \cdot \left[\rho (q_d e_d + q_v e_v) \mathbf{u}\right] \\ = \; & -p \nabla \cdot \mathbf{u} + Q_d + Q_v + \mathrm{DIFF}\left[(q_d + q_v) T^*\right] && (2.15) \\ & \frac{\partial \rho q_l e_l}{\partial t} + \nabla \cdot \left(\rho q_l e_l \mathbf{u}\right) + \frac{\partial \rho q_l e_l w_l}{\partial z} = Q_l + \mathrm{DIFF}\left[q_l T^*\right] && (2.16) \\ & \frac{\partial \rho q_l e_s}{\partial t} + \nabla \cdot \left(\rho q_s e_s \mathbf{u}\right) + \frac{\partial \rho q_s e_s w_s}{\partial z} = Q_s + \mathrm{DIFF}\left[q_s T^*\right] && (2.17) \end{aligned}$$

where T^* is some kind of potential temperature, discussed later. The internal energies are defined as

$$\begin{aligned} e_d &= c_{vd} T && (2.18) \\ e_v &= c_{vv} T && (2.19) \\ e_l &= c_l T && (2.20) \\ e_s &= c_s T, && (2.21) \end{aligned}$$

The summation of Eqs.(2.15)-(2.17) gives the following internal energy equations:

$$\begin{aligned} & \frac{\partial \rho e}{\partial t} + \nabla \cdot (\rho e \mathbf{u}) + \frac{\partial \rho q_l e_l w_l}{\partial z} + \frac{\partial \rho q_s e_s w_s}{\partial z} + p \nabla \cdot \mathbf{u} \\ = \quad & Q + \mathrm{DIFF}\left[T^*\right] \end{aligned} \tag{2.22}$$

where

$$e = q_d e_d + q_v e_v + q_l e_l + q_s e_s, \tag{2.23}$$

and the total diabatic heating is described as

$$Q = Q_d + Q_v + Q_l + Q_s. \tag{2.24}$$

2.4 Conseptual seperation for solving the set of equations

Eqs.(2.2)-(2.4),(2.7),(2.14), and (2.13) with Eq.(2.22) are the complete set of equations. For solving them easily, we seperate the set of equations conceptually as

$$\frac{\partial \phi}{\partial t} = \left(\frac{\partial \phi}{\partial t}\right)_{dynamics} + \left(\frac{\partial \phi}{\partial t}\right)_{physics} \tag{2.25}$$

The falling proccess of liquid and solid waters, the source and sink process of water vapor, and the diabatic heating process for energy equations are treated as physical process, the others are treated as dynamical proccess.

According to this scheme, the dynamical process can be written as

$$\frac{\partial \rho q_v}{\partial t} + \nabla \cdot (\rho q_v \mathbf{u}) = 0 \tag{2.26}$$

$$\frac{\partial \rho q_l}{\partial t} + \nabla \cdot (\rho q_l \mathbf{u}) = 0 \tag{2.27}$$

$$\frac{\partial \rho q_s}{\partial t} + \nabla \cdot (\rho q_s \mathbf{u}) = 0 \tag{2.28}$$

$$\frac{\partial \rho}{\partial t} + \nabla \cdot (\rho \mathbf{u}) = 0 \tag{2.29}$$

$$\frac{\partial \rho \mathbf{u}}{\partial t} + \nabla \cdot (\rho \mathbf{u} \otimes \mathbf{u}) = -\nabla p - \rho g \mathbf{e_z} \tag{2.30}$$

$$\frac{\partial \rho e}{\partial t} + \nabla \cdot (\rho e \mathbf{u}) + p \nabla \cdot \mathbf{u} = 0 \tag{2.31}$$

On the other hand, the physical processes are as follows:

$$\frac{\partial \rho q_v}{\partial t} = S_v + \mathrm{DIFF}\left[q_v\right] \tag{2.32}$$

$$\frac{\partial \rho q_l}{\partial t} + \frac{\partial \rho q_l w_l}{\partial z} = S_l + \mathrm{DIFF}\left[q_l\right] \tag{2.33}$$

$$\frac{\partial \rho q_s}{\partial t} + \frac{\partial \rho q_s w_s}{\partial z} = S_s + \mathrm{DIFF}\left[q_s\right] \tag{2.34}$$

$$\frac{\partial \rho}{\partial t} + \frac{\partial \rho q_l w_l}{\partial z} + \frac{\partial \rho q_s w_s}{\partial z} = 0 \tag{2.35}$$

$$\frac{\partial \rho \mathbf{u}}{\partial t} + \frac{\partial \rho q_l \mathbf{u} w_l}{\partial z} + \frac{\partial \rho q_s \mathbf{u} w_s}{\partial z} = \mathrm{DIFF}\left[\mathbf{u}\right] \tag{2.36}$$

$$\frac{\partial \rho e}{\partial t} + \frac{\partial \rho q_l e_l w_l}{\partial z} + \frac{\partial \rho q_s e_s w_s}{\partial z} = Q + \mathrm{DIFF}\left[T^*\right] \tag{2.37}$$

2.5 Conservation of thermodynamics in the dynamical process

Equation (2.31) is not a complete flux form, because the internal energy itself is not conserved both in the Euler sense and in the Lagrangian sense. In this section, we consider the conservative quantity for thermodynamics equation.

In the dry atmosphere, the potential temperature for dry air, which is defined as

$$\theta_d \quad = \quad T\left(\frac{p_{00}}{p}\right)^{R_d/c_{pd}}, \tag{2.38}$$

is used as a conserved quantity it is conserved along the Lagrange trajectory c_{pd} R_d are the specific heats at constant pressure and However, it is no longer satisfied when the water substances are included.

Sinece Eq.(2.29) is equivallent to

$$\frac{d\rho}{dt} + \rho \nabla \cdot \mathbf{u} = 0, \tag{2.39}$$

Equation (2.31) is

$$\rho \frac{de}{dt} - \frac{p}{\rho}\frac{d\rho}{dt} = 0. \tag{2.40}$$

Dividing by ρ, this equation can be written as

$$\frac{de}{dt} + p\frac{d}{dt}\left(\frac{1}{\rho}\right) = 0. \tag{2.41}$$

Substiting Eq.(2.13) into Eq.(2.41),

$$\begin{aligned} &\frac{dq_d c_{vd} T}{dt} + p\frac{d}{dt}\left[\frac{q_d R_d T}{p}\right] + \frac{dq_v c_{vv} T}{dt} + p\frac{d}{dt}\left[\frac{q_v R_v T}{p}\right] \\ &+\frac{dq_l c_l T}{dt} + \frac{dq_s c_s T}{dt} = 0 \end{aligned} \tag{2.42}$$

Since Eqs.(2.26)-(2.29) give

$$\frac{dq_d}{dt} = \frac{dq_v}{dt} = \frac{dq_l}{dt} = \frac{dq_s}{dt} = 0, \tag{2.43}$$

Equation (2.42) gives the following form:

$$\begin{aligned} & q_d \left[\frac{dc_{vd}T}{dt} + p\frac{d}{dt}\left[\frac{R_d T}{p}\right]\right] + q_v \left[\frac{dc_{vv}T}{dt} + p\frac{d}{dt}\left[\frac{R_v T}{p}\right]\right] \\ & + q_l \frac{dc_l T}{dt} + q_s \frac{dc_s T}{dt} = 0 \end{aligned} \tag{2.44}$$

Dividing this equation by T,

$$\begin{aligned} & q_d \left[c_{pd}\frac{1}{T}\frac{dT}{dt} + R_d p\frac{d}{dt}\left(\frac{1}{p}\right)\right] + q_v \left[c_{pv}\frac{1}{T}\frac{dT}{dt} + R_v p\frac{d}{dt}\left(\frac{1}{p}\right)\right] \\ & + q_l c_l \frac{1}{T}\frac{dT}{dt} + q_s c_s \frac{1}{T}\frac{dT}{dt} = 0 \end{aligned} \tag{2.45}$$

$$\begin{aligned} & q_d c_{pd} \left[\frac{d\ln T}{dt} + \frac{R_d}{c_{pd}}\frac{d}{dt}\left[\ln\left(\frac{1}{p}\right)\right]\right] + q_v c_{pv} \left[\frac{d\ln T}{dt} + \frac{R_v}{c_{pv}}\frac{d}{dt}\left[\ln\left(\frac{1}{p}\right)\right]\right] \\ & + q_l c_l \frac{d\ln T}{dt} + q_s c_s \frac{d\ln T}{dt} = 0 \end{aligned} \tag{2.46}$$

$$q_d c_{pd}\frac{d\ln\theta_d}{dt} + q_v c_{pv}\frac{d\ln\theta_v}{dt} + q_l c_l \frac{d\ln T}{dt} + q_s c_s \frac{d\ln T}{dt} = 0 \tag{2.47}$$

$$\frac{d}{dt}\left[\ln\left(\theta_d^{q_d c_{pd}}\theta_v^{q_v c_{pv}} T^{q_l c_l} T^{q_s c_s}\right)\right] = 0 \tag{2.48}$$

Thus,

$$\frac{d}{dt}\left[\theta_d^{q_d c_{pd}}\theta_v^{q_v c_{pv}} T^{q_l c_l} T^{q_s c_s}\right] = 0 \tag{2.49}$$

Thus, the following quantity is conserved along the flow trajectory;

$$\Theta = \theta_d^{q_d c_{pd}}\theta_v^{q_v c_{pv}} T^{q_l c_l} T^{q_s c_s} \tag{2.50}$$

where θ_v is the potential temperature for water vapor, defined as

$$\theta_v = T\left(\frac{p_{00}}{p}\right)^{R_v/c_{pv}} \tag{2.51}$$

The equation of state has the following expression using Θ.

$$\Theta = T^{q_d c_{pd}}\left(\frac{p_{00}}{p}\right)^{q_d R_d} T^{q_v c_{pv}}\left(\frac{p_{00}}{p}\right)^{q_v R_v} T^{q_l c_l} + T^{q_s c_s} \tag{2.52}$$

$$= T^{q_d c_{pd} + q_v c_{pv} + q_l c_l + q_s c_s}\left(\frac{p_{00}}{p}\right)^{q_d R_d + q_v R_v} \tag{2.53}$$

$$= T^{c_p^*}\left(\frac{p_{00}}{p}\right)^{R^*}, \tag{2.54}$$

where

$$c_p^* \equiv q_d c_{pd} + q_v c_{pv} + q_l c_l + q_s c_s \tag{2.55}$$

$$R^* \equiv q_d R_d + q_v R_v \tag{2.56}$$

We define a new potential temperature

$$\theta \equiv \Theta^{1/c_p^*} = T\left(\frac{p_{00}}{p}\right)^{R^*/c_p^*} \tag{2.57}$$

The pressure expression is derived diagnostically as follows:

$$p = \rho(q_d R_d + q_v R_v)\theta\left(\frac{p}{p_{00}}\right)^{\frac{R^*}{c_p^*}} \tag{2.58}$$

$$p^{1-\frac{R^*}{c_p^*}} = \rho R^*\theta\left(\frac{1}{p_{00}}\right)^{\frac{R^*}{c_p^*}} \tag{2.59}$$

$$p = p_{00}\left(\frac{\rho\theta R^*}{p_{00}}\right)^{\frac{c_p^*}{c_p^*-R^*}} \tag{2.60}$$

Note that

$$\frac{d\theta}{dt} = \frac{1}{a}\Theta^{1/a-1}\frac{d\Theta}{dt} = 0 \tag{2.61}$$

Therefore, $\rho\theta$ can be employed for the prognostic varaiable!

Figure 2.1(a) gives the vertical profile of the temperature in the U.S.standard atmosphere and Fig.2.1(b) shows the vetical profiles of θ/θ_d under this temperature condition when we assume that q_v is mass concentration of water vapor at the saturation, $q_l + q_s$ gives 0.0, 0.01, 0.02, and 0.04. The differnce between θ and θ_d becomes larger with the height and it may not be negligible.

2.6 Diabatic heating in the physical process

If the prognostic variable for thermodynamics is changed from the internal energy to the newly defined potential temperature θ, the diabatic heating in Eq.(2.37) should be modified. Through the manupulation from Eq.(2.40) to Eq.(2.48), Eq.(2.37) without turbulence term can be written as

$$\frac{d\ln\Theta}{dt} = \frac{Q}{\rho T} \tag{2.62}$$

On the other hand, Eq.(2.61) gives

$$\frac{d\theta}{dt} = \frac{1}{c_p^*}\Theta^{1/a}\frac{d\ln\Theta}{dt} \tag{2.63}$$

Substituting Eq.(2.62) into Eq.(2.63),

$$\frac{d\theta}{dt} = \frac{1}{c_p^*}\left(\frac{p}{p_{00}}\right)^{\frac{R^*}{c_p^*}}\frac{Q}{\rho} \tag{2.64}$$

2.7 Summary of equations in the dynamical process and physical process

2.7.1 The dynamical process

$$\frac{\partial \rho q_v}{\partial t} + \nabla \cdot (\rho q_v \mathbf{u}) = \left(\frac{\partial \rho q_v}{\partial t}\right)_{physics} \tag{2.65}$$

$$\frac{\partial \rho q_l}{\partial t} + \nabla \cdot (\rho q_l \mathbf{u}) = \left(\frac{\partial \rho q_l}{\partial t}\right)_{physics} \tag{2.66}$$

$$\frac{\partial \rho q_s}{\partial t} + \nabla \cdot (\rho q_s \mathbf{u}) = \left(\frac{\partial \rho q_s}{\partial t}\right)_{physics} \tag{2.67}$$

$$\frac{\partial \rho}{\partial t} + \nabla \cdot (\rho \mathbf{u}) = \left(\frac{\partial \rho}{\partial t}\right)_{physics} \tag{2.68}$$

$$\frac{\partial \rho \mathbf{u}}{\partial t} + \nabla \cdot (\rho \mathbf{u} \otimes \mathbf{u}) = -\nabla p - \rho g \mathbf{e_z} + \left(\frac{\partial \rho \mathbf{u}}{\partial t}\right)_{physics} \tag{2.69}$$

$$\frac{\partial \rho \theta}{\partial t} + \nabla \cdot (\rho \theta \mathbf{u}) = \left(\frac{\partial \rho \theta}{\partial t}\right)_{physics} \tag{2.70}$$

$$p = p_{00} \left(\frac{\rho \theta R^*}{p_{00}}\right)^{\frac{c_p^*}{c_p^* - R^*}} \tag{2.71}$$

where

$$c_p^* \equiv q_d c_{pd} + q_v c_{pv} + q_l c_l + q_s c_s \tag{2.72}$$

$$R^* \equiv q_d R_d + q_v R_v \tag{2.73}$$

2.7.2 The physical process

$$\left(\frac{\partial \rho q_v}{\partial t}\right)_{physics} = S_v + \text{DIFF}\left[q_v\right] \tag{2.74}$$

$$\left(\frac{\partial \rho q_l}{\partial t}\right)_{physics} = -\frac{\partial \rho q_l w_l}{\partial z} + S_l + \text{DIFF}\left[q_l\right] \tag{2.75}$$

$$\left(\frac{\partial \rho q_s}{\partial t}\right)_{physics} = -\frac{\partial \rho q_s w_s}{\partial z} + S_s + \text{DIFF}\left[q_s\right] \tag{2.76}$$

$$\left(\frac{\partial \rho}{\partial t}\right)_{physics} = -\frac{\partial \rho q_l w_l}{\partial z} - \frac{\partial \rho q_s w_s}{\partial z} \tag{2.77}$$

$$\left(\frac{\partial \rho \mathbf{u}}{\partial t}\right)_{physics} = -\frac{\partial \rho q_l \mathbf{u} w_l}{\partial z} - \frac{\partial \rho q_s \mathbf{u} w_s}{\partial z} + \text{DIFF}\left[\mathbf{u}\right] \tag{2.78}$$

$$\left(\frac{\partial \rho \theta}{\partial t}\right)_{physics} = \frac{1}{c_p^*}\left(\frac{p}{p_{00}}\right)^{\frac{R^*}{c_p^*}} \left[Q - \frac{\partial \rho q_l e_l w_l}{\partial z} - \frac{\partial \rho q_s e_s w_s}{\partial z}\right] + \text{DIFF}\left[\theta\right] \tag{2.79}$$

(a)

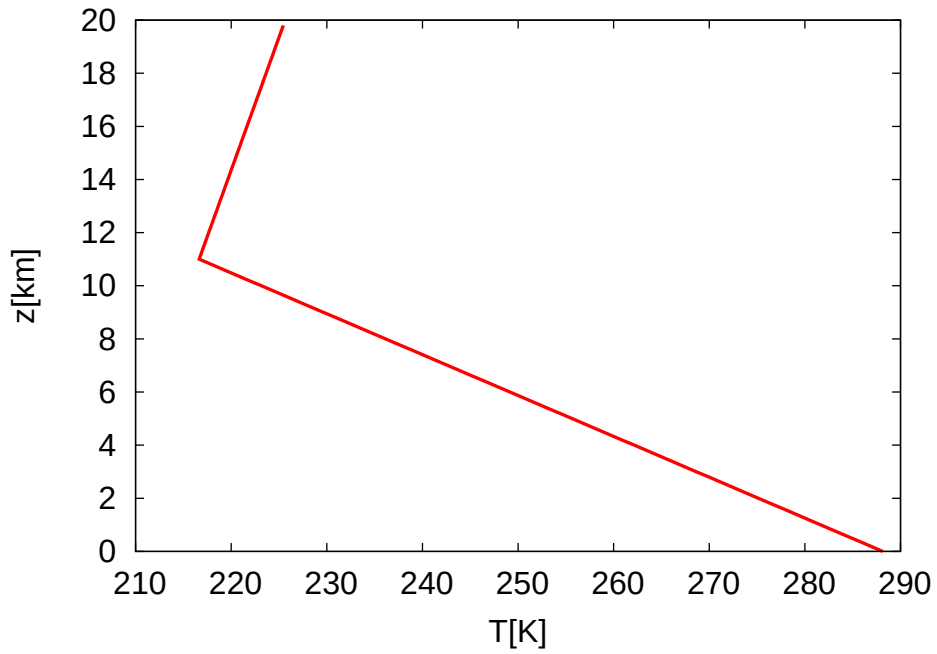

(b)

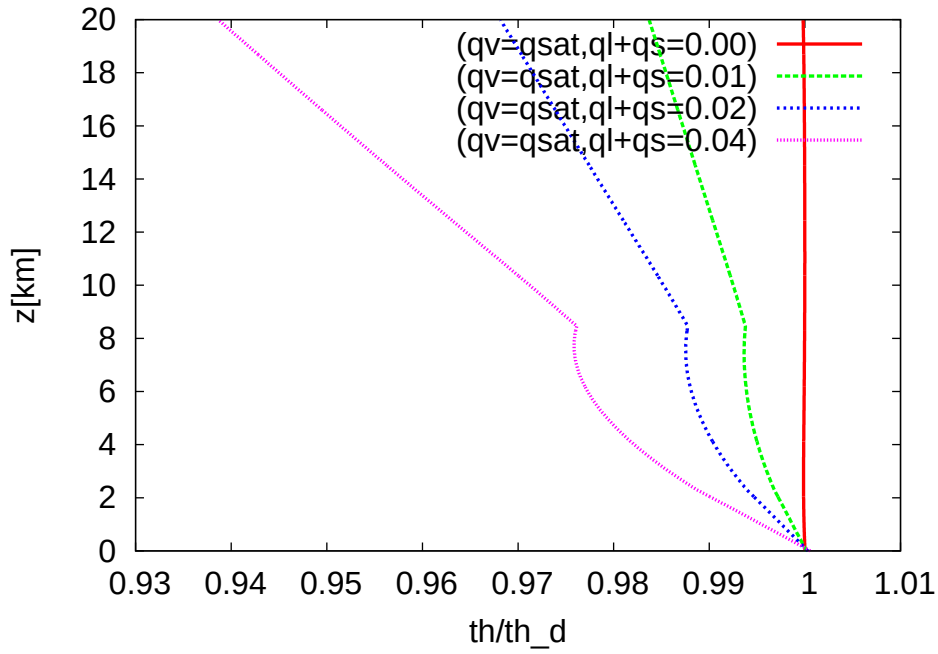

Figure 2.1: Thee vertical profile of (a) U.S. standard atmosphere, (b) Several profiles of θ/θ_d.

Chapter 3

Descretization of the dynamics

Corresponding author : Seiya Nishizawa

3.1 Temporal integration scheme

3.1.1 Runge-Kutta schemes

For the time integration of Eqs.(2.68)-(2.40), we adopt the full explicit scheme with the p step Runge-Kutta scheme.

$$\phi_0^* = \phi^t \tag{3.1}$$
$$k_1 = f(\phi^t) \tag{3.2}$$
$$k_2 = f(\phi^t + k_1 \Delta t \alpha_1) \tag{3.3}$$
$$\cdots$$
$$k_p = f(\phi^t + k_{p-1} \Delta t \alpha_{p-1}) \tag{3.4}$$
$$\phi^{t+\Delta t} = \phi^t + \Delta t \sum_p \beta_p k_p. \tag{3.5}$$

The 3 and 4 step Runge-Kutta scheme are implemented.

The Heun's three step scheme

$$k_1 = f(\phi^n), \tag{3.6}$$
$$k_2 = f\left(\phi^n + \frac{1}{3}\Delta t k_1\right), \tag{3.7}$$
$$k_3 = f\left(\phi^n + \frac{2}{3}\Delta t k_2\right), \tag{3.8}$$
$$\phi^{n+1} = \phi^n + \frac{1}{4}\Delta t(k_1 + 3k_3). \tag{3.9}$$

The Kutta's three step scheme

$$k_1 = f(\phi^n), \tag{3.10}$$
$$k_2 = f\left(\phi^n + \frac{1}{2}\Delta t k_1\right), \tag{3.11}$$
$$k_3 = f\left(\phi^n - \Delta t k_1 + 2\Delta t k_2\right), \tag{3.12}$$
$$\phi^{n+1} = \phi^n + \frac{1}{6}\Delta t(k_1 + 4k_2 + k_3). \tag{3.13}$$

The Wicker and Skamarock (2002)'s three step scheme

$$k_1 = f(\phi^n), \tag{3.14}$$
$$k_2 = f\left(\phi^n + \frac{1}{3}\Delta t k_1\right), \tag{3.15}$$
$$k_3 = f\left(\phi^n + \frac{1}{2}\Delta t k_2\right), \tag{3.16}$$
$$\phi^{n+1} = \phi^n + \Delta t k_3. \tag{3.17}$$

The four step scheme

$$k_1 = f(\phi^n), \tag{3.18}$$
$$k_2 = f\left(\phi^n + \frac{1}{2}\Delta t k_1\right), \tag{3.19}$$
$$k_3 = f\left(\phi^n + \frac{1}{2}\Delta t k_2\right), \tag{3.20}$$
$$k_4 = f\left(\phi^n + \Delta t k_3\right), \tag{3.21}$$
$$\phi^{n+1} = \phi^n + \frac{1}{6}\Delta t(k_1 + 2k_2 + 2k_3 + k_4). \tag{3.22}$$

The forward-backward scheme

In the short time step, the momentums are updated first and then density is updated with the updated momentums.

$$\rho u_i^{n+1} = \rho u_i^n + \Delta t f_{\rho u_i}(\rho^n), \tag{3.23}$$
$$\rho^{n+1} = \rho^n + \Delta t f_\rho(\rho u_i^{n+1}). \tag{3.24}$$

3.1.2 Numerical stability

A fully compressive equations of a acoustic mode is considered. The continuous and momentum equations is the followings:

$$\frac{\partial \rho}{\partial t} = -\frac{\partial \rho u_i}{\partial x_i} \tag{3.25}$$

$$\frac{\partial \rho u_i}{\partial t} = -\frac{\partial p}{\partial x_i} \tag{3.26}$$

$$p = p_0 \left(\frac{R\rho\theta}{p_0} \right)^{c_p/c_v}, \tag{3.27}$$

here the potential temperature θ is assumed to be constant.

In order to analize the numerical stability of equation, the equation of the state is linearized.

$$p \approx \bar{p} + c^2 \rho', \tag{3.28}$$

where c is the sound speed: $c^2 = \frac{c_p \bar{p}}{c_v \bar{\rho}}$.

We descritize the governing equation with the 2th order central difference.

$$\left.\frac{\partial \rho}{\partial t}\right|_{i,j,k} = -\frac{U_{i+1/2} - U_{i-1/2}}{\Delta x} - \frac{V_{j+1/2} - V_{j-1/2}}{\Delta y} - \frac{W_{k+1/2} - W_{k-1/2}}{\Delta z} \tag{3.29}$$

$$\left.\frac{\partial U}{\partial t}\right|_{i+1/2} = -c^2 \frac{\rho_{i+1} - \rho_i}{\Delta x} \tag{3.30}$$

$$\left.\frac{\partial V}{\partial t}\right|_{j+1/2} = -c^2 \frac{\rho_{j+1} - \rho_j}{\Delta y} \tag{3.31}$$

$$\left.\frac{\partial W}{\partial t}\right|_{i+1/2} = -c^2 \frac{\rho_{k+1} - \rho_k}{\Delta z}, \tag{3.32}$$

where U, V, and W is the momentum at the stagared grid point in x, y, and z direction, respectively.

The error of the spatial differenece of a wavenumber k component $\hat{\phi}_k$ is $\{\exp(ik\Delta x) - 1\}\,\hat{\phi}$, and the error of 2-grid mode is the largest: $\exp(i\pi) - 1 = -2$.

The temporal differential of the 2-grid mode is

$$\frac{\partial \rho}{\partial t} = -\frac{1 - \exp(-i\pi)}{\Delta x} U - \frac{1 - \exp(-i\pi)}{\Delta y} V - \frac{1 - \exp(-i\pi)}{\Delta z} W \tag{3.33}$$

$$\frac{\partial U}{\partial t} = -c^2 \frac{\exp(i\pi) - 1}{\Delta x} \rho \tag{3.34}$$

$$\frac{\partial V}{\partial t} = -c^2 \frac{\exp(i\pi) - 1}{\Delta y} \rho \tag{3.35}$$

$$\frac{\partial W}{\partial t} = -c^2 \frac{\exp(i\pi) - 1}{\Delta z} \rho. \tag{3.36}$$

The mode of which the U, V and W has the same phase is the most unstable:

$$\frac{\partial \rho}{\partial t} = -3 \frac{1 - \exp(-i\pi)}{\Delta x} U \tag{3.37}$$

$$\frac{\partial U}{\partial t} = -c^2 \frac{\exp(i\pi) - 1}{\Delta x} \rho \tag{3.38}$$

Writing matrix form,

$$\begin{pmatrix} \frac{\partial \rho}{\partial t} \\ \frac{\partial U}{\partial t} \end{pmatrix} = D \begin{pmatrix} \rho \\ U \end{pmatrix}, \tag{3.39}$$

where

$$D = \begin{pmatrix} 0 & -\frac{6}{\Delta x} \\ \frac{2c^2}{\Delta x} & 0 \end{pmatrix}. \tag{3.40}$$

The Euler scheme

With the Euler scheme,

$$\phi^{n+1} = \phi^n + \Delta t f(\phi^n) \tag{3.41}$$

The A is the matrix representing the time step, then

$$A = I + dtD, \tag{3.42}$$

$$= \begin{pmatrix} 1 & -6\frac{\Delta t}{\Delta x} \\ \frac{2c^2 \Delta t}{\Delta x} & 1 \end{pmatrix}. \tag{3.43}$$

The eigen value of A is larger than 1, and the Euler scheme is instable for any Δt.

The second step Runge-Kutta scheme

The Heun's second step Runge-Kutta scheme is

$$k_1 = f(\phi^n), \tag{3.44}$$

$$k_2 = f(\phi^n + \Delta t k_1), \tag{3.45}$$

$$\phi^{n+1} = \phi^n + \frac{\Delta t}{2}(k_1 + k_2). \tag{3.46}$$

$$A = I + \frac{\Delta t}{2}(K_1 + K_2), \tag{3.47}$$

$$K_1 = D, \tag{3.48}$$

$$K_2 = D(I + \Delta t K_1). \tag{3.49}$$

After all,

$$A = \begin{pmatrix} 1 - 6\nu^2 & -\frac{6\Delta t}{\Delta x} \\ \frac{2c^2 \Delta t}{\Delta x} & 1 - 6\nu^2 \end{pmatrix}, \tag{3.50}$$

where ν is the Courant number for the sound speed: $\frac{c\Delta t}{\Delta x}$. The eigen value of A is larger than 1, and the Euler scheme is instable for any Δt.

The third step Runge-Kutta scheme

With the Heun's third step Runge-Kutta scheme, the matrix A is written by

$$A = I + \frac{\Delta t}{4}(K_1 + 4K_3), \tag{3.51}$$

$$= \begin{pmatrix} 1 - 6\nu^2 & -\frac{6\Delta t}{\Delta x}(1 - 2\nu^2) \\ \frac{2c^2 \Delta t}{\Delta x}(1 - 2\nu^2) & 1 - 6\nu^2 \end{pmatrix}, \tag{3.52}$$

where

$$K_1 = D, \tag{3.53}$$

$$K_2 = D(I + \frac{\Delta t}{3} K_1), \tag{3.54}$$

$$K_3 = D(I + \frac{2\Delta t}{3} K_2). \tag{3.55}$$

The condition that all the eigen values are less than or equal to 1 is

$$\nu \leq \frac{1}{2}. \tag{3.56}$$

In the Kutta's three step Runge-Kutta scheme, the matrix A is

$$A = I + \frac{\Delta t}{6}(K_1 + 4K_2 + K_3), \tag{3.57}$$

where

$$K_1 = D, \tag{3.58}$$

$$K_2 = D\left(I + \frac{\Delta t}{2} K_1\right), \tag{3.59}$$

$$K_3 = D\left(I - \Delta t K_1 + 2\Delta t K_2\right). \tag{3.60}$$

It is the idential as that in the Heun's scheme (eq. 3.52). Thus, the stable condition is the same (eq. 3.56).

The Wicker and Skamarock (2002)'s Runge-Kutta scheme is described as

$$A = I + \Delta t K_3, \tag{3.61}$$

$$K_1 = D, \tag{3.62}$$

$$K_2 = D\left(I + \frac{\Delta t}{3} K_1\right), \tag{3.63}$$

$$K_3 = D\left(I + \frac{\Delta t}{2} K_2\right). \tag{3.64}$$

The A and the consequent stable condition are the identical as the above two schemes.

The four step Runge-Kutta scheme

The matrix A is

$$A = I + \frac{\Delta t}{6}(K_1 + 2K_2 + 2K_3 + K_4), \tag{3.65}$$

$$= \begin{pmatrix} 1 - 6\nu^2 + 6\nu^4 & -\frac{6\Delta t}{\Delta x}(1 - 2\nu^2) \\ \frac{2c^2\Delta t}{\Delta x}(1 - 2\nu^2) & 1 - 6\nu^2 + 6^4 \end{pmatrix}, \tag{3.66}$$

where

$$K_1 = D, \tag{3.67}$$

$$K_2 = D\left(I + \frac{\Delta t}{2} K_1\right), \tag{3.68}$$

$$K_3 = D\left(I + \frac{\Delta t}{2} K_2\right), \tag{3.69}$$

$$K_4 = D(I + \Delta t K_3). \tag{3.70}$$

The condition for stability is

$$\nu \leq \frac{\sqrt{6}}{3}. \tag{3.71}$$

The number of floating opint operations with the four step Runge-Kutta scheme is about 4/3 times larger than that with the three step scheme. Howere, the time step can be $2\sqrt{6}/3$ larger than that in the three step scheme. Since $2\sqrt{6}/3 > 4/3$, the four step Runge-Kutta scheme is more cost effective than the three step scheme in terms of numerical stability.

The forward-backward scheme

The stabitlity condition is

$$\nu \leq \frac{1}{\sqrt{3}}. \tag{3.72}$$

The forward-backward scheme can be used in each step in the Runge-Kutta schemes. The stability conditions are the followings:

The second step RK scheme

$$\nu \leq \frac{1}{\sqrt{3}}. \tag{3.73}$$

The Heun's three step RK scheme

$$\nu \leq \frac{1}{2}. \tag{3.74}$$

The Kutta's three step RK scheme

$$\nu \leq \frac{1}{2}. \tag{3.75}$$

TheWicker and Skamarock (2002)'s three step RK scheme

$$\nu \leq \frac{\sqrt{6}}{4}. \tag{3.76}$$

The four step RK scheme

$$\nu \leq 0.66 \tag{3.77}$$

Corresponding author : Hirofumi Tomita

3.2 Spatial descretization

We employ the Arakawa-C staggered grid with the 3-dimensional momentum $(\rho u, \rho v, \rho w)$, density (ρ) and mass-weighted potentail temperature$(\rho\theta)$ as the prognostic variables. Figure 3.1(a) shows the structure of the control volume for the mass, indicating the location of each of prognostic variables. Conceptually, we use the 4th order central difference scheme for the advection or convection terms and the 2nd order central difference scheme for the other terms. Before the descretization of differential equations, we should diagnose several quantities from the prognostic variables.

Full-level pressure and potential temperature

$$p_{i,j,k} = p_{00}\left[\frac{(\rho\theta)_{i,j,k}R^*}{p_{00}}\right]^{\frac{c_p^*}{c_p^*-R^*}} \tag{3.78}$$

$$\theta_{i,j,k} = \frac{(\rho\theta)_{i,j,k}}{\rho_{i,j,k}} \tag{3.79}$$

$$\tag{3.80}$$

Half-level density

$$\overline{\rho}_{i+\frac{1}{2},j,k} = \frac{\rho_{i+1,j,k}+\rho_{i,j,k}}{2} \tag{3.81}$$

$$\overline{\rho}_{i,j+\frac{1}{2},k} = \frac{\rho_{i,j+1,k}+\rho_{i,j,k}}{2} \tag{3.82}$$

$$\overline{\rho}_{i,j,k+\frac{1}{2}} = \frac{\Delta z_k\rho_{i,j,k+1}+\Delta z_{k+1}\rho_{i,j,k}}{\Delta z_k+\Delta z_{k+1}} \tag{3.83}$$

Half-level velocity

$$\overline{u}_{i+\frac{1}{2},j,k} = \frac{(\rho u)_{i+\frac{1}{2},j,k}}{\overline{\rho}_{i+\frac{1}{2},j,k}} \tag{3.84}$$

$$\overline{v}_{i,j+\frac{1}{2},k} = \frac{(\rho v)_{i,j+\frac{1}{2},k}}{\overline{\rho}_{i,j+\frac{1}{2},k}} \tag{3.85}$$

$$\overline{w}_{i,j,k+\frac{1}{2}} = \frac{(\rho w)_{i,j,k+\frac{1}{2}}}{\overline{\rho}_{i,j,k+\frac{1}{2}}} \tag{3.86}$$

Full-level velocity

$$\overline{u}_{i,j,k} = \frac{(\rho u)_{i+\frac{1}{2},j,k}+(\rho u)_{i-\frac{1}{2},j,k}}{2\rho_{i,j,k}} \tag{3.87}$$

$$\overline{v}_{i,j,k} = \frac{(\rho v)_{i,j+\frac{1}{2},k}+(\rho v)_{i,j-\frac{1}{2},k}}{2\rho_{i,j,k}} \tag{3.88}$$

$$\overline{w}_{i,j,k} = \frac{(\rho w)_{i,j,k+\frac{1}{2}}+(\rho w)_{i,j,k-\frac{1}{2}}}{2\rho_{i,j,k}} \tag{3.89}$$

3.2.1 Continuity equation

$$\left(\frac{\partial \rho}{\partial t}\right)_{i,j,k} = -\frac{(\rho u)_{i+\frac{1}{2},j,k} - (\rho u)_{i-\frac{1}{2},j,k}}{\Delta x} - \frac{(\rho v)_{i,j+\frac{1}{2},k} - (\rho v)_{i,j-\frac{1}{2},k}}{\Delta y} - \frac{(\rho w)_{i,j,k+\frac{1}{2}} - (\rho w)_{i,j,k-\frac{1}{2}}}{\Delta z} \tag{3.90}$$

3.2.2 Momentum equations

Figure 3.1(a) shows the structure of the control volume for the momentum in the x direction. The momentum equation is descretized as

$$\left(\frac{\partial \rho u}{\partial t}\right)_{i+\frac{1}{2},j,k} = -\frac{\overline{(\rho u)}_{i+1,j,k}\overline{u}_{i+1,j,k} - \overline{(\rho u)}_{i,j,k}\overline{u}_{i,j,k}}{\Delta x} - \frac{\overline{(\rho u)}_{i+\frac{1}{2},j+\frac{1}{2},k}\overline{v}_{i+\frac{1}{2},j+\frac{1}{2},k} - \overline{(\rho u)}_{i+\frac{1}{2},j-\frac{1}{2},k}\overline{v}_{i+\frac{1}{2},j-\frac{1}{2},k}}{\Delta y} - \frac{\overline{(\rho u)}_{i+\frac{1}{2},j,k+\frac{1}{2}}\overline{w}_{i+\frac{1}{2},j,k+\frac{1}{2}} - \overline{(\rho u)}_{i+\frac{1}{2},j,k-\frac{1}{2}}\overline{w}_{i+\frac{1}{2},j,k-\frac{1}{2}}}{\Delta z} - \frac{p_{i+1,j,k} - p_{i,j,k}}{\Delta x}, \tag{3.91}$$

where

$$\overline{(\rho u)}_{i,j,k} = \frac{-(\rho u)_{i+\frac{3}{2},j,k} + 7(\rho u)_{i+\frac{1}{2},j,k} + 7(\rho u)_{i-\frac{1}{2},j,k} - (\rho u)_{i-\frac{3}{2},j,k}}{12} \tag{3.92}$$

$$\overline{(\rho u)}_{i+\frac{1}{2},j+\frac{1}{2},k} = \frac{-(\rho u)_{i+\frac{1}{2},j+2,k} + 7(\rho u)_{i+\frac{1}{2},j+1,k} + 7(\rho u)_{i+\frac{1}{2},j,k} - (\rho u)_{i+\frac{1}{2},j-1,k}}{12} \tag{3.93}$$

$$\overline{(\rho u)}_{i+\frac{1}{2},j,k+\frac{1}{2}} = \frac{-(\rho u)_{i+\frac{1}{2},j,k+2} + 7(\rho u)_{i+\frac{1}{2},j,k+1} + 7(\rho u)_{i+\frac{1}{2},j,k} - (\rho u)_{i+\frac{1}{2},j,k-1}}{12} \tag{3.94}$$

and the velocities at the cell wall for the staggered control volume to x direction are defined as

$$\overline{u}_{i,j,k} = \frac{\overline{u}_{i+\frac{1}{2},j,k} + \overline{u}_{i-\frac{1}{2},j,k}}{2} \tag{3.95}$$

$$\overline{v}_{i+\frac{1}{2},j+\frac{1}{2},k} = \frac{\overline{v}_{i,j+\frac{1}{2},k} + \overline{v}_{i+1,j+\frac{1}{2},k}}{2} \tag{3.96}$$

$$\overline{w}_{i+\frac{1}{2},j,k+\frac{1}{2}} = \frac{\overline{w}_{i,j,k+\frac{1}{2}} + \overline{w}_{i+1,j,k+\frac{1}{2}}}{2} \tag{3.97}$$

In this form, the 4th order accuracy is guaranteed on the condition of the constant velocity.

The momentum equations in the y and z directions are descretized in the same way:

$$\begin{aligned}\left(\frac{\partial \rho v}{\partial t}\right)_{i,j+\frac{1}{2},k} = & -\frac{\overline{(\rho v)}_{i+\frac{1}{2},j+\frac{1}{2},k}\overline{u}_{i+\frac{1}{2},j+\frac{1}{2},k} - \overline{(\rho v)}_{i-\frac{1}{2},j+\frac{1}{2},k}\overline{u}_{i-\frac{1}{2},j+\frac{1}{2},k}}{\Delta x} \\ & -\frac{\overline{(\rho v)}_{i,j+1,k}\overline{v}_{i,j+1,k} - \overline{(\rho v)}_{i,j,k}\overline{v}_{i,j,k}}{\Delta y} \\ & -\frac{\overline{(\rho v)}_{i,j+\frac{1}{2},k+\frac{1}{2}}\overline{v}_{i,j+\frac{1}{2},k+\frac{1}{2}} - \overline{(\rho v)}_{i,j+\frac{1}{2},k-\frac{1}{2}}\overline{v}_{i,j+\frac{1}{2},k-\frac{1}{2}}}{\Delta z} \\ & -\frac{p_{i,j+1,k} - p_{i,j,k}}{\Delta y}, \end{aligned} \tag{3.98}$$

$$\begin{aligned}\left(\frac{\partial \rho w}{\partial t}\right)_{i,j,k+\frac{1}{2}} = & -\frac{\overline{(\rho w)}_{i+\frac{1}{2},j,k+\frac{1}{2}}\overline{u}_{i+\frac{1}{2},j,k+\frac{1}{2}} - \overline{(\rho w)}_{i-\frac{1}{2},j,k+\frac{1}{2}}\overline{u}_{i-\frac{1}{2},j,k+\frac{1}{2}}}{\Delta x} \\ & -\frac{\overline{(\rho w)}_{i,j+\frac{1}{2},k+\frac{1}{2}}\overline{w}_{i,j+\frac{1}{2},k+\frac{1}{2}} - \overline{(\rho w)}_{i,j-\frac{1}{2},k+\frac{1}{2}}\overline{w}_{i,j-\frac{1}{2},k+\frac{1}{2}}}{\Delta y} \\ & -\frac{\overline{(\rho w)}_{i,j,k+1}\overline{w}_{i,j,k+1} - \overline{(\rho w)}_{i,j,k}\overline{w}_{i,j,k}}{\Delta z} \\ & -\frac{p_{i,j,k+1} - p_{i,j,k}}{\Delta z} - \overline{\rho}_{i,j,k+\frac{1}{2}}g \end{aligned} \tag{3.99}$$

Pressure

Since the pressure pertubation is much smaller than the absolute value of the pressure, truncation error of floating point value is relatively large and its precision could become smaller. Therefore, the pressure gradient terms are calculated from the deviation from reference pressure field satisfing the hydrostatic balance. Additionally, the calculation of the pressure (eq. 2.60) is linearlized avoiding a power calculation, which numerically costs expensive.

$$\begin{aligned} p &\approx \bar{p} + \frac{c_p^*}{R^* C_v^*}\left(\frac{\rho\theta R^*}{p_{00}}\right)^{\frac{R^*}{c_v^*}}\{\rho\theta - \overline{\rho\theta}\} \\ &= \bar{p} + \frac{c_p^*}{c_v^*}\frac{\bar{p}}{\overline{\rho\theta}}(\rho\theta)' \end{aligned} \tag{3.100}$$

$$p - p_{\mathrm{ref}} = \bar{p} - p_{\mathrm{ref}} + \frac{c_p^*}{c_v^*}\frac{\bar{p}}{\overline{\rho\theta}}(\rho\theta)' \tag{3.101}$$

3.2.3 Energy equation

$$\begin{aligned}\left(\frac{\partial \rho\theta}{\partial t}\right)_{i,j,k} = & -\frac{(\rho u)_{i+\frac{1}{2},j,k}\overline{\theta}_{i+\frac{1}{2},j,k} - (\rho u)_{i-\frac{1}{2},j,k}\overline{\theta}_{i-\frac{1}{2},j,k}}{\Delta x} \\ & -\frac{(\rho v)_{i,j+\frac{1}{2},k}\overline{\theta}_{i,j+\frac{1}{2},k} - (\rho v)_{i,j-\frac{1}{2},k}\overline{\theta}_{i,j-\frac{1}{2},k}}{\Delta y} \\ & -\frac{(\rho w)_{i,j,k+\frac{1}{2}}\overline{\theta}_{i,j,k+\frac{1}{2}} - (\rho w)_{i,j,k-\frac{1}{2}}\overline{\theta}_{i,j,k-\frac{1}{2}}}{\Delta z} \end{aligned} \tag{3.102}$$

where

$$\overline{\theta}_{i+\frac{1}{2},j,k} = \frac{-\theta_{i+2,j,k} + 7\theta_{i+1,j,k} + 7\theta_{i,j,k} - \theta_{i-1,j,k}}{12} \tag{3.103}$$

$$\overline{\theta}_{i,j+\frac{1}{2},k} = \frac{-\theta_{i,j+2,k} + 7\theta_{i,j+1,k} + 7\theta_{i,j,k} - \theta_{i,j-1,k}}{12} \tag{3.104}$$

$$\overline{\theta}_{i,j,k+\frac{1}{2}} = \frac{-\theta_{i,j,k+2} + 7\theta_{i,j,k+1} + 7\theta_{i,j,k} - \theta_{i,j,k-1}}{12} \tag{3.105}$$

3.2.4 Tracer advection

The tracer advection process is done after the time integration of the dynamical variables (ρ, ρu, ρv, ρw, and $\rho\theta$). We impose two constraints to tracer advection:

Consistency With Continuity (CWC) On the condition without any source/sink, the mass concentration in the advection process should be conserved along the trajectory. It is, at least, necessary that the spatially constant mass concentration should be kept in any motion of fluid. In order to satisfy this condition, we use the same mass flux at the last Runge-Kutta process of Eqs.() and () for integration of tracers:

$$\begin{aligned}\frac{(\rho q)^{n+1}_{i,j,k} - (\rho q)^{n}_{i,j,k}}{\Delta t} = & -\frac{(\rho u)_{i+\frac{1}{2},j,k}\overline{q}_{i+\frac{1}{2},j,k} - (\rho u)_{i-\frac{1}{2},j,k}\overline{q}_{i-\frac{1}{2},j,k}}{\Delta x} \\ & -\frac{(\rho v)_{i,j+\frac{1}{2},k}\overline{q}_{i,j+\frac{1}{2},k} - (\rho v)_{i,j-\frac{1}{2},k}\overline{q}_{i,j-\frac{1}{2},k}}{\Delta y} \\ & -\frac{(\rho w)_{i,j,k+\frac{1}{2}}\overline{q}_{i,j,k+\frac{1}{2}} - (\rho w)_{i,j,k-\frac{1}{2}}\overline{q}_{i,j,k-\frac{1}{2}}}{\Delta z}\end{aligned} \tag{3.106}$$

Monotonicity In order to satisfy the monotonicity of tracer advection, we employ the Flux Corrected Trasport scheme, which is a hybrid scheme with the 4th order central difference scheme and 1st order upwind scheme. If The 4th order central difference is applied, $\overline{q}$ is descritized as

$$\overline{q}^{high}_{i+\frac{1}{2},j,k} = \frac{-q_{i+2,j,k} + 7q_{i+1,j,k} + 7q_{i,j,k} - q_{i-1,j,k}}{12} \tag{3.107}$$

$$\overline{q}^{high}_{i,j+\frac{1}{2},k} = \frac{-q_{i,j+2,k} + 7q_{i,j+1,k} + 7q_{i,j,k} - q_{i,j-1,k}}{12} \tag{3.108}$$

$$\overline{q}^{high}_{i,j,k+\frac{1}{2}} = \frac{-q_{i,j,k+2} + 7q_{i,j,k+1} + 7q_{i,j,k} - q_{i,j,k-1}}{12}. \tag{3.109}$$

On the other hand, in the 1st order upwind scheme $\overline{q}$ is described as

$$\overline{q}^{low}_{i+\frac{1}{2},j,k} = \begin{cases} q_{i,j,k} & ((\rho u)_{i+\frac{1}{2},j,k} > 0) \\ q_{i+1,j,k} & (\text{otherwise}) \end{cases} \tag{3.110}$$

$$\overline{q}^{low}_{i,j+\frac{1}{2},k} = \begin{cases} q_{i,j,k} & ((\rho u)_{i,j+\frac{1}{2},k} > 0) \\ q_{i,j+1,k} & (\text{otherwise}) \end{cases} \tag{3.111}$$

$$\overline{q}^{low}_{i,j,k+\frac{1}{2}} = \begin{cases} q_{i,j,k} & ((\rho u)_{i,j,k+\frac{1}{2}} > 0) \\ q_{i,j,k+1} & (\text{otherwise}) \end{cases} \tag{3.112}$$

The actual $\overline{q}$ is described as

$$\overline{q}_{i+\frac{1}{2},j,k} = C_{i+\frac{1}{2},j,k}\overline{q}^{high}_{i+\frac{1}{2},j,k} + \left(1 - C_{i+\frac{1}{2},j,k}\right)\overline{q}^{low}_{i+\frac{1}{2},j,k} \quad (3.113)$$

$$\overline{q}_{i,j+\frac{1}{2},k} = C_{i,j+\frac{1}{2},k}\overline{q}^{high}_{i,j+\frac{1}{2},k} + \left(1 - C_{i,j+\frac{1}{2},k}\right)\overline{q}^{low}_{i,j+\frac{1}{2},k} \quad (3.114)$$

$$\overline{q}_{i,j,k+\frac{1}{2}} = C_{i,j,k+\frac{1}{2}}\overline{q}^{high}_{i,j,k+\frac{1}{2}} + \left(1 - C_{i,j,k+\frac{1}{2}}\right)\overline{q}^{low}_{i,j,k+\frac{1}{2}} \quad (3.115)$$

See the appedix for the method to determine the flux limter.

3.3 boundary condition

The boundary condition only for the vertical velocity at the top and bottom boundaries is needed:

$$w_{i,j,k_{max}+\frac{1}{2}} = 0 \quad (3.116)$$

$$w_{i,j,k_{min}-\frac{1}{2}} = 0 \quad (3.117)$$

This leads to the boundary condition of the prognostic variable as

$$(\rho w)_{i,j,k_{max}+\frac{1}{2}} = 0 \quad (3.118)$$

$$(\rho w)_{i,j,k_{min}-\frac{1}{2}} = 0 \quad (3.119)$$

3.4 Numerical filters

We impose an explicit numerical filter using the numerical viscosity and diffusion. Although the filter is necessary for numerical stability, too strong a filter could dampen any physically meaningful variability. In this subsection, we describe the numerical filters used in this model, and discuss the strength of the filter.

In order to damp the higher wavenumber component selectively, we adopt the hyperviscosity and diffusion in the traditional way. The hyperviscosity and diffusion of the nth order is defined as

$$\frac{\partial}{\partial x}\left[\nu\rho\frac{\partial^{n-1}f}{\partial x^{n-1}}\right], \quad (3.120)$$

where f is an arbitrary variable ($f \in \rho, u, v, w, \theta, q$).

The Laplacian of f is discretized as

$$\Delta f_i = \frac{1}{\Delta x_i}\left[\frac{1}{\Delta x_{i+\frac{1}{2}}}f_{i+1} - \left(\frac{1}{\Delta x_{i+\frac{1}{2}}} + \frac{1}{\Delta x_{i-\frac{1}{2}}}\right)f_i + \frac{1}{\Delta x_{i-\frac{1}{2}}}f_{i-1}\right], \quad (3.121)$$

and

$$\Delta^{n/2} f_i = \frac{1}{\Delta x_i}\left[\frac{1}{\Delta x_{i+\frac{1}{2}}}\Delta^{n/2-1}f_{i+1} - \left(\frac{1}{\Delta x_{i+\frac{1}{2}}} + \frac{1}{\Delta x_{i-\frac{1}{2}}}\right)\Delta^{n/2-1}f_i + \frac{1}{\Delta x_{i-\frac{1}{2}}}\Delta^{n/2-1}f_{i-1}\right]. \quad (3.122)$$

Here we consider spatially dependent grid interval in calculating the Laplacian. If it is calculated with constant Δx_i as

$$\Delta f_i = \frac{1}{\Delta x_i^2}\left(f_{i+1} - 2f_i + f_{i-1}\right), \tag{3.123}$$

$$\Delta^{n/2} f_i = \frac{1}{\Delta x_i^2}\left(\Delta^{n/2-1} f_{i+1} - 2\Delta^{n/2-1} f_i + \Delta^{n/2-1} f_{i-1}\right), \tag{3.124}$$

non-negligible numerical noise appears where the grid spacing varies (e.g., stretching layer near the top boundary).

The hyperviscosity and diffusion can be discretized as

$$\frac{\partial}{\partial x}\left[\nu\rho\frac{\partial^{n-1} f}{\partial^{n-1} x}\right] \sim \frac{F_{i+\frac{1}{2}} - F_{i-\frac{1}{2}}}{\Delta x_i}, \tag{3.125}$$

where

$$F_{i+\frac{1}{2}} \frac{\nu_{i+\frac{1}{2}}\rho_{i+\frac{1}{2}}}{\Delta x_{i+\frac{1}{2}}}\left(\Delta^{n/2-1} f_{i+1} - \Delta^{n/2-1} f_i\right). \tag{3.126}$$

The coefficient, ν, is written as

$$\nu_{i+\frac{1}{2}} = (-1)^{n/2+1}\gamma\frac{\Delta x_{i+\frac{1}{2}}^n}{2^n \Delta t}, \tag{3.127}$$

where γ is a non-dimensional coefficient. One-dimensional sinusoidal two-grid noise will decay to $1/e$ with $1/\gamma$ time steps. Note that the theoretical e-folding time is $\frac{2^n}{\pi^n}\frac{\Delta t}{\gamma}$. However, it is $\frac{\Delta t}{\gamma}$ with the fourth-order central scheme used in this model.

For the numerical stability of the numerical filter itself, it should satisfy

$$\gamma < 1 \tag{3.128}$$

for the one-dimensional two-grid noise, and

$$\gamma < \frac{1}{3} \tag{3.129}$$

for the three-dimensional two-grid noise. The conditions might be stricter for other types of noise.

The flux, F, for the numerical filter is added to the advective flux as

$$(\rho u f)^{\dagger}_{i+\frac{1}{2}} = (\rho u f)_{i+\frac{1}{2}} + F_{i+\frac{1}{2}}, \tag{3.130}$$

where the first term of the right-hand side is the flux calculated by the advection scheme. In the present model, the advection scheme is the fourth-order central difference scheme. This concept is very important for the CWC condition in the tracer equations. The modified mass flux of the numerical filter should be used in the tracer advection, otherwise the CWC condition is violated.

The numerical viscosity and diffusion in the y and z directions are formulated in the same way as in the x direction, although a special treatment for the z direction is needed. At the top and bottom boundaries, the flux must be zero, $F_{k_{\max}+\frac{1}{2}} = F_{k_{\min}-\frac{1}{2}} = 0$. In order to calculate the $F_{k_{\max}-\frac{1}{2}}$ and $F_{k_{\min}+\frac{1}{2}}$,

values beyond the boundaries, $f_{k_{\max}+1}$ and $f_{k_{\min}-1}$, are required, then the mirror boundary condition is assumed; $f_{k_{\max}+1} = -f_{k_{\max}}$ and $f_{k_{\min}-1} = -f_{k_{\min}}$. This condition is appropriate to cause the decay the vertical two-grid noise.

Vertical profiles of density, potential temperature, and water vapor usually have significant (e.g., logarithmic) dependencies on height. Eq. (3.125) has a non-zero value even for the steady state, and the numerical filter produces artificial motion. To reduce this artificial motion, we introduce a reference profile which is a function of height, and deviation from the reference is used as f instead of ρ, θ, and q_{v} in calculating the numerical filter. The reference profile can be chosen arbitrarily, but a profile under hydrostatic balance is usually chosen.

(a) Control volume for the mass

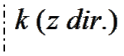

(b) Control volume for the momentum

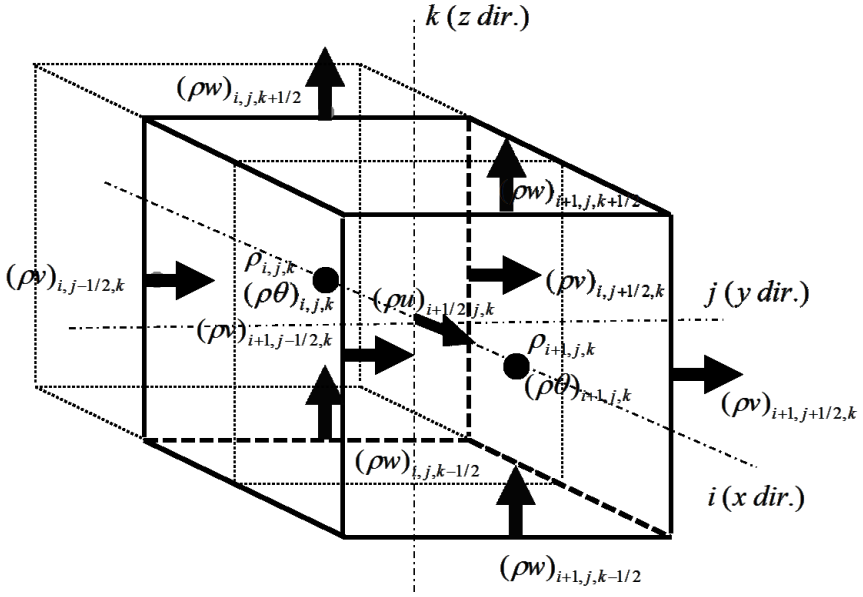

Figure 3.1: Control volume

Chapter 4

Terrain-following Coordinates

Corresponding author : Hisashi Yashiro

4.1 Geometry and Definitions

We introduce a terrain following coordinate system with a new vertical coordinate ξ. ξ-coordinate system is not deformable system. We use the relation between z and ξ as

$$\xi = \frac{z_{toa}(z - z_{sfc})}{z_{toa} - z_{sfc}}, \tag{4.1}$$

Where z_{toa} is the top of the model domain and z_{sfc} is the surface height, which depends on the horizontal location.

The metrics are defined as

$$G^{\frac{1}{2}} = \frac{\partial z}{\partial \xi}, \tag{4.2}$$

$$J^{\xi}_{13} = \left(\frac{\partial \xi}{\partial x}\right)_z = -\frac{J^z_{13}}{J^z_{33}}, \tag{4.3}$$

$$J^{\xi}_{23} = \left(\frac{\partial \xi}{\partial y}\right)_z = -\frac{J^z_{23}}{J^z_{33}}, \tag{4.4}$$

$$J^{\xi}_{33} = \frac{\partial \xi}{\partial z} = \frac{1}{J^z_{33}}, \tag{4.5}$$

where

$$J^z_{13} = \left(\frac{\partial z}{\partial x}\right)_{\xi}, \tag{4.6}$$

$$J^z_{23} = \left(\frac{\partial z}{\partial y}\right)_{\xi}, \tag{4.7}$$

$$J^z_{33} = G^{\frac{1}{2}} \tag{4.8}$$

If we use the Eqs.(4.1)-(4.5), we obtain following equations:

$$G^{\frac{1}{2}}\nabla\phi = \left[\left(\frac{\partial G^{\frac{1}{2}}\phi}{\partial x}\right)_{\xi} + \frac{\partial J^{\xi}_{13}G^{\frac{1}{2}}\phi}{\partial\xi}\right]\hat{\boldsymbol{e}}_x + \left[\left(\frac{\partial G^{\frac{1}{2}}\phi}{\partial y}\right)_{\xi} + \frac{\partial J^{\xi}_{23}G^{\frac{1}{2}}\phi}{\partial\xi}\right]\hat{\boldsymbol{e}}_y + \left[\frac{\partial J^{\xi}_{33}G^{\frac{1}{2}}\phi}{\partial\xi}\right]\hat{\boldsymbol{e}}_z, \tag{4.9}$$

$$G^{\frac{1}{2}}\nabla\cdot(\phi\mathbf{u}) = \left(\frac{\partial G^{\frac{1}{2}}\phi u}{\partial x}\right)_{\xi} + \left(\frac{\partial G^{\frac{1}{2}}\phi v}{\partial y}\right)_{\xi} + \frac{\partial G^{\frac{1}{2}}\phi\dot{\xi}}{\partial\xi} \tag{4.10}$$

where $\{\hat{\boldsymbol{e}}_x, \hat{\boldsymbol{e}}_y, \hat{\boldsymbol{e}}_z\}$ are unit vectors in Cartesian coordinate, and $\dot{\xi}$ is the vertical velocity component in the terrain following coordinate, giving by

$$\dot{\xi} \equiv \frac{d\xi}{dt} = J^{\xi}_{13}u + J^{\xi}_{23}v + J^{\xi}_{33}w. \tag{4.11}$$

4.2 Summary of modified equations in the dynamical process

Prognostic variables by multiplying $G^{\frac{1}{2}}$ are defined as

$$(\rho Q_v)_{i,j,k} = G^{\frac{1}{2}}_{i,j,k}(\rho q_v)_{i,j,k}, \tag{4.12}$$

$$(\rho Q_l)_{i,j,k} = G^{\frac{1}{2}}_{i,j,k}(\rho q_l)_{i,j,k}, \tag{4.13}$$

$$(\rho Q_s)_{i,j,k} = G^{\frac{1}{2}}_{i,j,k}(\rho q_s)_{i,j,k}, \tag{4.14}$$

$$R_{i,j,k} = G^{\frac{1}{2}}_{i,j,k}\rho_{i,j,k}, \tag{4.15}$$

$$(\rho U)_{i+\frac{1}{2},j,k} = G^{\frac{1}{2}}_{i+\frac{1}{2},j,k}(\rho u)_{i+\frac{1}{2},j,k}, \tag{4.16}$$

$$(\rho V)_{i,j+\frac{1}{2},k} = G^{\frac{1}{2}}_{i,j+\frac{1}{2},k}(\rho v)_{i,j+\frac{1}{2},k}, \tag{4.17}$$

$$(\rho W)_{i,j,k+\frac{1}{2}} = G^{\frac{1}{2}}_{i,j,k+\frac{1}{2}}(\rho w)_{i,j,k+\frac{1}{2}}, \tag{4.18}$$

$$(\rho\Theta)_{i,j,k} = G^{\frac{1}{2}}_{i,j,k}(\rho\theta)_{i,j,k}, \tag{4.19}$$

$$P_{i,j,k} = G^{\frac{1}{2}}_{i,j,k}p_{i,j,k}. \tag{4.20}$$

Eqs.(2.67)-(2.72) are modified using Eqs.(4.9)-(4.11),

$$\frac{\partial \rho Q_v}{\partial t} + \frac{\partial}{\partial x_j}\left(\rho Q_v u_j\right) = 0, \tag{4.21}$$

$$\frac{\partial \rho Q_l}{\partial t} + \frac{\partial}{\partial x_j}\left(\rho Q_l u_j\right) = 0, \tag{4.22}$$

$$\frac{\partial \rho Q_s}{\partial t} + \frac{\partial}{\partial x_j}\left(\rho Q_s u_j\right) = 0, \tag{4.23}$$

$$\frac{\partial R}{\partial t} + \frac{\partial}{\partial x_j}\left(R u_j\right) = 0, \tag{4.24}$$

$$\frac{\partial \rho U}{\partial t} + \frac{\partial}{\partial x_j}\left(\rho U u_j\right) = -\left(\frac{\partial P}{\partial x}\right)_\xi - \frac{\partial J^\xi_{13} P}{\partial \xi}, \tag{4.25}$$

$$\frac{\partial \rho V}{\partial t} + \frac{\partial}{\partial x_j}\left(\rho V u_j\right) = -\left(\frac{\partial P}{\partial y}\right)_\xi - \frac{\partial J^\xi_{23} P}{\partial \xi}, \tag{4.26}$$

$$\frac{\partial \rho W}{\partial t} + \frac{\partial}{\partial x_j}\left(\rho W u_j\right) = -\frac{\partial J^\xi_{33} P}{\partial \xi} - Rg, \tag{4.27}$$

$$\frac{\partial \rho \Theta}{\partial t} + \frac{\partial}{\partial x_j}\left(\rho \Theta u_j\right) = 0, \tag{4.28}$$

where Einstein summation has been used to implicitly sum over repeated indices, and $(x_1, x_2, x_3) = (x, y, \xi)$, $(u_1, u_2, u_3) = (u, v, \dot{\xi})$.

4.3 Spatial descretization

4.3.1 Continuity equation

$$\begin{aligned}\left(\frac{\partial R}{\partial t}\right)_{i,j,k} = -\Bigg[& \frac{(\rho U)_{i+\frac{1}{2},j,k} - (\rho U)_{i-\frac{1}{2},j,k}}{\Delta x} \\ & + \frac{(\rho V)_{i,j+\frac{1}{2},k} - (\rho V)_{i,j-\frac{1}{2},k}}{\Delta y} \\ & + \frac{(J^\xi_{13})_{i,j,k+\frac{1}{2}} \overline{\left(\widetilde{\rho U}\right)^x}^z_{i,j,k+\frac{1}{2}} - (J^\xi_{13})_{i,j,k-\frac{1}{2}} \overline{\left(\widetilde{\rho U}\right)^x}^z_{i,j,k-\frac{1}{2}}}{\Delta \xi} \\ & + \frac{(J^\xi_{23})_{i,j,k+\frac{1}{2}} \overline{\left(\widetilde{\rho V}\right)^y}^z_{i,j,k+\frac{1}{2}} - (J^\xi_{23})_{i,j,k-\frac{1}{2}} \overline{\left(\widetilde{\rho V}\right)^y}^z_{i,j,k-\frac{1}{2}}}{\Delta \xi} \\ & + \frac{(J^\xi_{33})_{i,j,k+\frac{1}{2}} (\rho W)_{i,j,k+\frac{1}{2}} - (J^\xi_{33})_{i,j,k+\frac{1}{2}} (\rho W)_{i,j,k-\frac{1}{2}}}{\Delta \xi} \Bigg] \end{aligned} \tag{4.29}$$

where

$$\overline{\left(\widetilde{\rho U}\right)^x}^z_{i,j,k+\frac{1}{2}} = G^{\frac{1}{2}}_{i,j,k+\frac{1}{2}} \frac{\left(\widetilde{\rho u}\right)^x_{i,j,k+1} + \left(\widetilde{\rho u}\right)^x_{i,j,k}}{2}, \tag{4.30}$$

$$\overline{\left(\widetilde{\rho V}\right)^y}^z_{i,j,k+\frac{1}{2}} = G^{\frac{1}{2}}_{i,j,k+\frac{1}{2}} \frac{\left(\widetilde{\rho v}\right)^y_{i,j,k+1} + \left(\widetilde{\rho v}\right)^y_{i,j,k}}{2}, \tag{4.31}$$

$\left(\widetilde{\rho u}\right)^x_{i,j,k}$ and $\left(\widetilde{\rho v}\right)^y_{i,j,k}$ are obtained by same manner in eq.(3.20)

4.3.2 Momentum equations

$$
\begin{aligned}
\left(\frac{\partial \rho U}{\partial t}\right)_{i+\frac{1}{2},j,k} = -\Bigg[& \frac{(\widetilde{\rho U})^{x}_{i+1,j,k}\overline{u}_{i+1,j,k} - (\widetilde{\rho U})^{x}_{i,j,k}\overline{u}_{i,j,k}}{\Delta x} \\
& + \frac{(\widetilde{\rho U})^{y}_{i+\frac{1}{2},j+\frac{1}{2},k}\overline{v}_{i+\frac{1}{2},j+\frac{1}{2},k} - (\widetilde{\rho U})^{y}_{i+\frac{1}{2},j-\frac{1}{2},k}\overline{v}_{i+\frac{1}{2},j-\frac{1}{2},k}}{\Delta y} \\
& + \frac{(J^{\xi}_{13})_{i+\frac{1}{2},j,k+\frac{1}{2}}(\widetilde{\rho U})^{z}_{i+\frac{1}{2},j,k+\frac{1}{2}}\overline{\overline{u}}^{z}_{i+\frac{1}{2},j,k+\frac{1}{2}} - (J^{\xi}_{13})_{i+\frac{1}{2},j,k-\frac{1}{2}}(\widetilde{\rho U})^{z}_{i+\frac{1}{2},j,k-\frac{1}{2}}\overline{\overline{u}}^{z}_{i+\frac{1}{2},j,k-\frac{1}{2}}}{\Delta \xi} \\
& + \frac{(J^{\xi}_{23})_{i+\frac{1}{2},j,k+\frac{1}{2}}(\widetilde{\rho U})^{z}_{i+\frac{1}{2},j,k+\frac{1}{2}}\overline{\overline{v}^{y}}^{xz}_{i+\frac{1}{2},j,k+\frac{1}{2}} - (J^{\xi}_{23})_{i+\frac{1}{2},j,k-\frac{1}{2}}(\widetilde{\rho U})^{z}_{i+\frac{1}{2},j,k-\frac{1}{2}}\overline{\overline{v}^{y}}^{xz}_{i+\frac{1}{2},j,k-\frac{1}{2}}}{\Delta \xi} \\
& + \frac{(J^{\xi}_{33})_{i+\frac{1}{2},j,k+\frac{1}{2}}(\widetilde{\rho U})^{z}_{i+\frac{1}{2},j,k+\frac{1}{2}}\overline{\overline{w}}^{x}_{i+\frac{1}{2},j,k+\frac{1}{2}} - (J^{\xi}_{33})_{i+\frac{1}{2},j,k-\frac{1}{2}}(\widetilde{\rho U})^{z}_{i+\frac{1}{2},j,k-\frac{1}{2}}\overline{\overline{w}}^{x}_{i+\frac{1}{2},j,k-\frac{1}{2}}}{\Delta \xi} \\
& + \frac{P_{i+1,j,k} - P_{i,j,k}}{\Delta x} \\
& + \frac{(J^{\xi}_{13})_{i+\frac{1}{2},j,k+\frac{1}{2}}\overline{P}^{xz}_{i+\frac{1}{2},j,k+\frac{1}{2}} - (J^{\xi}_{13})_{i+\frac{1}{2},j,k-\frac{1}{2}}\overline{P}^{xz}_{i+\frac{1}{2},j,k-\frac{1}{2}}}{\Delta \xi} \Bigg],
\end{aligned}
\tag{4.32}
$$

where $(\widetilde{\rho U})^{x}_{i,j,k}$, $(\widetilde{\rho U})^{y}_{i+\frac{1}{2},j+\frac{1}{2},k}$ and $(\widetilde{\rho U})^{z}_{i+\frac{1}{2},j,k+\frac{1}{2}}$ is obtained according to the method of eq(3.20)-(3.22). The velocities at the cell wall for the staggered control volume to x direction are defined by eq(3.23)-(3.25). $\overline{\overline{u}}^{z}$ and $\overline{\overline{v}^{y}}^{xz}$ are defined as

$$
\overline{\overline{u}}^{z}_{i+\frac{1}{2},j,k+\frac{1}{2}} = \frac{\overline{u}_{i+\frac{1}{2},j,k+1} + \overline{u}_{i+\frac{1}{2},j,k}}{2}, \tag{4.33}
$$

$$
\overline{\overline{v}^{y}}^{xz}_{i+\frac{1}{2},j,k+\frac{1}{2}} = \frac{\overline{v}^{y}_{i+1,j,k+1} + \overline{v}^{y}_{i+1,j,k} + \overline{v}^{y}_{i,j,k+1} + \overline{v}^{y}_{i,j,k}}{4}. \tag{4.34}
$$

$\overline{P}^{xz}$ is defined as

$$
\overline{P}^{xz}_{i+\frac{1}{2},j,k+\frac{1}{2}} = G^{\frac{1}{2}}_{i+\frac{1}{2},j,k+\frac{1}{2}} \frac{p_{i+1,j,k+1} + p_{i+1,j,k} + p_{i,j,k+1} + p_{i,j,k}}{4}. \tag{4.35}
$$

The momentum equations in the y and z directions are descretized in the

same way:

$$\left(\frac{\partial \rho V}{\partial t}\right)_{i,j+\frac{1}{2},k} = -\Bigg[\frac{(\widetilde{\rho V})^{x}_{i+\frac{1}{2},j+\frac{1}{2},k}\overline{u}_{i+\frac{1}{2},j+\frac{1}{2},k} - (\widetilde{\rho V})^{x}_{i-\frac{1}{2},j+\frac{1}{2},k}\overline{u}_{i-\frac{1}{2},j+\frac{1}{2},k}}{\Delta x}$$
$$+ \frac{(\widetilde{\rho V})^{y}_{i,j+1,k}\overline{v}_{i,j+1,k} - (\widetilde{\rho V})^{y}_{i,j,k}\overline{v}_{i,j,k}}{\Delta y}$$
$$+ \frac{(J^{\xi}_{13})_{i,j+\frac{1}{2},k+\frac{1}{2}}(\widetilde{\rho V})^{z}_{i,j+\frac{1}{2},k+\frac{1}{2}}\overline{\overline{u}^{x}}^{yz}_{i,j+\frac{1}{2},k+\frac{1}{2}} - (J^{\xi}_{13})_{i,j+\frac{1}{2},k-\frac{1}{2}}(\widetilde{\rho V})^{z}_{i,j+\frac{1}{2},k-\frac{1}{2}}\overline{\overline{u}^{x}}^{yz}_{i,j+\frac{1}{2},k-\frac{1}{2}}}{\Delta \xi}$$
$$+ \frac{(J^{\xi}_{23})_{i,j+\frac{1}{2},k+\frac{1}{2}}(\widetilde{\rho V})^{z}_{i,j+\frac{1}{2},k+\frac{1}{2}}\overline{\overline{v}}^{z}_{i,j+\frac{1}{2},k+\frac{1}{2}} - (J^{\xi}_{23})_{i,j+\frac{1}{2},k-\frac{1}{2}}(\widetilde{\rho V})^{z}_{i,j+\frac{1}{2},k-\frac{1}{2}}\overline{\overline{v}}^{z}_{i,j+\frac{1}{2},k-\frac{1}{2}}}{\Delta \xi}$$
$$+ \frac{(J^{\xi}_{33})_{i,j+\frac{1}{2},k+\frac{1}{2}}(\widetilde{\rho V})^{z}_{i,j+\frac{1}{2},k+\frac{1}{2}}\overline{\overline{w}}^{y}_{i,j+\frac{1}{2},k+\frac{1}{2}} - (J^{\xi}_{33})_{i,j+\frac{1}{2},k-\frac{1}{2}}(\widetilde{\rho V})^{z}_{i,j+\frac{1}{2},k-\frac{1}{2}}\overline{\overline{w}}^{y}_{i,j+\frac{1}{2},k-\frac{1}{2}}}{\Delta \xi}$$
$$+ \frac{P_{i,j+1,k} - P_{i,j,k}}{\Delta y}$$
$$+ \frac{(J^{\xi}_{23})_{i,j+\frac{1}{2},k+\frac{1}{2}}\overline{P}^{yz}_{i,j+\frac{1}{2},k+\frac{1}{2}} - (J^{\xi}_{23})_{i,j+\frac{1}{2},k-\frac{1}{2}}\overline{P}^{yz}_{i,j+\frac{1}{2},k-\frac{1}{2}}}{\Delta \xi}\Bigg], \tag{4.36}$$

$$\left(\frac{\partial \rho W}{\partial t}\right)_{i,j,k+\frac{1}{2}} = -\Bigg[\frac{(\widetilde{\rho W})^{x}_{i+\frac{1}{2},j,k+\frac{1}{2}}\overline{u}_{i+\frac{1}{2},j,k+\frac{1}{2}} - (\widetilde{\rho W})^{x}_{i-\frac{1}{2},j,k+\frac{1}{2}}\overline{u}_{i-\frac{1}{2},j,k+\frac{1}{2}}}{\Delta x}$$
$$+ \frac{(\widetilde{\rho W})^{y}_{i,j+\frac{1}{2},k+\frac{1}{2}}\overline{v}_{i,j+\frac{1}{2},k+\frac{1}{2}} - (\widetilde{\rho W})^{y}_{i,j-\frac{1}{2},k+\frac{1}{2}}\overline{v}_{i,j-\frac{1}{2},k+\frac{1}{2}}}{\Delta y}$$
$$+ \frac{(J^{\xi}_{13})_{i,j,k+1}(\widetilde{\rho W})^{z}_{i,j,k+1}\overline{u}^{x}_{i,j,k+1} - (J^{\xi}_{13})_{i,j,k}(\widetilde{\rho W})^{z}_{i,j,k}\overline{u}^{x}_{i,j,k}}{\Delta \xi}$$
$$+ \frac{(J^{\xi}_{23})_{i,j,k+1}(\widetilde{\rho W})^{z}_{i,j,k+1}\overline{v}^{y}_{i,j,k+1} - (J^{\xi}_{23})_{i,j,k}(\widetilde{\rho W})^{z}_{i,j,k}\overline{v}^{y}_{i,j,k}}{\Delta \xi}$$
$$+ \frac{(J^{\xi}_{33})_{i,j,k+1}(\widetilde{\rho W})^{z}_{i,j,k+1}\overline{w}^{z}_{i,j,k+1} - (J^{\xi}_{33})_{i,j,k}(\widetilde{\rho W})^{z}_{i,j,k}\overline{w}^{z}_{i,j,k}}{\Delta \xi}$$
$$+ \frac{(J^{\xi}_{33})_{i,j,k+1}P_{i,j,k+1} - (J^{\xi}_{33})_{i,j,k}P_{i,j,k}}{\Delta \xi}\Bigg]. \tag{4.37}$$

4.3.3 Energy equation

$$\left(\frac{\partial \rho\Theta}{\partial t}\right)_{i,j,k} = -\Bigg[\frac{(\rho U)_{i+\frac{1}{2},j,k}\overline{\theta}_{i+\frac{1}{2},j,k} - (\rho U)_{i-\frac{1}{2},j,k}\overline{\theta}_{i-\frac{1}{2},j,k}}{\Delta x} + \frac{(\rho V)_{i,j+\frac{1}{2},k}\overline{\theta}_{i,j+\frac{1}{2},k} - (\rho V)_{i,j-\frac{1}{2},k}\overline{\theta}_{i,j-\frac{1}{2},k}}{\Delta y} + \frac{(J^{\xi}_{13})_{i,j,k+\frac{1}{2}}\overline{\widetilde{(\rho U)}^{x}}^{z}_{i,j,k+\frac{1}{2}}\overline{\theta}_{i,j,k+\frac{1}{2}} - (J^{\xi}_{13})_{i,j,k-\frac{1}{2}}\overline{\widetilde{(\rho U)}^{x}}^{z}_{i,j,k-\frac{1}{2}}\overline{\theta}_{i,j,k-\frac{1}{2}}}{\Delta \xi} + \frac{(J^{\xi}_{23})_{i,j,k+\frac{1}{2}}\overline{\widetilde{(\rho V)}^{y}}^{z}_{i,j,k+\frac{1}{2}}\overline{\theta}_{i,j,k+\frac{1}{2}} - (J^{\xi}_{23})_{i,j,k-\frac{1}{2}}\overline{\widetilde{(\rho V)}^{y}}^{z}_{i,j,k-\frac{1}{2}}\overline{\theta}_{i,j,k-\frac{1}{2}}}{\Delta \xi} + \frac{(J^{\xi}_{33})_{i,j,k+\frac{1}{2}}(\rho W)_{i,j,k+\frac{1}{2}}\overline{\theta}_{i,j,k+\frac{1}{2}} - (J^{\xi}_{33})_{i,j,k+\frac{1}{2}}(\rho W)_{i,j,k-\frac{1}{2}}\overline{\theta}_{i,j,k-\frac{1}{2}}}{\Delta \xi}\Bigg] \tag{4.38}$$

where $\overline{\theta}_{i+\frac{1}{2},j,k}$, $\overline{\theta}_{i,j+\frac{1}{2},k}$ and $\overline{\theta}_{i,j,k+\frac{1}{2}}$ are obtained according to the method of eq(3.29)-(3.31).

Chapter 5

Map factor

Corresponding author : Seiya Nishizawa

5.1 Coordinate transform

A orthogonal rectangular coordinate (x, y, z). A orthogonal curvilinear coordinate (ξ, η, ζ).

The transform is defined by

$$\boldsymbol{e}_\xi = \frac{\partial x}{\partial \xi}\hat{\boldsymbol{e}}_x + \frac{\partial y}{\partial \xi}\hat{\boldsymbol{e}}_y + \frac{\partial z}{\partial \xi}\hat{\boldsymbol{e}}_z, \tag{5.1}$$

$$\boldsymbol{e}_\eta = \frac{\partial x}{\partial \eta}\hat{\boldsymbol{e}}_x + \frac{\partial y}{\partial \eta}\hat{\boldsymbol{e}}_y + \frac{\partial z}{\partial \eta}\hat{\boldsymbol{e}}_z, \tag{5.2}$$

$$\boldsymbol{e}_\zeta = \frac{\partial x}{\partial \zeta}\hat{\boldsymbol{e}}_x + \frac{\partial y}{\partial \zeta}\hat{\boldsymbol{e}}_y + \frac{\partial z}{\partial \zeta}\hat{\boldsymbol{e}}_z. \tag{5.3}$$

Reverse transform is

$$\hat{\boldsymbol{e}}_x = \frac{\partial \xi}{\partial x}\boldsymbol{e}_\xi + \frac{\partial \eta}{\partial x}\boldsymbol{e}_\eta + \frac{\partial \zeta}{\partial x}\boldsymbol{e}_\zeta, \tag{5.4}$$

$$\hat{\boldsymbol{e}}_y = \frac{\partial \eta}{\partial y}\boldsymbol{e}_\xi + \frac{\partial \eta}{\partial y}\boldsymbol{e}_\eta + \frac{\partial \zeta}{\partial y}\boldsymbol{e}_\zeta, \tag{5.5}$$

$$\hat{\boldsymbol{e}}_z = \frac{\partial \zeta}{\partial z}\boldsymbol{e}_\xi + \frac{\partial \eta}{\partial z}\boldsymbol{e}_\eta + \frac{\partial \zeta}{\partial z}\boldsymbol{e}_\zeta. \tag{5.6}$$

The Jacobian matrix is $\{\frac{\partial \xi^k}{\partial x^i}\}$.

The reverse transform after the transform of the transform after the reverse transform make a vector to the original vector;

$$\frac{\partial \xi^k}{\partial x^i}\frac{\partial x^i}{\partial \xi^l} = \delta^k_l, \tag{5.7}$$

$$\frac{\partial x^i}{\partial \xi^k}\frac{\partial \xi^k}{\partial x^j} = \delta^i_j, \tag{5.8}$$

where index which appares upper and lower suffix in a single term implies summation of the term over set $1, 2, 3$ (Einstein notation).

Spatial parial derivative is tranformed with the Jacobian matrix (covariant transform);

$$\frac{\partial}{\partial \xi^k} = \frac{\partial x^i}{\partial \xi^k}\frac{\partial}{\partial x^i}, \tag{5.9}$$

$$\frac{\partial}{\partial x^i} = \frac{\partial \xi^k}{\partial x^i}\frac{\partial}{\partial \xi^k}. \tag{5.10}$$

Velocity is transformed with the inverse of the Jacobian matrix (cotravariant transform);

$$d\xi^k = \frac{\partial \xi^k}{\partial x^i}dx^i, \tag{5.11}$$

$$dx^i = \frac{\partial x^i}{\partial \xi^k}d\xi^k. \tag{5.12}$$

The metric tensor, g_{kl} is defined by

$$\begin{aligned} g_{kl} = \boldsymbol{e}_k \cdot \boldsymbol{e}_l &= \left(\frac{\partial x^i}{\partial \xi_k}\hat{\boldsymbol{e}}_i\right)\cdot\left(\frac{\partial x^j}{\partial \xi_l}\hat{\boldsymbol{e}}_j\right) \\ &= \frac{\partial x^i}{\partial \xi_k}\frac{\partial x^i}{\partial \xi_l}. \end{aligned} \tag{5.13}$$

For orthogonal curvilinear coordinates, the matrix g_{kl} is diagonal. Metric factor, h_k is defined as

$$h_k^2 = g_{kk} = \sum_i \left(\frac{\partial x^i}{\partial \xi_k}\right)^2. \tag{5.14}$$

Here we define the matrix, $\boldsymbol{E}_\xi$ is

$$\boldsymbol{E}_\xi = (\boldsymbol{e}_\xi\ \boldsymbol{e}_\eta\ \boldsymbol{e}_\zeta)\cdot\boldsymbol{H}^{-1} = \boldsymbol{E}_x \cdot \left\{\frac{\partial x^i}{\partial \xi^k}\right\}\cdot\boldsymbol{H}^{-1}, \tag{5.15}$$

where $\boldsymbol{E}_x = (\hat{\boldsymbol{e}}_x\ \hat{\boldsymbol{e}}_y\ \hat{\boldsymbol{e}}_z)$, and

$$\boldsymbol{H} = \begin{pmatrix} h_1 & 0 & 0 \\ 0 & h_2 & 0 \\ 0 & 0 & h_3 \end{pmatrix}. \tag{5.16}$$

The vector $\frac{1}{h_k}\boldsymbol{e}_k$ is unit vector and orthogonal each other, so the inverse of the $\boldsymbol{E}_\xi$ is $\boldsymbol{E}_\xi^T$.

$$\left(\boldsymbol{E}_x \cdot \left\{\frac{\partial x^i}{\partial \xi^k}\right\}\cdot\boldsymbol{H}^{-1}\right)^{-1} = \left(\boldsymbol{E}_x \cdot \left\{\frac{\partial x^i}{\partial \xi^k}\right\}\cdot\boldsymbol{H}^{-1}\right)^T,$$

$$\boldsymbol{H}\cdot\left\{\frac{\partial \xi^i}{\partial x^k}\right\}\cdot\boldsymbol{E}_x^{-1} = \boldsymbol{H}^{-1}\cdot\left\{\frac{\partial x^i}{\partial \xi^k}\right\}^T\cdot\boldsymbol{E}_x^T,$$

$$\begin{aligned} \left\{\frac{\partial \xi^i}{\partial x^k}\right\} &= \boldsymbol{H}^{-2}\cdot\left\{\frac{\partial x^i}{\partial \xi^k}\right\}^T\cdot\boldsymbol{E}_x^T\cdot\boldsymbol{E}_x \\ &= \boldsymbol{H}^{-2}\cdot\left\{\frac{\partial x^k}{\partial \xi^i}\right\}. \end{aligned} \tag{5.17}$$

That is

$$\frac{\partial \xi^k}{\partial x^i} = \frac{1}{h_k^2}\frac{\partial x^i}{\partial \xi^k}. \tag{5.18}$$

5.2 Governing equations

5.2.1 Continuous equiation

Divergence of $\rho \boldsymbol{u}$ is

$$\begin{aligned}
\frac{\partial}{\partial x^i}(\rho dx^i) &= \frac{\partial \xi^k}{\partial x^i}\frac{\partial}{\partial \xi^k}\left(\rho \frac{\partial x^i}{\partial \xi^l} d\xi^l\right) \\
&= \frac{\partial \xi^k}{\partial x^i}\frac{\partial x^i}{\partial \xi^l}\frac{\partial}{\partial \xi^k}(\rho d\xi^l) + \rho d\xi^l \frac{\partial \xi^k}{\partial x^i}\frac{\partial^2 x^i}{\partial \xi^k \partial \xi^l} \\
&= \frac{\partial}{\partial \xi^k}(\rho d\xi^k) + \sum_k \frac{1}{h_k^2}\rho d\xi^l \frac{\partial x^i}{\partial \xi^k}\frac{\partial^2 x^i}{\partial \xi^k \partial \xi^l} \\
&= \frac{\partial}{\partial \xi^k}(\rho d\xi^k) + \sum_k \frac{1}{2h_k^2}\rho d\xi^l \frac{\partial}{\partial \xi^l}\left(\frac{\partial x^i}{\partial \xi^k}\right)^2 \\
&= \frac{\partial}{\partial \xi^k}(\rho d\xi^k) + \sum_k \frac{1}{2h_k^2}\rho d\xi^l \frac{\partial}{\partial \xi^l} h_k^2 \\
&= \frac{\partial}{\partial \xi^k}(\rho d\xi^k) + \sum_k \frac{1}{2}\rho d\xi^l \frac{\partial}{\partial \xi^l} \ln h_k^2 \\
&= \frac{\partial}{\partial \xi^k}(\rho d\xi^k) + \rho d\xi^k \frac{\partial}{\partial \xi^k} \ln(\prod_l h_l) \\
&= J\left\{J^{-1}\frac{\partial}{\partial \xi^k}(\rho d\xi^l) + \rho d\xi^k \frac{\partial}{\partial \xi^k} J^{-1}\right\} \\
&= J\frac{\partial}{\partial \xi^k}(J^{-1}\rho d\xi^k),
\end{aligned} \tag{5.19}$$

where J is the Jacobian of the Jacobian matrix and

$$J = \frac{1}{\prod_k h_k}. \tag{5.20}$$

The continuous equation is

$$\frac{\partial \rho}{\partial t} + J\frac{\partial}{\partial \xi^k}\frac{\rho d\xi^k}{J} = 0. \tag{5.21}$$

5.2.2 Momentum equation

$$\frac{\partial \rho d\xi^k}{\partial t} = \frac{\partial \xi^k}{\partial x^i}\frac{\partial \rho dx^i}{\partial t}. \tag{5.22}$$

Advection term

$$
\begin{aligned}
&\frac{\partial \xi^k}{\partial x^i}\frac{\partial \rho dx^i dx^j}{\partial x^j} \\
&= \frac{\partial \xi^k}{\partial x^i}\left(dx^j\frac{\partial \rho dx^i}{\partial x^j} + \rho dx^i\frac{\partial dx^j}{\partial x^j}\right) \\
&= \frac{\partial \xi^k}{\partial x^i}\left(\frac{\partial x^j}{\partial \xi^l}d\xi^l\right)\frac{\partial \xi^m}{\partial x^j}\frac{\partial}{\partial \xi^m}\left(\rho\frac{\partial x^i}{\partial \xi^n}d\xi^n\right) + \frac{\partial \xi^k}{\partial x^i}\rho\left(\frac{\partial x^i}{\partial \xi^l}d\xi^l\right)\frac{\partial \xi^m}{\partial x^j}\frac{\partial}{\partial \xi^m}\left(\frac{\partial x^j}{\partial \xi^n}d\xi^n\right) \\
&= d\xi^l\frac{\partial \xi^k}{\partial x^i}\frac{\partial}{\partial \xi^l}\left(\rho\frac{\partial x^i}{\partial \xi^n}d\xi^n\right) + \rho d\xi^k\frac{\partial \xi^m}{\partial x^j}\frac{\partial}{\partial \xi^m}\left(\frac{\partial x^j}{\partial \xi^n}d\xi^n\right) \\
&= d\xi^l\frac{\partial \xi^k}{\partial x^i}\left\{\frac{\partial x^i}{\partial \xi^n}\frac{\partial}{\partial \xi^l}\left(\rho d\xi^n\right) + \rho d\xi^n\frac{\partial^2 x^i}{\partial \xi^l \partial \xi^n}\right\} + \rho d\xi^k\frac{\partial \xi^m}{\partial x^j}\left(\frac{\partial x^j}{\partial \xi^n}\frac{\partial d\xi^n}{\partial \xi^m} + d\xi^n\frac{\partial^2 x^j}{\partial \xi^m \partial \xi^n}\right) \\
&= d\xi^l\frac{\partial}{\partial \xi^l}\left(\rho d\xi^k\right) + \rho d\xi^l d\xi^n\frac{\partial \xi^k}{\partial x^i}\frac{\partial^2 x^i}{\partial \xi^l \partial \xi^n} + \rho d\xi^k\frac{\partial d\xi^m}{\partial \xi^m} + \rho d\xi^k d\xi^n\frac{\partial \xi^m}{\partial x^j}\frac{\partial^2 x^j}{\partial \xi^m \partial \xi^n} \\
&= \frac{\partial}{\partial \xi^l}\left(\rho d\xi^k d\xi^l\right) + \rho d\xi^l d\xi^n\frac{\partial \xi^k}{\partial x^i}\frac{\partial^2 x^i}{\partial \xi^l \partial \xi^n} + \rho d\xi^k d\xi^l\frac{\partial \xi^m}{\partial x^i}\frac{\partial^2 x^i}{\partial \xi^l \partial \xi^m} \\
&= J\left\{J^{-1}\frac{\partial}{\partial \xi^l}(\rho d\xi^k d\xi^l) + \rho d\xi^k d\xi^l\frac{\partial J^{-1}}{\partial \xi^l}\right\} + \rho d\xi^l d\xi^m\frac{\partial \xi^k}{\partial x^i}\frac{\partial^2 x^i}{\partial \xi^l \partial \xi^m} \\
&= J\frac{\partial}{\partial \xi^l}J^{-1}\rho d\xi^k d\xi^l + \rho d\xi^l d\xi^m\Gamma^k_{lm},
\end{aligned}
\tag{5.23}
$$

where Γ is the Christoffel symbols of the second kind, and

$$
\begin{aligned}
\Gamma^k_{lm} &= \frac{\partial \xi^k}{\partial x^i}\frac{\partial^2 x^i}{\partial \xi^l \partial \xi^m} \\
&= \frac{1}{2}g^{kn}\left(\frac{\partial g_{mn}}{\partial \xi^l} + \frac{\partial g_{ln}}{\partial \xi^m} - \frac{\partial g_{lm}}{\partial \xi^n}\right) \\
&= \frac{1}{h_k^2}\left(h_k\frac{\partial h_k}{\partial \xi^l}\delta_{km} + h_k\frac{\partial h_k}{\partial \xi^m}\delta_{kl} - h_l\frac{\partial h_l}{\partial \xi^k}\delta_{lm}\right),
\end{aligned}
\tag{5.24}
$$

where $\{g^{kn}\}$ is inverse matrix of $\{g_{kn}\}$.

Coriolis term

$$
\frac{\partial \xi^k}{\partial x^i}\epsilon^{ijp}f^j\rho dx^p = \epsilon^{klm}\frac{1}{h_k h_l h_m}\hat{f}^l d\xi^m,
\tag{5.25}
$$

where ϵ is the Levi-Civita symbol, and

$$
\hat{f}^l = \frac{\partial \xi^l}{\partial x^j}f^j.
\tag{5.26}
$$

Pressure gradient term

$$
\begin{aligned}
\frac{\partial \xi^k}{\partial x^i}\frac{\partial p}{\partial x^i} &= \frac{\partial \xi^k}{\partial x^i}\left(\frac{\partial \xi^l}{\partial x^i}\frac{\partial p}{\partial \xi^l}\right) \\
&= \frac{1}{h_k^2}\frac{\partial x^i}{\partial \xi^k}\frac{\partial \xi^l}{\partial x^i}\frac{\partial p}{\partial \xi^l} \\
&= \frac{1}{h_k^2}\frac{\partial p}{\partial \xi^k}.
\end{aligned}
\tag{5.27}
$$

After all, momentum equation is

$$\frac{\partial}{\partial t}\rho d\xi^k + J\frac{\partial}{\partial \xi^l}\left(J^{-1}\rho d\xi^k d\xi^l\right) + \rho d\xi^l d\xi^m \Gamma^k_{lm} + \epsilon^{klm}\frac{1}{h_k h_l h_m}\hat{f}^l \rho d\xi^m = -\frac{1}{h_k^2}\frac{\partial p}{\partial \xi^k} + \rho g^p \frac{\partial \xi^k}{\partial x^p}. \tag{5.28}$$

5.3 Map factor

We introduce Map factor m, n.

$$\frac{1}{m}\frac{a+z}{a} = h_1, \tag{5.29}$$

$$\frac{1}{n}\frac{a+z}{a} = h_2, \tag{5.30}$$

$$1 = h_3, \tag{5.31}$$

where is a is radius of the planet. Assuming shallow atmospher,

$$m = h_1^{-1}, \tag{5.32}$$

$$n = h_2^{-1}. \tag{5.33}$$

Normalized velocity is defined as

$$\hat{u} = h_1\frac{d\xi}{dt} = \frac{1}{m}\frac{d\xi}{dt}, \tag{5.34}$$

$$\hat{v} = h_2\frac{d\eta}{dt} = \frac{1}{n}\frac{d\eta}{dt}, \tag{5.35}$$

$$\hat{w} = h_3\frac{d\zeta}{dt} = \frac{d\zeta}{dt}. \tag{5.36}$$

The continuous equation becomes

$$\frac{\partial \rho}{\partial t} + mn\frac{\partial}{\partial \xi}\frac{\rho\hat{u}}{n} + mn\frac{\partial}{\partial \eta}\frac{\rho\hat{v}}{m} + \frac{\partial}{\partial \zeta}\rho\hat{w} = 0 \tag{5.37}$$

The momentum equations are

$$\begin{aligned}\frac{\partial \rho\hat{u}^k}{\partial t} &+ mn\frac{\partial}{\partial \xi}\frac{\rho\hat{u}\hat{u}^k}{n} + mn\frac{\partial}{\partial \eta}\frac{\rho\hat{v}\hat{u}^k}{m} + \frac{\partial}{\partial \zeta}\rho\hat{w}\hat{u}^k \\ &- mm_k\rho\hat{u}\hat{u}^k\frac{\partial}{\partial \xi}\frac{1}{m_k} - nm_k\rho\hat{v}\hat{u}^k\frac{\partial}{\partial \eta}\frac{1}{m_k} \\ &+ mm_k\rho\hat{u}^2\frac{\partial}{\partial \xi^k}\frac{1}{m} + nm_k\rho\hat{v}^2\frac{\partial}{\partial \xi^k}\frac{1}{n} + \epsilon^{klm}m_l\hat{f}^l\rho\hat{u}^m \\ &= -m_k\frac{\partial p}{\partial \zeta^k} + \rho g\delta_{3k}.\end{aligned} \tag{5.38}$$

This equation may also be written as

$$\frac{\partial \rho u}{\partial t} + mn\frac{\partial}{\partial \xi}\frac{\rho u u}{n} + mn\frac{\partial}{\partial \eta}\frac{\rho u v}{m} + \frac{\partial}{\partial \zeta}\rho u w$$
$$- f\rho v + mn\rho v\left\{v\frac{\partial}{\partial \xi}\left(\frac{1}{n}\right) - u\frac{\partial}{\partial \eta}\left(\frac{1}{m}\right)\right\} = -m\frac{\partial p}{\partial \xi}, \tag{5.39}$$

$$\frac{\partial \rho v}{\partial t} + mn\frac{\partial}{\partial \xi}\frac{\rho u v}{n} + mn\frac{\partial}{\partial \eta}\frac{\rho v v}{m} + \frac{\partial}{\partial \zeta}\rho v w$$
$$+ f\rho u - mn\rho u\left\{v\frac{\partial}{\partial \xi}\left(\frac{1}{n}\right) - u\frac{\partial}{\partial \eta}\left(\frac{1}{m}\right)\right\} = -n\frac{\partial p}{\partial \eta}, \tag{5.40}$$

$$\frac{\partial \rho w}{\partial t} + mn\frac{\partial}{\partial \xi}\frac{\rho u w}{n} + mn\frac{\partial}{\partial \eta}\frac{\rho v w}{m} + \frac{\partial}{\partial \zeta}\rho w w = -\frac{\partial p}{\partial \zeta} - \rho g. \tag{5.41}$$

The thermodynamical and tracer equations

$$\frac{\partial \rho \phi}{\partial t} + mn\frac{\partial}{\partial \xi}\frac{\rho \hat{u}\phi}{n} + mn\frac{\partial}{\partial \eta}\frac{\rho \hat{v}\phi}{m} + \frac{\partial \rho \hat{w}\phi}{\partial \zeta} = 0. \tag{5.42}$$

Chapter 6

Horizontal explicit virtical implicit

Corresponding author : Seiya Nishizawa

6.1 Equations

$$\frac{\partial G^{\frac{1}{2}}\rho}{\partial t} = -\frac{\partial J_{33} G^{\frac{1}{2}}\rho w}{\partial \xi} + G^{\frac{1}{2}} S_{\rho}, \tag{6.1}$$

$$\frac{\partial G^{\frac{1}{2}}\rho w}{\partial t} = -\frac{\partial J_{33} G^{\frac{1}{2}} p}{\partial \xi} - G^{\frac{1}{2}}\rho g + G^{\frac{1}{2}} S_{\rho w}, \tag{6.2}$$

$$\frac{\partial G^{\frac{1}{2}}\rho\theta}{\partial t} = -\frac{\partial J_{33} G^{\frac{1}{2}}\rho w\theta}{\partial \xi} + G^{\frac{1}{2}} S_{\rho\theta}, \tag{6.3}$$

$$p = P_{00}\left(\frac{R\rho\theta}{P_{00}}\right)^{c_p/c_v}, \tag{6.4}$$

where

$$\begin{aligned} G^{\frac{1}{2}} S_{\rho} &= -G^{\frac{1}{2}}\frac{\partial \rho u}{\partial x} - G^{\frac{1}{2}}\frac{\partial \rho v}{\partial y} \\ &= -\frac{\partial G^{\frac{1}{2}}\rho u}{\partial x^*} - \frac{\partial G^{\frac{1}{2}}\rho v}{\partial y^*} - \frac{\partial J_{13} G^{\frac{1}{2}}\rho u + J_{23} G^{\frac{1}{2}}\rho v}{\partial \xi}, \end{aligned} \tag{6.5}$$

$$\begin{aligned} G^{\frac{1}{2}} S_{\rho w} &= -G^{\frac{1}{2}}\frac{\partial u\rho w}{\partial x} - G^{\frac{1}{2}}\frac{\partial v\rho w}{\partial y} - G^{\frac{1}{2}}\frac{\partial w\rho w}{\partial z} \\ &= -\frac{\partial G^{\frac{1}{2}} u\rho w}{\partial x^*} - \frac{\partial G^{\frac{1}{2}} v\rho w}{\partial y^*} - \frac{\partial}{\partial \xi}(J_{13} G^{\frac{1}{2}} u\rho w + J_{23} G^{\frac{1}{2}} v\rho w + J_{33} G^{\frac{1}{2}} w\rho w), \end{aligned} \tag{6.6}$$

$$\begin{aligned} G^{\frac{1}{2}} S_{\rho\theta} &= -G^{\frac{1}{2}}\frac{\partial u\rho\theta}{\partial x} - G^{\frac{1}{2}}\frac{\partial v\rho\theta}{\partial y} \\ &= -\frac{\partial G^{\frac{1}{2}} u\rho\theta}{\partial x^*} - \frac{\partial G^{\frac{1}{2}} v\rho\theta}{\partial y^*} - \frac{\partial J_{13} G^{\frac{1}{2}} u\rho\theta + J_{23} G^{\frac{1}{2}} v\rho\theta}{\partial \xi}. \end{aligned} \tag{6.7}$$

6.2 Descritization

For the temporal discritization, backward temporal integrations are employed for the terms related to acoustic wave in vertical direction.

$$\frac{\rho^{n+1}-\rho^n}{\Delta t} = -G^{-\frac{1}{2}}\frac{\partial}{\partial\xi}\{J_{33}G^{\frac{1}{2}}(\rho w)^{n+1}\} + S_\rho^n, \tag{6.8}$$

$$\frac{(\rho w)^{n+1}-(\rho w)^n}{\Delta t} = -G^{-\frac{1}{2}}\frac{\partial}{\partial\xi}(J_{33}G^{\frac{1}{2}}p^{n+1}) - g\rho^{n+1} + S_{\rho w}^n, \tag{6.9}$$

$$\frac{p^{n+1}-p^n}{\Delta t} = \frac{c_p^n}{c_v^n}\frac{p^n}{(\rho\theta)^n}\frac{\partial\rho\theta}{\partial t}, \tag{6.10}$$

$$\frac{\partial\rho\theta}{\partial t} = -G^{-\frac{1}{2}}\frac{\partial}{\partial\xi}\{J_{33}G^{\frac{1}{2}}\theta^n(\rho w)^{n+1}\} + S_{\rho\theta}^n. \tag{6.11}$$

Note that the potential temperature at previous step, θ^n, is used.

Eliminating $p^{n+1}, (\rho\theta)^{n+1}$, and ρ^{n+1}, the Helmholtz equation for $(\rho w)^{n+1}$ is obtained:

$$\begin{aligned}
&(\rho w)^{n+1} - \frac{\Delta t^2 g}{G^{\frac{1}{2}}}\frac{\partial}{\partial\xi}\{J_{33}G^{\frac{1}{2}}(\rho w)^{n+1}\} - \frac{\Delta t^2}{G^{\frac{1}{2}}}\frac{\partial}{\partial\xi}\left(J_{33}\frac{c_p^n p^n}{c_v^n(\rho\theta)^n}\frac{\partial J_{33}G^{\frac{1}{2}}\theta^n(\rho w)^{n+1}}{\partial\xi}\right)\\
&= (\rho w)^n - \frac{\Delta t}{G^{\frac{1}{2}}}\frac{\partial}{\partial\xi}\left\{J_{33}G^{\frac{1}{2}}p^n\left(1+\frac{\Delta t c_p^n S_{\rho\theta}^n}{c_v^n(\rho\theta)^n}\right)\right\} - \Delta t g(\rho^n + \Delta t S_\rho^n) + \Delta t S_{\rho w}^n.
\end{aligned} \tag{6.12}$$

Vertical differencials are discritized as follows:

$$\begin{aligned}
&(\rho w)_{k+1/2}^{n+1} - \frac{\Delta t^2 g}{(\Delta z_{k+1}+\Delta z_k)G_{k+1/2}^{\frac{1}{2}}}\left\{J_{33}G^{\frac{1}{2}}(\rho w)_{k+3/2}^{n+1} - J_{33}G^{\frac{1}{2}}(\rho w)_{k-1/2}^{n+1}\right\}\\
&- \frac{\Delta t^2}{\Delta z_{k+1/2}G_{k+1/2}^{\frac{1}{2}}}\left\{\left(J_{33}\frac{c_p p}{c_v\rho\theta}\right)_{k+1}\frac{J_{33}G^{\frac{1}{2}}(\rho w)_{k+3/2}\hat{\theta}_{k+3/2} - J_{33}G^{\frac{1}{2}}(\rho w)_{k+1/2}\hat{\theta}_{k+1/2}}{\Delta z_{k+1}}\right.\\
&\qquad\left. - \left(J_{33}\frac{c_p p}{c_v\rho\theta}\right)_k\frac{J_{33}G^{\frac{1}{2}}(\rho w)_{k+1/2}\hat{\theta}_{k+1/2} - J_{33}G^{\frac{1}{2}}(\rho w)_{k-1/2}\hat{\theta}_{k-1/2}}{\Delta z_k}\right\}\\
&= (\rho w)_{k+1/2}^n\\
&- \frac{\Delta t}{\Delta z_{k+1/2}G_{k+1/2}^{\frac{1}{2}}}\left\{J_{33}G^{\frac{1}{2}}p_{k+1}\left(1+\frac{\Delta t c_p S_{\rho\theta}}{c_v\rho\theta}\right)_{k+1} - J_{33}G^{\frac{1}{2}}p_k\left(1+\frac{\Delta t c_p S_{\rho\theta}}{c_v\rho\theta}\right)_k\right\}\\
&- \frac{\Delta t g}{2}\{(\rho+\Delta t S_\rho)_{k+1} + (\rho+\Delta t S_\rho)_k\} + \Delta t S_{\rho w},
\end{aligned} \tag{6.13}$$

where

$$\hat{\theta}_{k+1/2} = \frac{1}{12}\left(-\theta_{k+2} + 7\theta_{k+1} + 7\theta_k - \theta_{k-1}\right). \tag{6.14}$$

Finally we obtained

$$
\begin{aligned}
&- \frac{1}{G^{\frac{1}{2}}_{k+1/2}} \left\{ \frac{\hat{\theta}_{k+3/2}}{\Delta z_{k+1/2}} A_{k+1} + B_{k+1/2} \right\} (\rho w)^{n+1}_{k+3/2} && (6.15)\\
&+ \left\{ 1 + \frac{\hat{\theta}_{k+1/2}}{\Delta z_{k+1/2} G^{\frac{1}{2}}_{k+1/2}} (A_{k+1} + A_k) \right\} (\rho w)^{n+1}_{k+1/2} && (6.16)\\
&- \frac{1}{G^{\frac{1}{2}}_{k+1/2}} \left\{ \frac{\hat{\theta}_{k-1/2}}{\Delta z_{k+1/2}} A_k - B_{k+1/2} \right\} (\rho w)^{n+1}_{k-1/2} && (6.17)\\
&= C_{k+1/2}, && (6.18)
\end{aligned}
$$

where

$$
\begin{aligned}
A_k &= \frac{\Delta t^2 J_{33} G^{\frac{1}{2}}}{\Delta z_k} \left(J_{33} \frac{c_p p}{c_v \rho \theta} \right)_k , && (6.19)\\
B_{k+1/2} &= \frac{\Delta t^2 g J_{33} G^{\frac{1}{2}}}{\Delta z_{k+1} + \Delta z_k}, && (6.20)\\
C_{k+1/2} &= (\rho w)^n_{k+1/2} \\
&\quad - \Delta t \frac{J_{33} G^{\frac{1}{2}} p_{k+1} \left(1 + \Delta t \frac{c_p S_{\rho\theta}}{c_v \rho \theta} \right)_{k+1} - J_{33} G^{\frac{1}{2}} p_k \left(1 + \Delta t \frac{c_p S_{\rho\theta}}{c_v \rho \theta} \right)_k}{\Delta z_{k+1/2} G^{\frac{1}{2}}_{k+1/2}} \\
&\quad - \Delta t g \frac{(\rho + \Delta t S_\rho)_{k+1} + (\rho + \Delta t S_\rho)_k}{2} + \Delta t S_{\rho w}. && (6.21)
\end{aligned}
$$

Chapter 7

Horizontally and virtically implicit

Corresponding author : Seiya Nishizawa

7.1 Equations

The governing equation is the followings:

$$\frac{\partial G^{\frac{1}{2}}\rho'}{\partial t} = -\frac{\partial G^{\frac{1}{2}}\rho u}{\partial x^*} - \frac{\partial G^{\frac{1}{2}}\rho v}{\partial y^*} - \frac{\partial J_{33}G^{\frac{1}{2}}\rho w}{\partial \xi} + G^{\frac{1}{2}}S_\rho, \tag{7.1}$$

$$\frac{\partial G^{\frac{1}{2}}\rho u}{\partial t} = -\frac{\partial G^{\frac{1}{2}}p'}{\partial x^*} + G^{\frac{1}{2}}S_{\rho u}, \tag{7.2}$$

$$\frac{\partial G^{\frac{1}{2}}\rho v}{\partial t} = -\frac{\partial G^{\frac{1}{2}}p'}{\partial y^*} + G^{\frac{1}{2}}S_{\rho v}, \tag{7.3}$$

$$\frac{\partial G^{\frac{1}{2}}\rho w}{\partial t} = -\frac{\partial J_{33}G^{\frac{1}{2}}p'}{\partial \xi} - G^{\frac{1}{2}}\rho' g + G^{\frac{1}{2}}S_{\rho w}, \tag{7.4}$$

$$\frac{\partial G^{\frac{1}{2}}\rho\theta}{\partial t} = -\frac{\partial G^{\frac{1}{2}}u\rho\theta}{\partial x^*} - \frac{\partial G^{\frac{1}{2}}v\rho\theta}{\partial y^*} - \frac{\partial J_{33}G^{\frac{1}{2}}w\rho\theta}{\partial \xi} + G^{\frac{1}{2}}S_{\rho\theta}, \tag{7.5}$$

$$p = P_{00}\left(\frac{R\rho\theta}{P_{00}}\right)^{c_p/c_v}, \tag{7.6}$$

where

$$G^{\frac{1}{2}}S_\rho = -\frac{\partial J_{13}G^{\frac{1}{2}}\rho u + J_{23}G^{\frac{1}{2}}\rho v}{\partial \xi}, \tag{7.7}$$

$$G^{\frac{1}{2}}S_{\rho u} = -\frac{\partial G^{\frac{1}{2}}u\rho u}{\partial x^*} - \frac{\partial G^{\frac{1}{2}}v\rho u}{\partial y^*} - \frac{\partial}{\partial \xi}(J_{13}G^{\frac{1}{2}}u\rho u + J_{23}G^{\frac{1}{2}}v\rho u + J_{33}G^{\frac{1}{2}}w\rho u) - \frac{\partial}{\partial \xi}(J_{13}G^{\frac{1}{2}}p'), \tag{7.8}$$

$$G^{\frac{1}{2}}S_{\rho v} = -\frac{\partial G^{\frac{1}{2}}u\rho v}{\partial x^*} - \frac{\partial G^{\frac{1}{2}}v\rho v}{\partial y^*} - \frac{\partial}{\partial \xi}(J_{13}G^{\frac{1}{2}}u\rho v + J_{23}G^{\frac{1}{2}}v\rho v + J_{33}G^{\frac{1}{2}}w\rho v), - \frac{\partial}{\partial \xi}(J_{23}G^{\frac{1}{2}}p'), \tag{7.9}$$

$$G^{\frac{1}{2}}S_{\rho w} = -\frac{\partial G^{\frac{1}{2}}u\rho w}{\partial x^*} - \frac{\partial G^{\frac{1}{2}}v\rho w}{\partial y^*} - \frac{\partial}{\partial \xi}(J_{13}G^{\frac{1}{2}}u\rho w + J_{23}G^{\frac{1}{2}}v\rho w + J_{33}G^{\frac{1}{2}}w\rho w), \tag{7.10}$$

$$G^{\frac{1}{2}}S_{\rho\theta} = -\frac{\partial J_{13}G^{\frac{1}{2}}u\rho\theta + J_{23}G^{\frac{1}{2}}v\rho\theta}{\partial \xi}. \tag{7.11}$$

Prime describes deviation from a reference state, and the reference state depends only z and satisfies in hydrostatic barance:

$$p' = p - \bar{p}, \tag{7.12}$$

$$\rho' = \rho - \bar{\rho}, \tag{7.13}$$

$$\frac{d\bar{p}(z)}{dz} = -\bar{\rho}(z)g. \tag{7.14}$$

7.2 Descritization

For the temporal discritization, backward temporal integrations are employed for the terms related to acoustic wave.

$$\frac{\rho'^{n+1} - \rho'^n}{\Delta t} = -G^{-\frac{1}{2}}\frac{\partial}{\partial x^*}\{G^{\frac{1}{2}}(\rho u)^{n+1}\} - G^{-\frac{1}{2}}\frac{\partial}{\partial y^*}\{G^{\frac{1}{2}}(\rho v)^{n+1}\} - G^{-\frac{1}{2}}\frac{\partial}{\partial \xi}\{J_{33}G^{\frac{1}{2}}(\rho w)^{n+1}\} + S^n_\rho, \tag{7.15}$$

$$\frac{(\rho u)^{n+1} - (\rho u)^n}{\Delta t} = -G^{-\frac{1}{2}}\frac{\partial}{\partial x^*}(G^{\frac{1}{2}}p'^{n+1}) + S^n_{\rho u}, \tag{7.16}$$

$$\frac{(\rho v)^{n+1} - (\rho v)^n}{\Delta t} = -G^{-\frac{1}{2}}\frac{\partial}{\partial y^*}(G^{\frac{1}{2}}p'^{n+1}) + S^n_{\rho v}, \tag{7.17}$$

$$\frac{(\rho w)^{n+1} - (\rho w)^n}{\Delta t} = -G^{-\frac{1}{2}}\frac{\partial}{\partial \xi}(J_{33}G^{\frac{1}{2}}p'^{n+1}) - g\rho'^{n+1} + S^n_{\rho w}, \tag{7.18}$$

$$\frac{p'^{n+1} - p'^n}{\Delta t} = P_{00}\left(\frac{R}{P_{00}}\right)^{\kappa^n}\kappa^n(\rho\theta)^{n\kappa^n - 1}\frac{\partial \rho\theta}{\partial t} = \kappa^n\frac{p^n}{(\rho\theta)^n}\frac{\partial \rho\theta}{\partial t}, \tag{7.19}$$

$$\frac{\partial \rho\theta}{\partial t} = -G^{-\frac{1}{2}}\frac{\partial}{\partial x^*}\{G^{\frac{1}{2}}\theta^n(\rho u)^{n+1}\} - G^{-\frac{1}{2}}\frac{\partial}{\partial y^*}\{G^{\frac{1}{2}}\theta^n(\rho v)^{n+1}\} - G^{-\frac{1}{2}}\frac{\partial}{\partial \xi}\{J_{33}G^{\frac{1}{2}}\theta^n(\rho w)^{n+1}\} + S^n_{\rho\theta}, \tag{7.20}$$

where $\kappa = c_p/c_v$. Note that the potential temperature at previous step, θ^n, is used.

In order to obtain Helmholtz equation, a linearlized equation for the density is used instead of Eq. 7.15.

$$\rho'^{n+1} \sim \rho'^n + \frac{1}{\kappa^n}\frac{\rho^n}{p^n}\left\{p'^{n+1} - p'^n\right\}. \tag{7.21}$$

Here we assume that the potential temperature does not change during a temporal step due to acoustic wave.

Eliminating $(\rho u)^{n+1}, (\rho v)^{n+1}(\rho w)^{n+1},$, and ρ'^{n+1}, the Helmholtz equation for p'^{n+1} is obtained.

$$\begin{aligned}
&\frac{\partial}{\partial x^*}\left(\theta^n \frac{\partial G^{\frac{1}{2}} p'^{n+1}}{\partial x^*}\right) + \frac{\partial}{\partial y^*}\left(\theta^n \frac{\partial G^{\frac{1}{2}} p'^{n+1}}{\partial y^*}\right) + \frac{\partial}{\partial \xi}\left(J_{33}\theta^n \frac{\partial J_{33} G^{\frac{1}{2}} p'^{n+1}}{\partial \xi}\right) \\
&+ g\frac{\partial}{\partial \xi}\left(\frac{J_{33} G^{\frac{1}{2}} \theta^n p'^{n+1}}{C_s^{2n}}\right) - \frac{G^{\frac{1}{2}}\theta^n p'^{n+1}}{\Delta t^2 C_s^{2n}} \\
&= \frac{1}{\Delta t}\left[\frac{\partial G^{\frac{1}{2}}\theta^n\left\{(\rho u)^n + \Delta t S^n_{\rho u}\right\}}{\partial x^*} + \frac{\partial G^{\frac{1}{2}}\theta^n\left\{(\rho v)^n + \Delta t S^n_{\rho v}\right\}}{\partial y^*} + \frac{\partial J_{33} G^{\frac{1}{2}}\theta^n\left\{(\rho w)^n + \Delta t S^n_{\rho w}\right\}}{\partial \xi}\right] \\
&\quad + g\frac{\partial}{\partial \xi}\left\{\frac{J_{33} G^{\frac{1}{2}}\theta^n p'^n}{C_s^{2n}} - J_{33} G^{\frac{1}{2}}(\rho'\theta)^n\right\} + \frac{G^{\frac{1}{2}} S_{\rho\theta}}{\Delta t} - \frac{G^{\frac{1}{2}}\theta^n p'^n}{\Delta t^2 C_s^{2n}},
\end{aligned} \tag{7.22}$$

where

$$C_s^2 = \kappa\frac{p}{\rho}. \tag{7.23}$$

Spatial differentials are descritized.

$$
\begin{aligned}
&\frac{1}{\Delta x_i}\left(\hat{\theta}_{i+1/2}\frac{(G^{\frac{1}{2}}p'^{n+1})_{i+1}-G^{\frac{1}{2}}p'^{n+1}}{\Delta x_{i+1/2}}-\hat{\theta}_{i-1/2}\frac{G^{\frac{1}{2}}p'^{n+1}-(G^{\frac{1}{2}}p'^{n+1})_{i-1}}{\Delta x_{i-1/2}}\right)\\
&+\frac{1}{\Delta y_j}\left(\hat{\theta}_{j+1/2}\frac{(G^{\frac{1}{2}}p'^{n+1})_{j+1}-G^{\frac{1}{2}}p'^{n+1}}{\partial y_{j+1/2}}-\hat{\theta}_{j-1/2}\frac{G^{\frac{1}{2}}p'^{n+1}-(G^{\frac{1}{2}}p'^{n+1})_{j-1}}{\partial y_{j-1/2}}\right)\\
&+\frac{1}{\Delta z_k}\left\{(J_{33})_{k+1/2}\hat{\theta}_{k+1/2}\frac{J_{33}G^{\frac{1}{2}}p'^{n+1}_{k+1}-J_{33}G^{\frac{1}{2}}p'^{n+1}}{\Delta z_{k+1/2}}-(J_{33})_{k-1/2}\hat{\theta}_{k-1/2}\frac{J_{33}G^{\frac{1}{2}}p'^{n+1}-J_{33}G^{\frac{1}{2}}p'^{n+1}_{k-1}}{\Delta z_{k-1/2}}\right)\\
&+g\frac{1}{\Delta_{k+1/2}+\Delta z_{k-1/2}}\left\{\frac{J_{33}G^{\frac{1}{2}}\theta p'^{n+1}_{k+1}}{C^2_{sk+1}}-\frac{J_{33}G^{\frac{1}{2}}\theta p'^{n+1}_{k-1}}{C^2_{sk-1}}\right\}-\frac{G^{\frac{1}{2}}\theta p'^{n+1}}{\Delta t^2C_s^2}\\
&=\frac{1}{\Delta t}\left[\frac{G^{\frac{1}{2}}_{i+1/2}\hat{\theta}_{i+1/2}\left\{(\rho u)_{i+1/2}+\Delta t(S_{\rho u})_{i+1/2}\right\}-G^{\frac{1}{2}}_{i-1/2}\hat{\theta}_{i-1/2}\left\{(\rho u)_{i-1/2}+\Delta t(S_{\rho u})_{i-1/2}\right\}}{\Delta x_i}\right.\\
&+\frac{G^{\frac{1}{2}}_{j+1/2}\hat{\theta}_{j+1/2}\left\{(\rho v)_{j+1/2}+\Delta t(S_{\rho v})_{j+1/2}\right\}-G^{\frac{1}{2}}_{j-1/2}\hat{\theta}_{j-1/2}\left\{(\rho v)_{j-1/2}+\Delta t'S_{\rho v})_{j-1/2}\right\}}{\Delta y_j}\\
&\left.+\frac{J_{33}G^{\frac{1}{2}}\hat{\theta}_{k+1/2}\left\{(\rho w)_{k+1/2}+\Delta t(S_{\rho w})_{k+1/2}\right\}-J_{33}G^{\frac{1}{2}}\hat{\theta}_{k-1/2}\left\{(\rho w)_{k-1/2}+\Delta t(S_{\rho w})_{k-1/2}\right\}}{\Delta z_k}\right]\\
&\quad+g\frac{1}{\Delta z_{k+1/2}+\Delta z_{k-1/2}}\left\{\frac{J_{33}G^{\frac{1}{2}}\theta p'^n_{k+1}}{C^2_{sk+1}}-\frac{J_{33}G^{\frac{1}{2}}\theta p'^n_{k-1}}{C^2_{sk-1}}-J_{33}G^{\frac{1}{2}}\{(\rho'\theta)_{k+1}-(\rho'\theta)_{k-1}\}\right\}\\
&+\frac{G^{\frac{1}{2}}S_{\rho\theta}}{\Delta t}-\frac{G^{\frac{1}{2}}\theta p'^n}{\Delta t^2C_s^2}. \qquad (7.24)
\end{aligned}
$$

Chapter 8

The physical parameterization

8.1 Turbulence

Correnspoinding author : Seiya Nishizawa

8.1.1 Spatial filter

The governing euqations are the followings:

$$\frac{\partial \rho}{\partial t} + \frac{\partial u_i \rho}{\partial x_i} = 0 \tag{8.1}$$

$$\frac{\partial \rho u_i}{\partial t} + \frac{\partial u_j \rho u_i}{\partial x_j} = -\frac{\partial p}{\partial x_i} + g\rho\delta_{i3} \tag{8.2}$$

$$\frac{\partial \rho \theta}{\partial t} + \frac{\partial u_i \rho \theta}{\partial x_i} = Q \tag{8.3}$$

Spatial filtering the continuity equation yields

$$\frac{\partial \overline{\rho}}{\partial t} + \frac{\partial \overline{u_i \rho}}{\partial x_i} = 0, \tag{8.4}$$

where $\overline{\phi}$ means the spatial filtered quantity of an arbitrary variable ϕ. The Favre filtering (Favre, 1983) defined by

$$\widetilde{\phi} = \frac{\overline{\rho\phi}}{\overline{\rho}} \tag{8.5}$$

makes the equation (8.4)

$$\frac{\partial \overline{\rho}}{\partial t} + \frac{\partial \widetilde{u}_i \overline{\rho}}{\partial x_i} = 0. \tag{8.6}$$

The momentam equations become

$$\frac{\partial \overline{\rho u_i}}{\partial t} + \frac{\partial \overline{u_j \rho u_i}}{\partial x_j} = -\frac{\partial \overline{p}}{\partial x_i} + \overline{\rho} g \delta_{i3} \tag{8.7}$$

$$\frac{\partial \overline{\rho}\widetilde{u_i}}{\partial t} + \frac{\partial \widetilde{u_j}\,\overline{\rho}\widetilde{u_i}}{\partial x_j} = -\frac{\partial \overline{p}}{\partial x_i} + g\overline{\rho}\delta_{i3} - \frac{\partial}{\partial x_j}\left(\overline{u_i \rho u_j} - \widetilde{u_j}\overline{\rho}\widetilde{u_i}\right) \tag{8.8}$$

$$\frac{\partial \overline{\rho}\widetilde{u_i}}{\partial t} + \frac{\partial \widetilde{u_j}\,\overline{\rho}\widetilde{u_i}}{\partial x_j} = -\frac{\partial \overline{p}}{\partial x_i} + g\overline{\rho}\delta_{i3} - \frac{\partial}{\partial x_j}\overline{\rho}\left(\widetilde{u_i u_j} - \widetilde{u_j}\widetilde{u_i}\right). \tag{8.9}$$

As the same matter, the thermal equation becomes

$$\frac{\partial \overline{\rho}\widetilde{\theta}}{\partial t} + \frac{\partial \widetilde{u_i}\overline{\rho}\widetilde{\theta}}{\partial x_i} = Q - \frac{\partial}{\partial x_i}\overline{\rho}\left(\widetilde{u_i\theta} - \widetilde{u_i}\widetilde{\theta}\right). \tag{8.10}$$

Then, the govering equations for the prognositic variables ($\overline{\rho}, \overline{\rho}\widetilde{u_i}$, and $\overline{\rho}\widetilde{\theta}$) are

$$\frac{\partial \overline{\rho}}{\partial t} + \frac{\partial \widetilde{u_i}\overline{\rho}}{\partial x_i} = 0, \tag{8.11}$$

$$\frac{\partial \overline{\rho}\widetilde{u_i}}{\partial t} + \frac{\partial \widetilde{u_j}\overline{\rho}\widetilde{u_i}}{\partial x_j} = -\frac{\partial \overline{p}}{\partial x_i} + g\overline{\rho}\delta_{i3} - \frac{\partial \overline{\rho}\tau_{ij}}{\partial x_j}, \tag{8.12}$$

$$\frac{\partial \overline{\rho}\widetilde{\theta}}{\partial t} + \frac{\partial \widetilde{u_i}\overline{\rho}\widetilde{\theta}}{\partial x_i} = Q - \frac{\partial \overline{\rho}\tau_i^D}{\partial x_i}, \tag{8.13}$$

where

$$\tau_{ij} = \widetilde{u_i u_j} - \widetilde{u_i}\widetilde{u_j}, \tag{8.14}$$

$$\tau_i^D = \widetilde{u_i\theta} - \widetilde{u_i}\widetilde{\theta}. \tag{8.15}$$

Hereafter, we omite overline and tilde representing spatial and the Favre filters.

8.1.2 SGS model

Smagorinsky-Lilly model

The eddy momentum flux is

$$\tau_{ij} - \frac{1}{3}\tau_{kk}\delta_{ij} = -2\nu_{SGS}\left(S_{ij} - \frac{1}{3}S_{kk}\delta_{ij}\right), \tag{8.16}$$

where S_{ij} is the strain tensor,

$$S_{ij} = \frac{1}{2}\left(\frac{\partial u_i}{\partial x_j} + \frac{\partial u_j}{\partial x_i}\right), \tag{8.17}$$

and

$$\nu_{SGS} = (C_s\lambda)^2 |S|. \tag{8.18}$$

C_s is the Smagorinsky constant, λ is a characteristic SGS length scale, and $|S|$ is scale of the tensor S,

$$|S| = \sqrt{2S_{ij}S_{ij}}. \tag{8.19}$$

Then the eddy momentum flux is

$$\tau_{ij} = -2\nu_{SGS}\left(S_{ij} - \frac{1}{3}S_{kk}\delta_{ij}\right) + \frac{2}{3}TKE\delta_{ij}, \tag{8.20}$$

where

$$TKE = \frac{1}{2}\tau_{ii} = \left(\frac{\nu_{SGS}}{C_k\lambda}\right)^2, \tag{8.21}$$

where C_k is a SGS constant and assumed to be 0.1 by following Deardorff (1980) and Moeng and Wyngaard (1988).

The eddy heat flux is

$$\tau_i^D = -D_{SGS}\frac{\partial\theta}{\partial x_i}, \tag{8.22}$$

where

$$D_{SGS} = \frac{1}{Pr}\nu_{SGS}. \tag{8.23}$$

Pr is the turbulent Prandtl number. For the other scalar constants such as water vaper, D_{SGS} is also used as their diffusivity.

To include buoyancy effects, the extension of the basic Smagorinsky developed by Brown et al. (1994) is used.

$$\nu_{SGS} = (C_s\lambda)^2|S|\sqrt{1 - Rf}, \tag{8.24}$$

where Rf is the flux Richardson number ($Rf = Ri/Pr$). Ri is the local (pointwise) gradient Richardson number,

$$Ri = \frac{N^2}{|S|^2}, \tag{8.25}$$

and N^2 is the Brunt-Visala frequency,

$$N^2 = \frac{g}{\theta}\frac{\partial\theta}{\partial z}. \tag{8.26}$$

The Prandtl number is an unknow parameter, and it depends on the Richardson number, while it is offten assumed a constant value. For the unstable conditions ($Ri < 0$),

$$\nu_{SGS} = (C_s\lambda)^2|S|\sqrt{1 - cRi}, \tag{8.27}$$

$$D_{SGS} = \frac{1}{Pr_N}(C_s\lambda)^2|S|\sqrt{1 - bRi}, \tag{8.28}$$

where Pr_N is the Prandtl number in neutral condtions. The values of c, b, Pr_N are set 16, 40, and 0.7, respectively. Then the Prandtl number is

$$Pr = Pr_N\sqrt{\frac{1 - cRi}{1 - bRi}}. \tag{8.29}$$

For the stable condtions, when the Richardson number is smaller than the critical Richardson number, $Ri_c(= 0.25)$,

$$\nu_{SGS} = (C_s\lambda)^2|S|\left(1 - \frac{Ri}{Ri_c}\right)^4, \tag{8.30}$$

$$D_{SGS} = \frac{1}{Pr_N}(C_s\lambda)^2|S|\left(1 - \frac{Ri}{Ri_c}\right)^4(1 - gRi). \tag{8.31}$$

The constant g is determined as the Prandtl number becomes 1 in the limit of $Ri \to Ri_C$ and then is $(1 - Pr_N)/Ri_c$. The Prandtl number is

$$Pr = Pr_N \left\{ 1 - (1 - Pr_N) \frac{Ri}{Ri_c} \right\}^{-1}. \tag{8.32}$$

For the strongly stable condistions ($Ri > Ri_c$), the eddy viscosity and the diffusivity for scalars are 0;

$$\nu_{SGS} = 0, \tag{8.33}$$
$$D_{SGS} = 0. \tag{8.34}$$

The Prandtl number is $Pr = 1$.

Scotti et al. (1993) suggested that the length scale should depend on the grid aspect ratio. In the equilibrium condition with the universal Kolmogorov spectrum, energy cascaded to the SGS turbulence, which equals to SGS dissipation, must not depend on grid aspect ratio. The energy flux or dissipation can be written as function of S_{ij} and the length scale, λ. The S_{ij} depends on the grid aspect ratio, so the length scale should have dependency on the aspect ratio which cancels the dependency of the S_{ij}. With some approximations, they obtained an approximate function of the length scale [1] :

$$\lambda = f(a)\Delta, \tag{8.35}$$

where $f(a)$ is a function of grid aspect ratio, a, and

$$\begin{aligned} f(a) = 1.736 a^{1/3} \{ & \\ & 4P_1(b_1)a^{1/3} + 0.222P_2(b_1)a^{-5/3} + 0.077P_3(b_1)a^{-11/3} \\ & - 3b_1 + 4P_1(b_2) + 0.222P_2(b_2) + 0.077P_3(b_2) - 3b_2 \\ & \}^{-3/4}. \end{aligned} \tag{8.36}$$

Here $b_1 = \arctan(1/a), b_2 = \arctan(a) = \pi/2 - b_1$, and

$$P_1(z) = 2.5P_2(z) - 1.5(\cos(z))^{2/3}\sin(z), \tag{8.37}$$
$$P_2(z) = 0.98z + 0.073z^2 - 0.418z^3 + 0.120z^4, \tag{8.38}$$
$$P_3(z) = 0.976z + 0.188z^2 + 1.169z^3 + 0.755z^4 - 0.151z^5. \tag{8.39}$$

For instance, $f(2) = 1.036, f(5) = 1.231, f(10) = 1.469$, and $f(20) = 1.790$. Δ is the filter length, and is defined to be proportional to $(\Delta x \Delta y \Delta z)^{1/3}$ here. In this model, we introduce a numerical filter to reduce two-grid noise discussed above. This filter reduces two-grid scale physical variability as well. This means that two-grid scale would be preferred for the filter length in this model rather than grid spacing itself, that is,

$$\Delta = 2(\Delta x \Delta y \Delta z)^{1/3}. \tag{8.40}$$

[1] They considered two grid aspect ratios, while we here think only one, i.e. $\Delta x = \Delta y$.

Terrain-following coordinate

Tendencies representing effect of the sub-grid scale turbulence with the terrain-following coordinate are following [2];

$$\frac{\partial G^{\frac{1}{2}}\rho u}{\partial t} = -\frac{\partial G^{\frac{1}{2}}\rho\tau_{11}}{\partial x^*} - \frac{\partial G^{\frac{1}{2}}\rho\tau_{12}}{\partial y^*} - \frac{\partial J_{13}G^{\frac{1}{2}}\rho\tau_{11} + J_{23}G^{\frac{1}{2}}\rho\tau_{12} + J_{33}G^{\frac{1}{2}}\rho\tau_{13}}{\partial\xi}, \tag{8.41}$$

$$\frac{\partial G^{\frac{1}{2}}\rho v}{\partial t} = -\frac{\partial G^{\frac{1}{2}}\rho\tau_{21}}{\partial x^*} - \frac{\partial G^{\frac{1}{2}}\rho\tau_{22}}{\partial y^*} - \frac{\partial J_{13}G^{\frac{1}{2}}\rho\tau_{21} + J_{23}G^{\frac{1}{2}}\rho\tau_{22} + J_{33}G^{\frac{1}{2}}\rho\tau_{23}}{\partial\xi}, \tag{8.42}$$

$$\frac{\partial G^{\frac{1}{2}}\rho w}{\partial t} = -\frac{\partial G^{\frac{1}{2}}\rho\tau_{31}}{\partial x^*} - \frac{\partial G^{\frac{1}{2}}\rho\tau_{32}}{\partial y^*} - \frac{\partial J_{13}G^{\frac{1}{2}}\rho\tau_{31} + J_{23}G^{\frac{1}{2}}\rho\tau_{32} + J_{33}G^{\frac{1}{2}}\rho\tau_{33}}{\partial\xi}, \tag{8.43}$$

$$\frac{\partial G^{\frac{1}{2}}\rho\theta}{\partial t} = -\frac{\partial G^{\frac{1}{2}}\rho\tau_1^D}{\partial x^*} - \frac{\partial G^{\frac{1}{2}}\rho\tau_2^D}{\partial y^*} - \frac{\partial J_{13}G^{\frac{1}{2}}\rho\tau_1^D + J_{23}G^{\frac{1}{2}}\rho\tau_2^D + J_{33}G^{\frac{1}{2}}\rho\tau_3^D}{\partial\xi} \tag{8.44}$$

$$G^{\frac{1}{2}}S_{11} = \frac{\partial G^{\frac{1}{2}}u}{\partial x^*} + \frac{\partial J_{13}G^{\frac{1}{2}}u}{\partial\xi}, \tag{8.45}$$

$$G^{\frac{1}{2}}S_{22} = \frac{\partial G^{\frac{1}{2}}v}{\partial y^*} + \frac{\partial J_{23}G^{\frac{1}{2}}v}{\partial\xi}, \tag{8.46}$$

$$G^{\frac{1}{2}}S_{33} = \frac{\partial J_{33}G^{\frac{1}{2}}w}{\partial\xi}, \tag{8.47}$$

$$G^{\frac{1}{2}}S_{12} = \frac{1}{2}\left(\frac{\partial G^{\frac{1}{2}}u}{\partial y^*} + \frac{\partial G^{\frac{1}{2}}v}{\partial x^*} + \frac{\partial J_{23}G^{\frac{1}{2}}u + J_{13}G^{\frac{1}{2}}v}{\partial\xi}\right), \tag{8.48}$$

$$G^{\frac{1}{2}}S_{23} = \frac{1}{2}\left(\frac{\partial G^{\frac{1}{2}}w}{\partial y^*} + \frac{\partial J_{33}G^{\frac{1}{2}}v + J_{23}G^{\frac{1}{2}}w}{\partial\xi}\right), \tag{8.49}$$

$$G^{\frac{1}{2}}S_{31} = \frac{1}{2}\left(\frac{\partial G^{\frac{1}{2}}w}{\partial x^*} + \frac{\partial J_{13}G^{\frac{1}{2}}w + J_{33}G^{\frac{1}{2}}u}{\partial\xi}\right), \tag{8.50}$$

$$G^{\frac{1}{2}}\tau_1^D = -D_{SGS}\left(\frac{\partial G^{\frac{1}{2}}\theta}{\partial x^*} + \frac{\partial J_{13}G^{\frac{1}{2}}\theta}{\partial\xi}\right), \tag{8.51}$$

$$G^{\frac{1}{2}}\tau_2^D = -D_{SGS}\left(\frac{\partial G^{\frac{1}{2}}\theta}{\partial y^*} + \frac{\partial J_{23}G^{\frac{1}{2}}\theta}{\partial\xi}\right), \tag{8.52}$$

$$G^{\frac{1}{2}}\tau_3^D = -D_{SGS}\frac{\partial J_{33}G^{\frac{1}{2}}\theta}{\partial\xi}, \tag{8.53}$$

$$G^{\frac{1}{2}}N^2 = \frac{g}{\theta}\frac{\partial J_{33}G^{\frac{1}{2}}\theta}{\partial\xi}. \tag{8.54}$$

[2]Equations which are not changed in the terrain-following coordinate are ommited.

8.1.3 descretization

Spatial descretization

We use the 4th order differnce scheme for the advection term as mentioned in the chapter 3. The τ_{ij} and τ_i^D are propotional to the square of the grid spacing (Δ^2). Due to the consistency with the advection term in terms of order for spatial difference, the second order central difference scheme is used for terms of the sub-grid scale turburence. In the following part in this sub-section, overline, and i, j, k mean as they are in the chapter 3.

Momentam equation The tendencies in the momentam equation related to the sub-grid scale mode are

$$\begin{aligned}\frac{\partial G^{\frac{1}{2}}\rho u}{\partial t}_{i+\frac{1}{2},j,k} =& -\frac{(G^{\frac{1}{2}}\rho\tau_{11})_{i+1,j,k} - (G^{\frac{1}{2}}\rho\tau_{11})_{i,j,k}}{\Delta x} \\ & -\frac{(G^{\frac{1}{2}}\overline{\rho}\tau_{12})_{i+\frac{1}{2},j+\frac{1}{2},k} - (G^{\frac{1}{2}}\overline{\rho}\tau_{12})_{i+\frac{1}{2},j-\frac{1}{2},k}}{\Delta y} \\ & -\frac{\{G^{\frac{1}{2}}\overline{\rho}(J_{13}\tau_{11} + J_{23}\tau_{12} + J_{33}\tau_{13})\}_{i+\frac{1}{2},j,k+\frac{1}{2}} - \{G^{\frac{1}{2}}\overline{\rho}(J_{13}\tau_{11} + J_{23}\tau_{12} + J_{33}\tau_{13})\}_{i+\frac{1}{2},j,k-\frac{1}{2}}}{\Delta z},\end{aligned} \tag{8.55}$$

$$\begin{aligned}\frac{\partial G^{\frac{1}{2}}\rho v}{\partial t}_{i,j+\frac{1}{2},k} =& -\frac{(G^{\frac{1}{2}}\overline{\rho}\tau_{21})_{i+\frac{1}{2},j+\frac{1}{2},k} - (G^{\frac{1}{2}}\overline{\rho}\tau_{21})_{i-\frac{1}{2},j+\frac{1}{2},k}}{\Delta x} \\ & -\frac{(G^{\frac{1}{2}}\rho\tau_{22})_{i,j+1,k} - (G^{\frac{1}{2}}\rho\tau_{22})_{i,j,k}}{\Delta y} \\ & -\frac{\{G^{\frac{1}{2}}\overline{\rho}(J_{13}\tau_{21} + J_{23}\tau_{22} + J_{33}\tau_{23})\}_{i,j+\frac{1}{2},k+\frac{1}{2}} - \{G^{\frac{1}{2}}\overline{\rho}(J_{13}\tau_{21} + J_{23}\tau_{22} + J_{33}\tau_{23})\}_{i,j+\frac{1}{2},k-\frac{1}{2}}}{\Delta z},\end{aligned} \tag{8.56}$$

$$\begin{aligned}\frac{\partial G^{\frac{1}{2}}\rho w}{\partial t}_{i,j,k+\frac{1}{2}} =& -\frac{(G^{\frac{1}{2}}\overline{\rho}\tau_{31})_{i+\frac{1}{2},j,k+\frac{1}{2}} - (G^{\frac{1}{2}}\overline{\rho}\tau_{31})_{i-\frac{1}{2},j,k+\frac{1}{2}}}{\Delta x} \\ & -\frac{(G^{\frac{1}{2}}\overline{\rho}\tau_{32})_{i,j+\frac{1}{2},k+\frac{1}{2}} - (G^{\frac{1}{2}}\overline{\rho}\tau_{32})_{i,j-\frac{1}{2},k+\frac{1}{2}}}{\Delta y} \\ & -\frac{\{(G^{\frac{1}{2}}\rho(J_{13}\tau_{31} + J_{23}\tau_{32} + J_{33}\tau_{33})\}_{i,j,k+1} - \{(G^{\frac{1}{2}}\rho(J_{13}\tau_{31} + J_{23}\tau_{32} + J_{33}\tau_{33})\}_{i,j,k}}{\Delta z}.\end{aligned} \tag{8.57}$$

The $\overline{\rho}$ is

$$\overline{\rho}_{i,j+\frac{1}{2},k+\frac{1}{2}} = \frac{\rho_{i,j+1,k+1} + \rho_{i,j+1,k} + \rho_{i,j,k+1} + \rho_{i,j,k}}{4}, \tag{8.58}$$

$$\overline{\rho}_{i+\frac{1}{2},j,k+\frac{1}{2}} = \frac{\rho_{i+1,j,k+1} + \rho_{i+1,j,k} + \rho_{i,j,k+1} + \rho_{i,j,k}}{4}, \tag{8.59}$$

$$\overline{\rho}_{i+\frac{1}{2},j+\frac{1}{2},k} = \frac{\rho_{i+1,j+1,k} + \rho_{i+1,j,k} + \rho_{i,j+1,k} + \rho_{i,j,k}}{4}. \tag{8.60}$$

Thermal equation The tendency in the thermal equation related to the subgrid scale model is

$$\begin{aligned}\frac{\partial G^{\frac{1}{2}}\rho\theta}{\partial t}_{i,j,k} =& -\frac{(G^{\frac{1}{2}}\overline{\rho}\tau_1^D)_{i+\frac{1}{2},j,k} - (G^{\frac{1}{2}}\overline{\rho}\tau_1^D)_{i-\frac{1}{2},j,k}}{\Delta x} \\ & -\frac{(G^{\frac{1}{2}}\overline{\rho}\tau_2^D)_{i,j+\frac{1}{2},k} - (G^{\frac{1}{2}}\overline{\rho}\tau_2^D)_{i,j-\frac{1}{2},k}}{\Delta y} \\ & -\frac{\{G^{\frac{1}{2}}\overline{\rho}(J_{13}\tau_1^D + J_{23}\tau_2^D + J_{33}\tau_3^D)\}_{i,j,k+\frac{1}{2}} - \{G^{\frac{1}{2}}\overline{\rho}(J_{13}\tau_1^D + J_{23}\tau_2^D + J_{33}\tau_3^D)\}_{i,j,k-\frac{1}{2}}}{\Delta z}.\end{aligned} \tag{8.61}$$

The $\overline{\rho}$ at half-level is eq.(3.81)-(3.83).

The eddy diffution flux, τ^D, at half-level is

$$(G^{\frac{1}{2}}\tau_1^D)_{i+\frac{1}{2},j,k} = -D_{SGS,i+\frac{1}{2},j,k}\left\{\frac{(G^{\frac{1}{2}}\theta)_{i+1,j,k} - (G^{\frac{1}{2}}\theta)_{i,j,k}}{\Delta x} + \frac{(J_{13}G^{\frac{1}{2}}\overline{\theta})_{i+\frac{1}{2},j,k+\frac{1}{2}} - (J_{13}G^{\frac{1}{2}}\overline{\theta})_{i+\frac{1}{2},j,k-\frac{1}{2}}}{\Delta z}\right\}, \tag{8.62}$$

$$(G^{\frac{1}{2}}\tau_2^D)_{i,j+\frac{1}{2},k} = -D_{SGS,i,j+\frac{1}{2},k}\left\{\frac{(G^{\frac{1}{2}}\theta)_{i,j+1,k} - (G^{\frac{1}{2}}\theta)_{i,j,k}}{\Delta y} + \frac{(J_{23}G^{\frac{1}{2}}\overline{\theta})_{i,j+\frac{1}{2},k+\frac{1}{2}} - (J_{23}G^{\frac{1}{2}}\overline{\theta})_{i,j+\frac{1}{2},k-\frac{1}{2}}}{\Delta z}\right\}, \tag{8.63}$$

$$(G^{\frac{1}{2}}\tau_3^D)_{i,j,k+\frac{1}{2}} = -D_{SGS,i,j,k+\frac{1}{2}}\frac{J_{33}G^{\frac{1}{2}}\theta_{i,j,k+1} - J_{33}G^{\frac{1}{2}}\theta_{i,j,k}}{\Delta z}. \tag{8.64}$$

Strain tensor All the strain tensor, eq.(8.17), have to be calculated at full-level (grid cell center), and some of them are at cell edges.

- cell center (i,j,k)

$$(G^{\frac{1}{2}}S_{11})_{i,j,k} = \frac{(G^{\frac{1}{2}}\overline{u})_{i+\frac{1}{2},j,k} - (G^{\frac{1}{2}}\overline{u})_{i-\frac{1}{2},j,k}}{\Delta x} + \frac{(J_{13}G^{\frac{1}{2}}\overline{u})_{i+\frac{1}{2},j,k+\frac{1}{2}} - (J_{13}G^{\frac{1}{2}}\overline{u})_{i+\frac{1}{2},j,k-\frac{1}{2}}}{\Delta z}, \tag{8.65}$$

$$(G^{\frac{1}{2}}S_{22})_{i,j,k} = \frac{(G^{\frac{1}{2}}\overline{v})_{i,j+\frac{1}{2},k} - (G^{\frac{1}{2}}\overline{v})_{i,j-\frac{1}{2},k}}{\Delta y} + \frac{(J_{23}G^{\frac{1}{2}}\overline{v})_{i,j+\frac{1}{2},k+\frac{1}{2}} - (J_{23}G^{\frac{1}{2}}\overline{v})_{i,j+\frac{1}{2},k-\frac{1}{2}}}{\Delta z}, \tag{8.66}$$

$$(G^{\frac{1}{2}}S_{33})_{i,j,k} = \frac{J_{33}G^{\frac{1}{2}}\overline{w}_{i,j,k+\frac{1}{2}} - J_{33}G^{\frac{1}{2}}\overline{w}_{i,j,k-\frac{1}{2}}}{\Delta z}, \tag{8.67}$$

$$(G^{\frac{1}{2}}S_{12})_{i,j,k} = \frac{1}{2}\left\{\frac{(G^{\frac{1}{2}}\overline{u})_{i,j+\frac{1}{2},k} - (G^{\frac{1}{2}}\overline{u})_{i,j-\frac{1}{2},k}}{\Delta y} + \frac{(G^{\frac{1}{2}}\overline{v})_{i+\frac{1}{2},j,k} - (G^{\frac{1}{2}}\overline{v})_{i-\frac{1}{2},j,k}}{\Delta x} + \frac{(J_{23}G^{\frac{1}{2}}\overline{u})_{i,j,k+\frac{1}{2}} - (J_{23}G^{\frac{1}{2}}\overline{u})_{i,j,k-\frac{1}{2}} + (J_{13}G^{\frac{1}{2}}\overline{v})_{i,j,k+\frac{1}{2}} - (J_{13}G^{\frac{1}{2}}\overline{v})_{i,j,k-\frac{1}{2}}}{\Delta z}\right\}, \tag{8.68}$$

$$(G^{\frac{1}{2}}S_{23})_{i,j,k} = \frac{1}{2}\left\{\frac{(G^{\frac{1}{2}}\overline{w})_{i,j+\frac{1}{2},k} - (G^{\frac{1}{2}}\overline{w})_{i,j-\frac{1}{2},k}}{\Delta y} + \frac{J_{33}G^{\frac{1}{2}}\overline{v}_{i,j,k+\frac{1}{2}} - J_{33}G^{\frac{1}{2}}\overline{v}_{i,j,k-\frac{1}{2}} + (J_{23}G^{\frac{1}{2}}\overline{w})_{i,j,k+\frac{1}{2}} - (J_{23}G^{\frac{1}{2}}\overline{w})_{i,j,k-\frac{1}{2}}}{\Delta z}\right\}, \tag{8.69}$$

$$(G^{\frac{1}{2}}S_{31})_{i,j,k} = \frac{1}{2}\left\{\frac{(G^{\frac{1}{2}}\overline{w})_{i+\frac{1}{2},j,k} - (G^{\frac{1}{2}}\overline{w})_{i-\frac{1}{2},j,k}}{\Delta x} + \frac{J_{33}G^{\frac{1}{2}}\overline{u}_{i,j,k+\frac{1}{2}} - J_{33}G^{\frac{1}{2}}\overline{u}_{i,j,k-\frac{1}{2}} + (J_{13}G^{\frac{1}{2}}\overline{w})_{i,j,k+\frac{1}{2}} - (J_{13}G^{\frac{1}{2}}\overline{w})_{i,j,k-\frac{1}{2}}}{\Delta z}\right\}. \tag{8.70}$$

- z edge $(i+\frac{1}{2}, j+\frac{1}{2}, k)$

$$(G^{\frac{1}{2}}S_{12})_{i+\frac{1}{2},j+\frac{1}{2},k} = \frac{1}{2}\left\{\frac{(G^{\frac{1}{2}}\overline{u})_{i+\frac{1}{2},j+1,k} - (G^{\frac{1}{2}}\overline{u})_{i+\frac{1}{2},j,k}}{\Delta y} + \frac{(G^{\frac{1}{2}}\overline{v})_{i+1,j+\frac{1}{2},k} - (G^{\frac{1}{2}}\overline{v})_{i,j+\frac{1}{2},k}}{\Delta x} + \frac{(J_{23}G^{\frac{1}{2}}\overline{u})_{i+\frac{1}{2},j+\frac{1}{2},k+\frac{1}{2}} - (J_{23}G^{\frac{1}{2}}\overline{u})_{i+\frac{1}{2},j+\frac{1}{2},k-\frac{1}{2}} + (J_{13}G^{\frac{1}{2}}\overline{v})_{i+\frac{1}{2},j+\frac{1}{2},k+\frac{1}{2}} - (J_{13}G^{\frac{1}{2}}\overline{v})}{\Delta z}\right. \tag{8.71}$$

- x edge $(i, j+\frac{1}{2}, k+\frac{1}{2})$

$$(G^{\frac{1}{2}}S_{23})_{i,j+\frac{1}{2},k+\frac{1}{2}} = \frac{1}{2}\left\{\frac{(G^{\frac{1}{2}}\overline{w})_{i,j+1,k+\frac{1}{2}} - (G^{\frac{1}{2}}\overline{w})_{i,j,k+\frac{1}{2}}}{\Delta y} + \frac{J_{33}G^{\frac{1}{2}}\overline{v}_{i,j+\frac{1}{2},k+1} - J_{33}G^{\frac{1}{2}}\overline{v}_{i,j+\frac{1}{2},k} + (J_{23}G^{\frac{1}{2}}\overline{w})_{i,j+\frac{1}{2},k+1} - (J_{23}G^{\frac{1}{2}}\overline{w})_{i,j+\frac{1}{2},k}}{\Delta z}.\right\} \tag{8.72}$$

- y edge $(i+\frac{1}{2}, j, k+\frac{1}{2})$

$$(G^{\frac{1}{2}}S_{31})_{i+\frac{1}{2},j,k+\frac{1}{2}} = \frac{1}{2}\left\{ \frac{(G^{\frac{1}{2}}\overline{w})_{i+1,j,k+\frac{1}{2}} - (G^{\frac{1}{2}}\overline{w})_{i,j,k+\frac{1}{2}}}{\Delta x} + \frac{J_{33}G^{\frac{1}{2}}\overline{u}_{i+\frac{1}{2},j,k+1} - J_{33}G^{\frac{1}{2}}\overline{u}_{i+\frac{1}{2},j,k} + (J_{13}G^{\frac{1}{2}}\overline{w})_{i+\frac{1}{2},j,k+1} - (J_{13}G^{\frac{1}{2}}\overline{w})_{i+\frac{1}{2},j,k}}{\Delta z}. \right\}. \tag{8.73}$$

velocity Calculattion of the strain tensor requires value of velocity at cell center, plane center, edge center, and vertex. The velocities at cell center (full-level) are eq.(3.87-3.89).

- x-y plane center $(i, j, k+\frac{1}{2})$

$$\overline{u}_{i,j,k+\frac{1}{2}} = \frac{\overline{u}_{i,j,k+1} + \overline{u}_{i,j,k}}{2}, \tag{8.74}$$

$$\overline{v}_{i,j,k+\frac{1}{2}} = \frac{\overline{v}_{i,j,k+1} + \overline{v}_{i,j,k}}{2}, \tag{8.75}$$

$$\overline{w}_{i,j,k+\frac{1}{2}} = \frac{(\rho w)_{i,j,k+\frac{1}{2}}}{\overline{\rho}_{i,j,k+\frac{1}{2}}}. \tag{8.76}$$

- y-z plane center $(i+\frac{1}{2}, j, k)$

$$\overline{u}_{i+\frac{1}{2},j,k} = \frac{(\rho u)_{i+\frac{1}{2},j,k}}{\overline{\rho}_{i+\frac{1}{2},j,k}}, \tag{8.77}$$

$$\overline{v}_{i+\frac{1}{2},j,k} = \frac{\overline{v}_{i+1,j,k} + \overline{v}_{i,j,k}}{2}, \tag{8.78}$$

$$\overline{w}_{i+\frac{1}{2},j,k} = \frac{\overline{w}_{i+1,j,k} + \overline{w}_{i,j,k}}{2}. \tag{8.79}$$

- z-x plane center $(i, j+\frac{1}{2}, k)$

$$\overline{u}_{i,j+\frac{1}{2},k} = \frac{\overline{u}_{i,j+1,k} + \overline{u}_{i,j,k}}{2}, \tag{8.80}$$

$$\overline{v}_{i,j+\frac{1}{2},k} = \frac{(\rho v)_{i,j+\frac{1}{2},k}}{\overline{\rho}_{i,j+\frac{1}{2},k}}, \tag{8.81}$$

$$\overline{w}_{i,j+\frac{1}{2},k} = \frac{\overline{w}_{i,j+1,k} + \overline{w}_{i,j,k}}{2}. \tag{8.82}$$

- x edge center $(i, j+\frac{1}{2}, k+\frac{1}{2})$

$$\overline{u}_{i,j+\frac{1}{2},k+\frac{1}{2}} = \frac{\overline{u}_{i,j+1,k+1} + \overline{u}_{i,j+1,k} + \overline{u}_{i,j,k+1} + \overline{u}_{i,j,k}}{4}, \tag{8.83}$$

$$\overline{v}_{i,j+\frac{1}{2},k+\frac{1}{2}} = \frac{\overline{v}_{i,j+\frac{1}{2},k+1} + \overline{v}_{i,j+\frac{1}{2},k}}{2}, \tag{8.84}$$

$$\overline{w}_{i,j+\frac{1}{2},k+\frac{1}{2}} = \frac{\overline{w}_{i,j+1,k+\frac{1}{2}} + \overline{w}_{i,j,k+\frac{1}{2}}}{2}. \tag{8.85}$$

- y edge center $(i+\frac{1}{2}, j, k+\frac{1}{2})$

$$\overline{u}_{i+\frac{1}{2},j,k+\frac{1}{2}} = \frac{\overline{u}_{i+\frac{1}{2},j,k+1} + \overline{u}_{i+\frac{1}{2},j,k}}{2}, \tag{8.86}$$

$$\overline{v}_{i+\frac{1}{2},j,k+\frac{1}{2}} = \frac{\overline{v}_{i+1,j,k+1} + \overline{v}_{i+1,j,k} + \overline{v}_{i,j,k+1} + \overline{v}_{i,j,k}}{4}, \tag{8.87}$$

$$\overline{w}_{i+\frac{1}{2},j,k+\frac{1}{2}} = \frac{\overline{w}_{i+1,j,k+\frac{1}{2}} + \overline{w}_{i,j,k+\frac{1}{2}}}{2}. \tag{8.88}$$

- z edge center $(i+\frac{1}{2}, j+\frac{1}{2}, k)$

$$\overline{u}_{i+\frac{1}{2},j+\frac{1}{2},k} = \frac{\overline{u}_{i+\frac{1}{2},j+1,k} + \overline{u}_{i+\frac{1}{2},j,k}}{2}, \tag{8.89}$$

$$\overline{v}_{i+\frac{1}{2},j+\frac{1}{2},k} = \frac{\overline{v}_{i+1,j+\frac{1}{2},k} + \overline{v}_{i,j+\frac{1}{2},k}}{2}, \tag{8.90}$$

$$\overline{w}_{i+\frac{1}{2},j+\frac{1}{2},k} = \frac{\overline{w}_{i+1,j+1,k} + \overline{w}_{i+1,j,k} + \overline{w}_{i,j+1,k} + \overline{w}_{i,j,k}}{4}. \tag{8.91}$$

- vertex $(i+\frac{1}{2}, j+\frac{1}{2}, k+\frac{1}{2})$

$$\overline{u}_{i+\frac{1}{2},j+\frac{1}{2},k+\frac{1}{2}} = \frac{\overline{u}_{i+\frac{1}{2},j+1,k+1} + \overline{u}_{i+\frac{1}{2},j+1,k} + \overline{u}_{i+\frac{1}{2},j,k+1} + \overline{u}_{i+\frac{1}{2},j,k}}{4}, \tag{8.92}$$

$$\overline{v}_{i+\frac{1}{2},j+\frac{1}{2},k+\frac{1}{2}} = \frac{\overline{v}_{i+1,j+\frac{1}{2},k+1} + \overline{v}_{i+1,j+\frac{1}{2},k} + \overline{v}_{i,j+\frac{1}{2},k+1} + \overline{v}_{i,j+\frac{1}{2},k}}{4}, \tag{8.93}$$

$$\overline{w}_{i+\frac{1}{2},j+\frac{1}{2},k+\frac{1}{2}} = \frac{\overline{w}_{i+1,j+1,k+\frac{1}{2}} + \overline{w}_{i+1,j,k+\frac{1}{2}} + \overline{w}_{i,j+1,k+\frac{1}{2}} + \overline{w}_{i,j,k+\frac{1}{2}}}{4}. \tag{8.94}$$

Eddy viscosity/diffusion coefficient The eddy viscosity/diffusion coefficient, ν_{SGS} / D_{SGS}, is calculated at full-level with S and Ri at full-level and it at half level is interporated one at full-level.

Brunt-Visala frequency The Brunt-Visala frequency, N^2 is required to calculate the Richardson number at full-level.

$$(G^{\frac{1}{2}}N^2)_{i,j,k} = \frac{g}{\theta_{i,j,k}} \frac{J_{33}G^{\frac{1}{2}}\theta_{i,j,k+1} - J_{33}G^{\frac{1}{2}}\theta_{i,j,k-1}}{2\Delta z}. \tag{8.95}$$

8.2 Boundary layer turbulence model

Corrensponding author : Seiya Nishizawa

8.2.1 Mellor-Yamada Nakanishi-Niino model

level 2.5

$$\frac{\partial \rho u}{\partial t} = -\frac{\partial}{\partial z}\rho\overline{u'w'}, \tag{8.96}$$

$$\frac{\partial \rho v}{\partial t} = -\frac{\partial}{\partial z}\rho\overline{v'w'}, \tag{8.97}$$

$$\frac{\partial \rho \theta_l}{\partial t} = -\frac{\partial}{\partial z}\rho\overline{\theta_l'w'}, \tag{8.98}$$

$$\frac{\partial \rho q_a}{\partial t} = -\frac{\partial}{\partial z}\rho\overline{q_a'w'}, \tag{8.99}$$

$$\frac{\partial}{\partial t}\rho q^2 = -2\left(\rho\overline{u'w'}\frac{\partial u}{\partial z} + \rho\overline{v'w'}\frac{\partial v}{\partial z}\right) + 2\frac{g}{\theta_0}\rho\overline{\theta_v'w'} - \frac{\partial}{\partial z}\rho\overline{q^2w'} - 2\rho\epsilon, \tag{8.100}$$

where

$$q_a = q_v + q_c + q_r + q_i + q_s + q_g, \tag{8.101}$$

and q^2 is doubled tubulence kinetic energy;

$$q^2 = u'^2 + v'^2 + w'^2. \tag{8.102}$$

The higher order moments and the disipation term are parameterized as followings:

$$\overline{u'w'} = -LqS_M\frac{\partial u}{\partial z}, \tag{8.103}$$

$$\overline{v'w'} = -LqS_M\frac{\partial v}{\partial z}, \tag{8.104}$$

$$\overline{\theta_l'w'} = -LqS_H\frac{\partial \theta_l}{\partial z}, \tag{8.105}$$

$$\overline{q_a'w'} = -LqS_H\frac{\partial q_a}{\partial z}, \tag{8.106}$$

$$\overline{q^2w'} = -3LqS_M\frac{\partial q^2}{\partial z}, \tag{8.107}$$

$$\overline{\theta_v'w'} = \beta_\theta\overline{\theta_l'w'} + \beta_q\overline{q_a'w'}, \tag{8.108}$$

$$\epsilon = \frac{q^3}{B_1L}, \tag{8.109}$$

where

$$S_M = \alpha_c A_1\frac{\Phi_3 - 3C_1\Phi_4}{D_{2.5}}, \tag{8.110}$$

$$S_H = \alpha_c A_2\frac{\Phi_2 + 3C_1\Phi_5}{D_{2.5}}, \tag{8.111}$$

$$\beta_\theta = 1 + 0.61q_a - 1.61Q_l - \tilde{R}abc, \tag{8.112}$$

$$\beta_q = 0.61\theta + \tilde{R}ac. \tag{8.113}$$

$$D_{2.5} = \Phi_2\Phi_4 + \Phi_5\Phi_3, \tag{8.114}$$

$$\Phi_1 = 1 - 3\alpha_c^2 A_2 B_2 (1 - C_3) G_H, \tag{8.115}$$

$$\Phi_2 = 1 - 9\alpha_c^2 A_1 A_2 (1 - C_2) G_H, \tag{8.116}$$

$$\Phi_3 = \Phi_1 + 9\alpha_c^2 A_2^2 (1 - C_2)(1 - C_5) G_H, \tag{8.117}$$

$$\Phi_4 = \Phi_1 - 12\alpha_c^2 A_1 A_2 (1 - C_2) G_H, \tag{8.118}$$

$$\Phi_5 = 6\alpha_c^2 A_1^2 G_M, \tag{8.119}$$

$$\alpha_c = \begin{cases} q/q_2, & q < q_2 \\ 1, & q \geq q_2 \end{cases}, \tag{8.120}$$

$$G_M = \frac{L^2}{q^2}\left\{\left(\frac{\partial u}{\partial z}\right)^2 + \left(\frac{\partial v}{\partial z}\right)^2\right\}, \tag{8.121}$$

$$G_H = -\frac{L^2}{q^2} N^2, \tag{8.122}$$

$$R = \frac{1}{2}\left\{1 + \mathrm{erf}\left(\frac{Q_1}{\sqrt{2}}\right)\right\}, \tag{8.123}$$

$$\tilde{R} = R - \frac{Q_l}{2\sigma_s}\frac{1}{\sqrt{2\pi}}\exp\left(-\frac{q_1^2}{2}\right), \tag{8.124}$$

$$Q_l = 2\sigma_s\left\{RQ_1 + \frac{1}{\sqrt{2\pi}}\exp\left(-\frac{Q_1^2}{2}\right)\right\}, \tag{8.125}$$

$$Q_1 = \frac{a}{2\sigma_s}(q_a - Q_{sl}), \tag{8.126}$$

$$\sigma_s^2 = \frac{1}{4}a^2 L^2 \alpha_c B_2 S_H \left(\frac{\partial q_a}{\partial z} - b\frac{\partial \theta_l}{\partial z}\right)^2, \tag{8.127}$$

$$\delta Q_{sl} = \left.\frac{\partial Q_s}{\partial T}\right|_{T=T_l}, \tag{8.128}$$

$$a = \left(1 + \frac{L}{C_p}\delta Q_{sl}\right)^{-1}, \tag{8.129}$$

$$b = \frac{T}{\theta}\delta Q_{sl}, \tag{8.130}$$

$$c = (1 + 0.61q_a - 1.61Q_l)\frac{\theta}{T}\frac{L_v}{C_p} - 1.61\theta, \tag{8.131}$$

and Q_{sl} is the satulation specific humidity at the temperature $T_l (= \theta_l T/\theta)$.

The buoyancy flux term, which is the third term of the left hand side in eq. 8.100 is

$$\begin{aligned} 2\frac{g}{\theta_0}\overline{\theta_v' w'} &= 2\frac{g}{\theta_0}\left(-\beta_\theta L q S_H \frac{\partial \theta_l}{\partial z} - \beta_q L q S_H \frac{\partial q_a}{\partial z}\right) \\ &= -2Lq S_H \frac{g}{\theta_0}\left(\beta_\theta \frac{\partial \theta_l}{\partial z} + \beta_q \frac{\partial q_a}{\partial z}\right) \\ &= -2Lq S_H \frac{g}{\theta_0}\frac{\partial \theta_v}{\partial z} \\ &= -2Lq S_H N^2, \end{aligned} \tag{8.132}$$

where N^2 is square of the Brunt-Vaisala frequency.

$$\frac{\partial}{\partial t}\rho q^2 = 2\rho L q S_M \left\{ \left(\frac{\partial u}{\partial z}\right)^2 + \left(\frac{\partial v}{\partial z}\right)^2 \right\} - 2\rho L q S_H N^2 + \frac{\partial}{\partial z}\left(3\rho L q S_M \frac{\partial}{\partial z} q^2\right) - 2\rho \frac{q^3}{B_1 L} \tag{8.133}$$

S_{M2}, S_{H2}, and q_2 is for level 2 scheme corresponding to S_M, S_H, and q, respectively;

$$S_{M2} = \frac{A_1 F_1}{A_2 F_2} \frac{R_{f1} - Rf}{R_{f2} - Rf} S_{H2}, \tag{8.134}$$

$$S_{H2} = 3A_2(\gamma_1 + \gamma_2)\frac{Rf_c - Rf}{1 - Rf}, \tag{8.135}$$

$$q_2^2 = B_1 L^2 S_{M2}(1 - Rf)\left\{ \left(\frac{\partial u}{\partial z}\right)^2 + \left(\frac{\partial v}{\partial z}\right)^2 \right\}. \tag{8.136}$$

Rf and Rf_c are the flux Richardson number and the critical flux Richardson number, respectively. The gradient Richardson number, Ri, is

$$Ri = Rf \frac{S_{M2}}{S_{H2}}. \tag{8.137}$$

Then the Rf is

$$Rf = \frac{1}{2}\frac{A_2 F_2}{A_1 F_1}\left\{ Ri + \frac{A_1 F_1}{A_2 F_2} R_{f1} - \sqrt{Ri^2 + 2\frac{A_1 F_1}{A_2 F_2}(R_{f1} - 2R_{f2})Ri + \left(\frac{A_1 F_1}{A_2 F_2} R_{f1}\right)^2} \right\}, \tag{8.138}$$

$$Rf_C = \frac{\gamma_1}{\gamma_1 + \gamma_2}, \tag{8.139}$$

$$\tag{8.140}$$

where

$$R_{f1} = B_1 \frac{\gamma_1 - C_1}{F_1}, \tag{8.141}$$

$$R_{f2} = B_1 \frac{\gamma_1}{F_2}. \tag{8.142}$$

The turbulent length scale, L, is determined by the smallest length scale among the three length scales;

$$\frac{1}{L} = \frac{1}{L_s} + \frac{1}{L_T} + \frac{1}{L_B}. \tag{8.143}$$

he surface layer scale, L_s, the boundary layer scale, L_T, and buoyancy length

scale, T_B;

$$L_S = \begin{cases} kz/3.7, & \zeta \geq 1 \\ kz/(1+2.7\zeta), & 0 \leq \zeta < 1 \\ kz(1-100\zeta)^{0.2}, & \zeta < 0 \end{cases}, \tag{8.144}$$

$$L_T = 0.23 \frac{\int_0^\infty qzdz}{\int_0^\infty qdz}, \tag{8.145}$$

$$L_B = \begin{cases} q/N, & \partial\theta_v/\partial z > 0 \text{ and } \zeta \geq 0 \\ \{1+5(q_c/L_T N)^{1/2}\}q/N, & \partial\theta_v/\partial z > 0 \text{ and } \zeta < 0 \\ \infty, & \partial\theta_v/\partial z \leq 0 \end{cases}, \tag{8.146}$$

where ζ is the dimensionless height;

$$\zeta = \frac{z}{L_M}. \tag{8.147}$$

L_M is the Monin-Obukhov length;

$$L_M = -\frac{\theta_0 u_*^3}{kg\overline{\theta'_v w'}_g}, \tag{8.148}$$

where u_* is the friction velocity, and the subscript g denotes the ground surface. q_c is a velocity scale defined similarly as the convective velocity w_*, except that the depth z_i of the convective boundary layer is replaced by L_t;

$$q_c = \left\{ \frac{g}{\theta_0} \overline{\theta'_v w'}_g L_T \right\}^{1/3} \tag{8.149}$$

$$A_1 = B_1 \frac{1-3\gamma_1}{6}, \tag{8.150}$$

$$A_2 = \frac{1}{3\gamma_1 B_1^{1/3} Pr_N}, \tag{8.151}$$

$$B_1 = 24.0, \tag{8.152}$$

$$B_2 = 15.0, \tag{8.153}$$

$$C_1 = \gamma_1 - \frac{1}{3A_1 B_1^{1/3}}, \tag{8.154}$$

$$C_2 = 0.75, \tag{8.155}$$

$$C_3 = 0.352, \tag{8.156}$$

$$C_5 = 0.2, \tag{8.157}$$

$$\gamma_1 = 0.235, \tag{8.158}$$

$$\gamma_2 = \frac{2A_1(3-2C_2) + B_2(1-C_3)}{B_1}, \tag{8.159}$$

$$F_1 = B_1(\gamma_1 - C_1) + 2A_1(3-2C_2) + 3A_2(1-C_2)(1-C_5), \tag{8.160}$$

$$F_2 = B_1(\gamma_1 + \gamma_2) - 3A_1(1-C_2), \tag{8.161}$$

$$Pr_N = 0.74. \tag{8.162}$$

descretization

The diffusion equations for q^2a is solved implicitly.

$$\rho_k \frac{(q_k^2)^{n+1} - (q_k^2)^n}{\Delta t} = 2\rho_k \left[(LqS_M)_k \left\{ \left(\frac{\partial u}{\partial z} \right)^2 + \left(\frac{\partial v}{\partial z} \right)^2 \right\} + (LqS_H N^2)_k \right] + \frac{1}{\Delta z_k} \left\{ (3\rho LqS_M)_{k+\frac{1}{2}} \frac{(q_{k+1}^2)^{n+1} - (q_k^2)^{n+1}}{\Delta z_{k+\frac{1}{2}}} - (3\rho LqS_M)_{k-\frac{1}{2}} \frac{(q_k^2)^{n+1} - (q_{k-1}^2)^{n+1}}{\Delta z_{k-\frac{1}{2}}} \right\} - \frac{2\rho_k q_k}{B_1 L_k} (q_k^2)^{n+1}. \tag{8.163}$$

$$a_k (q_{k+1}^2)^{n+1} + b_k (q_k^2)^{n+1} + c_k (q_{k-1}^2)^{n+1} = d_k, \tag{8.164}$$

where

$$a_k = -\frac{\Delta t}{\Delta z_{k+\frac{1}{2}} \Delta z_k \rho_k} (3\rho LqS_M)_{k+\frac{1}{2}}, \tag{8.165}$$

$$b_k = -a_k - c_k + 1 + \frac{2\Delta t q_k}{B_1 L}, \tag{8.166}$$

$$c_k = -\frac{\Delta t}{\Delta z_k \Delta z_{k-\frac{1}{2}} \rho_k} (3\rho LqS_M)_{k-\frac{1}{2}}, \tag{8.167}$$

$$d_k = (q_k^2)^n + 2\Delta t \left[LqS_M \left\{ \left(\frac{\partial u}{\partial z} \right)^2 + \left(\frac{\partial v}{\partial z} \right)^2 \right\} - LqS_H N^2 \right] \tag{8.168}$$

$$(q_k^2)^{n+1} = e_k (q_{k+1}^2)^{n+1} + f_k, \tag{8.169}$$

where

$$e_k = -\frac{a_k}{b_k + c_k e_{k-1}}, \tag{8.170}$$

$$f_k = \frac{d_k - c_k f_{k-1}}{b_k + c_k e_{k-1}}. \tag{8.171}$$

Vertical flux for $\rho u, \rho v, \rho\theta, \rho q_x$ is also solved implicitly. For instance, the flux for ρu, F_u is calculated by

$$F_{u,k+\frac{1}{2}} = (\rho LqSM)_{k+\frac{1}{2}} \frac{u_{k+1}^{n+1} - u_k^{n+1}}{\Delta z_{k+\frac{1}{2}}}. \tag{8.172}$$

u^{n+1} is calculated as the same way with the q^2, but

$$a_k = -\frac{\Delta t}{\Delta z_{k+\frac{1}{2}} \Delta z_k \rho_k} (\rho LqS_M)_{k+\frac{1}{2}}, \tag{8.173}$$

$$b_k = -a_k - c_k + 1, \tag{8.174}$$

$$c_k = -\frac{\Delta t}{\Delta z_k \Delta z_{k-\frac{1}{2}} \rho_k} (\rho LqS_M)_{k-\frac{1}{2}}, \tag{8.175}$$

$$d_k = u_k^n. \tag{8.176}$$

8.3 Microphysics

Corresponding author : Yousuke Sato

The SCALE-RM has three types of cloud microphysics models. We will show description of these models below.

8.3.1 Kessler Parameterization

An one-moment bulk microphysical scheme, which treats only warm cloud (cloud and rain), is implemented in SCALE. This scehem predicts mixing ratio of cloud (Q_{cloud}) and rain (Q_{rain}). Cloud microphysical processes treated in this scheme is saturation adjustment (corresponding to nucleatioin, evaporation, and condensation of cloud), evaporation, auto-conversion, accretion, and sedimentation. The tendency of Q_{cloud}, Q_{rain}, and Q_v (vapor mixing ratio) is given as

$$\frac{\partial Q_{cloud}}{\partial t} = dQ|_{sat} - dQ|_{auto} - dQ|_{acc} \tag{8.177}$$

$$\frac{\partial Q_{rain}}{\partial t} = dQ|_{auto} + dQ|_{acc} - dQ|_{evap} - F_{Q_r}|_{sed} \tag{8.178}$$

$$\frac{\partial Q_v}{\partial t} = dQ|_{evap} - dQ|_{sat} \tag{8.179}$$

where $dQ|_{sat}$, $dQ|_{auto}$, $dQ|_{acc}$, and $dQ|_{evap}$ represents tendency of mixing ratio by saturation adjustment, auto-conversion, accretion, and evaporation, respectively. $F_{Q_r}|_{sed}$ represents flux of Q_r by sedimentation.
$dQ|_{auto}$, $dQ|_{acc}$, and $dQ|_{evap}$ are given as

$$dQ_{auto} = \begin{cases} Q_{cloud} * 10^{-3} & (Q_{cloud} > 10^{-3}) \\ 0 & (else) \end{cases} \tag{8.180}$$

$$dQ_{acc} = 2.2 \times Q_{cloud} \times Q_{rain}^{0.875} \tag{8.181}$$

$$dQ_{evap} = \begin{cases} f_{vent} \frac{q_s - Q_{cloud}}{q_s \rho} \frac{(\rho * Q_{rain})^{0.525}}{5.4 \times 10^5 + \frac{2.55 \times 10^8}{p q_s}} & (q_s > Q_{cloud}) \\ 0 & (else) \end{cases} \tag{8.182}$$

where f_{vent} is ventiration factor ($f_{vent} = 1.6 + 124.9(\rho Q_{rain})^{0.2046}$), and unit of dQ_{***} is [kg/kg/s]. p, q_s, and ρ is pressure, saturation vapor mixing ratio, and total density.
The $dQ|_{sat}$ is given as

$$dQ|_{sat} = Q_v - q_s. \tag{8.183}$$

Terminal velocity of cloud ($V_{t,c}$) and rain ($V_{t,r}$) is given as

$$V_{t,c} = 0 \tag{8.184}$$

$$V_{t,r} = 36.34(\rho Q_{rain})^{0.1364} [m/s] \tag{8.185}$$

8.3.2 Double-Moment BulkSeiki and Nakajima (2014)

Treatment of hydrometeors

Generally, characteristics of cloud particles are determined by their size, shape and chemical properties of solute in them. Representation of these characteristics needs a multi-dimensional parameter space of size, shape and chemical compositions. Since development of a cloud resolving model (CRM) coupled with an aerosol transport model is beyond the scope of this study, we consider a two-dimensional parameter space of size and shape of cloud particles. We then categorize cloud models into two major groups according to their representation of cloud particles. One is the bin method, with discretized particle size bins, predicting the population density of particles in each bin. The other is the bulk method in which the particle size distributions are approximated by several prescribed modes, predicting the total populations of partilces of each mode. The treatment of hydrometeors adopted in this study is described in the following sections.

Droplet Size Distribution

The Seiki and Nakajima (2014)Seiki and Nakajima (2014) scheme is designed to maintain the self-consistency of the assumptions regarding droplet size distribution (DSD) and the shapes of ice particles among the cloud microphysical processes. Following Seifert and Beheng (2006; hereafter, SB06), Seiki and Nakajima(2014)Seiki and Nakajima (2014) predicts the moments of the DSDs of each hydrometeor assuming the generalized gamma distribution to analytically formulate the cloud microphysics as follows:

$$f_a(r) = \alpha_a x^{\nu_a} \exp(-\lambda x) \tag{8.186}$$

where the index a $\in$ (c,r,i,s,g) represents cloud water, rain, cloud ice, snow, and graupel. For a given DSD, the k-th moment of a DSD can be defined as follows:

$$M_a^{(k)} \equiv \int_0^\infty x^k f_a(r) dx, \quad (k \in \mathbf{R}) \tag{8.187}$$

For example, the 0-th moment of a DSD is the number concentration N_a, and the 1st moment of a DSD is the mass concentration $L_a = \rho q_a$. The evolutions of DSDs are represented by updating α_a and λ_a using N_a and L_a with two fixed parameters, ν_a and μ_a, respectively. The diagnostic parameters α_a and λ_a are calculated as follows:

$$\alpha_a = \frac{\mu_a \lambda_a}{\Gamma\left(\frac{\nu_a+1}{\mu_a}\right)} \lambda_a^{\frac{\nu_a+1}{\mu_a}} \tag{8.188}$$

$$\lambda_a = \left[\frac{\Gamma\left(\frac{\nu_a+1}{\mu_a}\right)}{\Gamma\left(\frac{\nu_a+2}{\mu_a}\right)}\right]^{-\nu_a}$$

where the mean particle mass $\bar{x} \equiv L_a/N_a$. We maintain the self-consistency of the shape of ice particles by assuming power law relationships between: 1) the particle mass and the maximum dimension D and 2) the particle mass and the projected area to the flow A as follows:

$$D = a_m x^{b_m} \tag{8.189}$$
$$A = a_{ax} x^{b_m} \tag{8.190}$$

where a_m, b_m, a_{ax}, and b_{ax} are constant coefficients. We chose to use constant parameters in the representations of DSDs following SB06 for cloud water, cloud ice, snow, and graupel; and following Seifert (2008) for rain (assuming the collisional-breakup equilibrium condition). The shapes of ice particles are those given by Mitchell (1996) assuming cloud ice as hexagonal plates, snow as assemblages of planer polycrystals in cirrus clouds, and graupel as lump graupel. The abovementioned constant parameters for each hydrometeor are summarized in Table 8.1.

Table 8.1: Constant parameters chosen for the generalized gamma distribution; power law coefficients used for maximum dimensions and the projected area; and ranges of lower- and upper limits of mean mass.

	cloud water	rain	cloud ice	snow	graupel
ν	1	-1/3	1	1	1
μ	1	1/3	1/3	1/3	1/3
a_m[m kg^{-bm}]	0.124	0.124	1.24	1.24	0.346
b_m	1/3	1/3	0.408	0.408	0.357
$a_{ax}[m^2 kg^{-bA}]$	0.0121	0.0121	0.178	0.196	0.0599
b_{ax}	2/3	2/3	0.755	0.768	0.714
$\bar{x_{min}}[kg]$	4.2×10^{-12}	4.2×10^{-12}	4.2×10^{-12}	4.2×10^{-12}	4.2×10^{-12}
$\bar{x_{max}}[kg]$	2.6×10^{-10}	2.6×10^{-10}	2.6×10^{-10}	2.6×10^{-10}	2.6×10^{-10}

Terminal velocity of hydrometeors

In the same manner as in Seifert and Beheng (2006a), the terminal velocities of particles are formulated in power laws except for the gravitational sedimentation which is described in accurate formula, because the gravitational sedimentation is directly compared with precipitation data. The terminal velocities of hydrometeors are determined by the balance between the drag force and gravitational force. Traditionally, the terminal velocity for small spherical particles, small Reynolds number (N_{Re}), are described by Stokes Law,

$$\nu_{t,stokes}(r) = \frac{2g(\rho_w - \rho)}{9\eta_a} r^2 \tag{8.191}$$

where $g = 9.80616\ [ms^{-2}]$ is the gravitational acceleration, $\rho w = 1000\ kgm^{-3}$ is the density of liquid water, ρ is the density of air and η_a is the dynamic viscosity of air. Laboratory experiments showed that the terminal velocity departed from Stokes Law as the Reynolds number increases (Gunn and Kinzer, 1948;

Beard and Pruppacher, 1969). Thus, other formulas are required for larger droplets such as rain droplets and ice crystals.
In the case of liquid water droplets, the terminal velocity is well determined by laboratory experiments because of simplicity of the shape. In contrast, in the case of ice particles, there are many observation data of the terminal velocity for various shapes of ice crystals. Bohm (1989), Bohm (1992) and Mitchell (1996) proposed the general formulations of the terminal velocities of ice particles based on the boundary layer theory and their studies showed good agreement with observational data. In this study, we calculated terminal velocities for each ice particle based on Mitchell (1996) and then made a fitting curve by a power law in the suitable range of diameter.
In the theoretical formulas, the terminal velocities of hydrometeors are dependent on diameter, shape, the Reynolds number and the Best (or Davies) number (N_X). Application of these dependencies to cloud microphysics are so complicated that here we have applied a simplified approach suggested by Beard (1980),
1. The terminal velocity is calculated for the reference atmosphere.
2. The terminal velocity in the atmosphere are adjusted from the reference value.
In the following paragraphs, we describe the terminal velocities for the reference atmosphere and the adjustment technique.

Terminal velocity of liquid water droplets for the reference atmosphere

In the case of liquid water droplets, absence of shape variability makes formulation easier than ice particles. Here, we only consider the dependency on the diameter of droplets. Seifert and Beheng (2006) applied the formulation of Rogers et al. (1993), which is the analytical approximation to the observation data of Gunn and Kinzer (1948),

$$\nu_t(D) = \begin{cases} a_{R_s} D(1 - exp(-b_{R_s} D)), & (D < D_{0,r}) \\ a_{R_l} - b_{R_l} exp(-c_{R_l} D), & (D > D_{0,r}) \end{cases} \tag{8.192}$$

where $a_{R_s} = 4000s^{-1}$, $b_{R_s} = 12000m^{-1}$, $a_{R_l} = 9.65ms^{-1}$, $b_{R_l} = 10.43ms^{-1}$, $c_{R_l} = 600m^{-1}$, and D_0, $r = 7.45 \times 10^{-4}$ m. This formulation approaches the quadratic form of Stokes Law in the limit for small diameter. In addition, the data of Gunn and Kinzer (1948) agrees well with the terminal velocities calculated by theoretical formulation based on the boundary layer theory (Bohm, 1992). Therefore, we applied eq.8.192 for the sedimentation of rain (Fig. 8.12 11). Here it is mentioned that the reference atmosphere of the formulation is $T = 293K$, $p = 1000hPa$, and relative humidity is 0.5 (Gunn and Kinzer, 1948).

Terminal velocity of solid water particles for the reference atmosphere

In the case of ice particles, we derive the theoretical formulation of the terminal velocity following to Mitchell (1996). In general the aerodynamic drag force F_D on a particle is expressed as follows,

$$F_D \equiv \frac{1}{2} \rho \nu_t^2 A C_D \tag{8.193}$$

where C_D is the drag coefficient. Terminal velocity is determined by the equilibrium condition between the drag force and the gravitational acceleration,

$$\nu_t = \Big(\frac{2xg}{\rho A C_D}\Big)^{1/2} \tag{8.194}$$

The problem of derivation of the terminal velocity is reduced to derivation of the drag coefficient indepenently on the terminal velocity. In practice, Mitchell (1996) and many other researchers calculated the terminal velocity by the definition of the Best number (N_X) as follows,

$$N_x \equiv C_D N_{R_e}^2 = \frac{2xg\rho D^2}{A\eta_a^2} \tag{8.195}$$

Where N_{R_e} is the Reynolds number. The terminal velocity can be calculated after the relationship between the Best number and the Reynolds number is determined. In the relationship, it is convenient that the drag coefficient is determined by the Reynolds number although the dependency of the drag coefficient is complicated. A theoretical formulation of the drag coefficient was proposed by Abraham (1970). The drag coefficient is the dimensionless number defined by the drag force, the dynamic pressure and the projection area of the particle (see eq.8.193). Abraham (1970) assumed that the effective projection area of the particle contained the projection area of the particle itself and also the boundary layer surrounding the particle as follows,

$$F_D = \frac{1}{2}\rho\nu_t^2 C_0 A\big(1 + \frac{\delta_b}{r_A}\big)^2 \tag{8.196}$$

where C_0 is the drag coefficient which is due to the pressure of the fluid and should be determined independently of the shape, δ_b is the boundary layer depth and r_A is the radius of a circle with the equivalent projection area. Furthermore, the ratio of the boundary layer depth to the radius is expressed as follows,

$$\frac{\delta_b}{r_A} = \frac{\delta_0}{N_{R_e}^{1/2}} \tag{8.197}$$

where δ_0 is non-dimensional constant. Substituting eq.8.197 into eq.8.196, the drag coefficient which also includes the effect of the boundary layer is corresponding to the following,

$$C_D = C_0\big(1 + \frac{\delta_0}{N_{R_e}^{1/2}}\big)^2 \tag{8.198}$$

Thus the drag coefficient is expressed by the Reynolds number. The relationship between the Reynolds number and the Best number is derived by substituting eq.8.198 into eq.8.195

$$N_{R_e} = \frac{\delta_0^2}{4}\Big[\big(1 + \frac{4N_X^{1/2}}{\delta_0^2 C_0^{1/2}}\big)^{1/2} - 1\Big]^2 \tag{8.199}$$

Here we use $C_0 = 0.6$ and $\delta_0 = 5.83$ as provided by Bohm (1989). Finally the terminal velocity of ice particles is calculated by substituting eq.8.195 and eq.8.199 into the definition of the Reynolds number,

$$\begin{aligned} \nu_t &= \frac{N_{Re}\eta_a}{D\rho} \\ &= \frac{\eta_a}{D\rho}\frac{\delta_0^2}{4}\Big[\Big[1+\frac{4}{\delta_0^2 C_0^{1/2}}\Big(\frac{2xg\rho D^2}{A\eta_a^2}\Big)^{1/2}\Big]^{1/2}-1\Big]^2 \end{aligned} \tag{8.200}$$

In this formulation, required variables are mass, projection area, maximum dimension of ice particles and thermodynamical variables. Here we use several piecewise-constant mass-maximum dimension and projection area-maximum dimension relationships provided by Mitchell (1996). The terminal velocities of various ice particles are plotted in Fig.8.2. As shown in Fig.8.1 there is less difference between hexagonal plates and stellar crystals with broad arms with the diameter less than a few hundred micrometers. Therefore we only consider hexagonal column and hexagonal plate as representatives of the category of ice.

Adjustment factor of terminal velocity

Beard (1980) suggested that calculation of the terminal velocity using the Best number could be simplified with use of an adjustment factor (f_{vt}) defined as,

$$\nu_t = \nu_{t0} f_{vt} \tag{8.201}$$

where v_{t0} is a reference terminal velocity. He demonstrated that f_{vt} was not sensitive to the shape of hydrometeors. When electrical force is not considered in the cloud microphysics, formulas of f_{vt} are as follows,

$$f_{vt} = f_{vt0} \quad (N_{Re_0} \leq 0.2) \tag{8.202}$$

$$f_{vt} = f_{vt\infty} \quad (N_{Re_0} \geq 1000) \tag{8.203}$$

$$\begin{aligned} f_{vt} &= f_{vt0} \\ &+ (f_{vt\infty} - f_{vt0})(1.61 + lnN_{R_e 0})/8.52 \quad (N_{Re_0} < 1000) \end{aligned} \tag{8.204}$$

$$f_{vt0} \equiv (\eta_0/\eta) \tag{8.205}$$

$$f_{vt\infty} \equiv (\rho_0/\rho)^{0.5} \tag{8.206}$$

$$N_{R_e 0} \equiv \rho_0 D v_{t0}/\eta_0 \tag{8.207}$$

The upper limit of the Reynolds number ($N_{R_e} = 1000$) corresponds to a diameter of several milimeters and the lower limit of the Reynolds number ($N_{R_e} = 0.2$) corresponds to a diameter of tens of micrometers. Seifert and Beheng (2006) applied a further simplified adjustment factor based on eq.8.205 and eq.8.206 as follows,

$$f_{vt,n} = (\rho_0/\rho)^{\gamma_n}, \quad (n = c, r, i, s, g) \tag{8.208}$$

where $\gamma_c = 1.0$ and $\gamma_r = \gamma_i = \gamma_s = \gamma_g = 0.5$ This simplification formula of the adjustment factor is intended to avoid the dependency on the Reynolds number. However, $\gamma_n = 0.5$ is valid only for high Reynolds number particles whose

diameters are more than several millimeters as shown in eq.8.200. Therefore, the above formula always underestimates the terminal velocity of cirrus clouds. Another simplified formula for cirrus clouds was suggested by Heymsfield and Iaquinta (2000) as follows,

$$f_{vt} = (p/p_0)^{-0.178}(T/T_0)^{-0.394} \tag{8.209}$$

where $T_0 = 233$ K and $p_0 = 300$ hPa. By using these adjustment factors, we can only consider the terminal velocity for the reference atmosphere. Adjustment factors used for each hydrometeor in this study are summarized in Table 8.2.

Table 8.2: Adjustment factor for the reference terminal velocity.

	cloud	rain	Ice	snow	graupel
f_{vt}	1	$(\rho_0/\rho)^{0.5}$	$(p/p_0)^{-0.178}(T/T_0)^{-0.394}$	$(p/p_0)^{-0.178}(T/T_0)^{-0.394}$	$(p/p_0)^{-0.178}(T/T_0)^{-0.394}$

Weightend mean terminal velocity

In gravitational sedimentation, the mean terminal velocity weighted by the k-th moments of DSD ($\bar{\mathbf{v}}_{\mathbf{k,nq}}$) is calculated straightforward as follows

$$\bar{v}_{k,nq} = \int_0^\infty x^k f_{nq}(x) v_{t,nq}(x) dx \tag{8.210}$$

However, the formulas of the terminal velocities, eq.8.193 and eq.8.200 are too complicated to analytically integrate eq.8.210. Seifert and Beheng (2006) and Seifert (2008) approximately used the large branch of eq.8.193 for rain droplets and simple power laws derived by observation for other hydrometeors. Here we made more accurate formulations to calculate the weighted terminal velocities.

As shown above, the dependency of the terminal velocity on the diameter varies among the aerodynamical regimes. In other words, the dependency varies among the range of diameter. Therefore, firstly we prepared two branches of the terminal velocities of hydrometeors except for cloud droplets so as to integrate the DSDs analytically. For cloud droplets, we use the same power law provided by Seifert and Beheng (2006) which is based on Stokes law. For the rain droplets, we directly use the formulation of eq.8.193 because we can integrate each branch analytically. In contrast, we need to derive two fitting curves for ice particles. The formulation of the terminal velocity of ice particles is described as a power law of the diameter made by the least-square method as follows,

$$
\begin{aligned}
v_{t,js} &= a_{v,js} x^{b_{v,js}}, \quad (js = i, s, g) && (8.211)\\
(RMSE)_{k,js} &= \sum_{id=1}^{id_max} \left(ln v_{k,\bar{js},true}(\bar{D_{id}}) - ln \bar{v_{k,js}}(\bar{D_{id}}) \right)^2 && (8.212)\\
\frac{\partial (RMSE)_{k,js}}{\partial a_{v,js}} &= 0, \; \frac{\partial (RMSE)_{k,js}}{\partial b_{v,js}} = 0 \\
\bar{v_{k,js}}(\bar{D_{id}}) &= \int_0^\infty a_{v,js} x^{b_{v,js}+k} f(x, \bar{D_{id}}, L) dx / L \\
&= a_{v,js} \frac{\Gamma\left(\frac{v_{js}+b_{v,js}+k+1}{\mu_{js}}\right)}{\Gamma\left(\frac{v_{js}+k+1}{\mu_{js}}\right)} \left[\frac{\Gamma\left(\frac{v_{js}+1}{\mu_{js}}\right)}{\Gamma\left(\frac{v_{js}+2}{\mu_{js}}\right)} \right]^{b_{v,js}} \bar{x_{id,js}^{b_{v,js}}} && (8.213)\\
\bar{v_{k,js},true}(\bar{D_{id}}) &= \sum_{i=1}^{imax} x^k v_{t,js,true} f_{logD}(ln D_i, \bar{D_{id}}, L) \Delta ln D / L
\end{aligned}
$$

where $D_1 = 10\mu m$, $D_{imax} = 10mm$, $i_{max} = 1000$, and L is arbitrary constant. The fitting ranges of the mean volume diameter in eq.8.212 are from 20 to 400 μm for the small branch and from 200 to 2000 μm for the large branch. The derived parameters are summarized in Table 8.3.
Secondly the terminal velocity with a certain mean diameter is calculated by interpolating between the two branches in the logaritgmic scale of the diameter. Here we practically use the mean diameter weighted by the kth moments of DSD in the interpolation. The formulation of the weighted terminal velocities of the rain droplets and solid particles are as shown in the following,

$$
\begin{aligned}
\bar{v_{k,nq}} &= w_{k,nq} v_k, \bar{lrg}, nq + (1 - w_{k,nq}) v_{k,\bar{lrg},nq}, \quad (nq = r, i, s, g) && (8.214)\\
w_{k,r} &= 0.5(1 + tanh(\pi ln(\bar{D_{k,r}} / D_{0,k,r}))) \\
w_{k,js} &= max(0.0, \; min(1.0, 0.5(1 + ln(\bar{D_{k,js}} / D_{0,k,js})))) \quad (js = i, s, g) \\
\bar{D_{k,nq}} &= \frac{\int_0^\infty D_{nq}(x) x^k f_{nq}(x) dx}{\int_0^\infty x^k f_{nq}(x) dx} \\
&= \bar{D_{nq}} \frac{\Gamma\left(\frac{v_{nq}+b_{m,nq}+k+1}{\mu_{nq}}\right)}{\Gamma\left(\frac{v_{nq}+k+1}{\mu_{nq}}\right)} \left[\frac{\Gamma\left(\frac{v_{nq}+1}{/mu_{nq}}\right)}{\Gamma\left(\frac{v_{nq}+2}{\mu_{nq}}\right)} \right]^{b_{m,nq}} && (8.215)\\
\bar{v_{k,sml},r} &= \frac{f_{vt,r}}{M_r^k} \int_0^\infty \left[a_{R_s} D (1 - exp(-b_{R_s} D)) \right] x^k N_r(D) dD \\
&= a_{R_s} \frac{(1 + \mu_{D,r} + 3k)}{\lambda_{D,r}} \\
&\times \left[1 - \left(1 + \frac{b_{R_s}}{\lambda_{D,r}} \right)^{-2-\mu_{D,r}-3k} \right] \left(\frac{\rho_0}{\rho} \right)^{1/2} && (8.216)\\
\bar{v_{k,lrg},r} &= \frac{f_{vt,r}}{M_r^k} \int_0^\infty \left[a_{Rl} - b_{Rl} exp(-c_{Rl} D) \right] x^k N_r(D) dD \\
&= a_{Rl} - b_{Rl} \left(1 + \frac{c_{Rl}}{\lambda_{D,r}} \right)^{-1-\mu_{D,r}-3k} \left(\frac{\rho_0}{\rho} \right)^{1/2} && (8.217)\\
N_r(D) &= N_{0,r} D^{-\mu_{D,r}} exp(-\lambda_{D,r} D) && (8.218)
\end{aligned}
$$

where $D_{0,r}$ and $D_{0,js}$ are the branch points of the fitting curves (see Table 8.4). Here we apply the form of the modified gamma distribution for the diameter as a DSD of rain droplets. Derivation and correspondences of the coefficient $N_{0,r}$ the slope parameter λ_D,r and shape parameter μD appeared in the modified gamma distribution are described in Appendix B. Weighted terminl velocities of ice particles for two branches, and, are calculated by eq.8.213. Fig.8.3 shows the terminal velocity of rain droplets weighted by number and mass concentration. Our method gives better results than the results by the approximated method applied in Seifert and Beheng (2006) in the range within their upper and lower limit. Fig.8.4 shows terminal velocities of ice particles weighted by the number and the mass concentration.

Table 8.3: Coefficients and exponents of the relationship between the mass and the terminal velocity of each hydrometeor used in the gravitational sedimentation and other processes.

Hydrometeors	Sedimentation of mass	Sedimentation of mass	Sedimentation of number	Sedimentation number	other process
	Small	Large	Small	Larg	
Cloud	$a_v = 3.75 \times 10^5, b_v = 2/3$	$a_v = 3.75 \times 10^5, b_v = 2/3$	$a_v = 3.75 \times 10^5, b_v = 2/3$	$a_v = 3.75 \times 10^5, b_v = 2/3$	$a_v = 3.75 \times 10^5, b_v = 2/3$
Rain	8.193	8.193	8.193	8.193	8.193
Hexagonal plate	$a_v = 5800, b_v = 0.505$	$a_v = 167, b_v = 0.325$	$a_v = 1.24 \times 10^5, b_v 0.549$	$a_v = 422, b_v = 0.385$	$a_v = 5800, b_v = 0.505$
Hexagonal columns	$a_v = 2900, b_v = 0.466$	$a_v = 32.2, b_v = 0.224$	$a_v = 9698, b_v 0.531$	$a_v = 64.2, b_v = 0.274$	$a_v = 2900, b_v = 0.466$
Aggregates of planar polycrystals	$a_v = 1.52 \times 10^5, b_v = 0.528$	$a_v = 306.0, b_v = 0.330$	$a_v = 2.93 \times 10^5, b_v 0.567$	$a_v = 818, b_v = 0.394$	$a_v = 1.52 \times 10^5 b_v = 0.528$
Lump graupel	$a_v = 1.55 \times 10^5, b_v = 0.535$	$a_v = 312.0, b_v = 0.330$	$a_v = 2.76 \times 10^5, b_v 0.571$	$a_v = 698, b_v = 0.387$	$a_v = 1.55 \times 10^5 b_v = 0.535$

Table 8.4: Branch points of the weighted terminal velocity.

Hydrometeors	Branch points of the weighted terminal velocity [m]
Cloud	Not used
Rain	$D_{0,r} = 7.45 \times 10^{-4}$
Hexagonal plates	$D_{0,0,i} = 262 \times 10^{-6}, D_{0,1,i} = 399 \times 10^{-6}$
Hexagonal columns	$D_{0,0,i} = 240.5 \times 10^{-6}, D_{0,1,i} = 330 \times 10^{-6}$
Aggrgates of planar polycrystals	$D_{0,0,s} = 270 \times 10^{-6}, D_{0,1,s} = 270 \times 10^{-6}$
Lump graupel	$D_{0,0,g} = 269 \times 10^{-6}, D_{0,1,g} = 376 \times 10^{-6}$

Detailed description of cloud microphysics

Cloud microphysics is mainly categorized into two physics. One is phase change among the gas, liquid, and solid phases. Another is the collection process among all the particles. In addition, all the hydrometeors are vertically transported by gravitational sedimentation. Phase change depends on the thermodynamics of environment air and affects thermodynamics itself through latent heat release. In contrast, collection is an internal growth process with less interaction with the atmosphere. Since the growth speed of the collection process is much faster than that of phase change, the role of the collection process is a key to determine the lifetime of cloud (e.g. lifetime effect). Finally, gravitational sedimentation determines the removal rate of cloud from the atmosphere. Directly it removes cloud by transportation, and indirectly by the collection process via collision volume (swept volume).
The cloud microphysics scheme developed in this study basically follows Seifert and Beheng (2006). Their two-moment bulk cloud microphysics scheme is remarkable in improvement of the collection process by using a bin cloud mi-

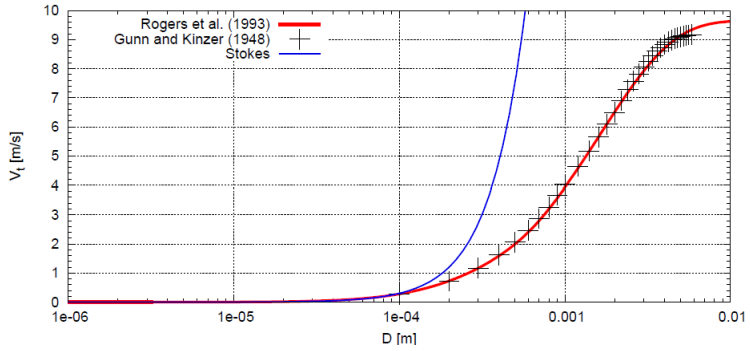

Figure 8.1: Dependency of terminal velocity of liquid water droplet on diameter. Marks are from Gunn and Kinzer (1948), red line is from Rogers et al. (1993) and blue line is calculated by Stokes law (eq.8.191) under the condition T=293K, p=1000hPa.

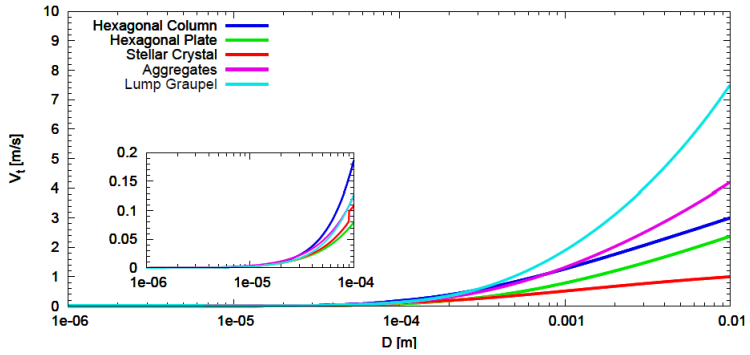

Figure 8.2: Dependency of terminal velocity of liquid water droplet in maximum dimension. Each color of solid line is corresponding to different ice particle type based on Mitchell (1996). Hexagonal columns is blue, hexagonal plates is green, stellar crystal with broad arms is red, Aggregates of planar polycrystals in cirrus clouds is purple and lump graupel is light blue.

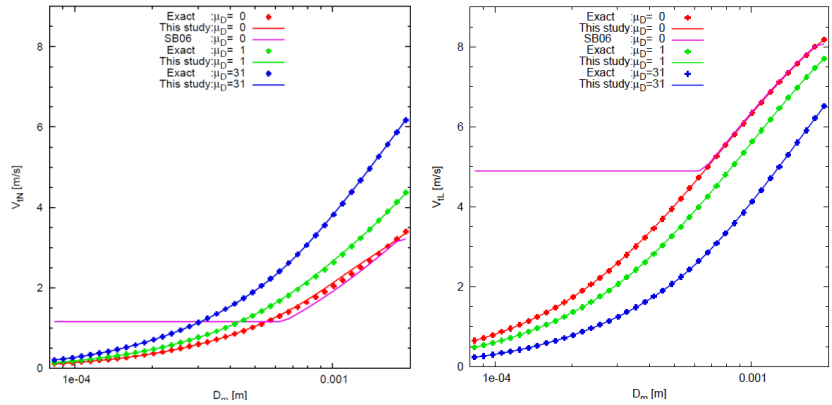

Figure 8.3: Dependencies of number weighted terminal velocity (v_{tN}) (left) and mass weighted terminal velocity (v_{tL}) (right) of rain droplets on mean volume diameter (D_m). Abscissa is the mean volume diameter and vertical axis is the terminal velocity. Dots show exactly integrated value and solid lines show approximated value by this study (red, green and blue) and Seifert and Beheng (2006) (purple). Red and purple ones are calculated with $\mu D = 0$, green ones are calculated with $\mu D = 1$ and blue ones are calculated with $\mu D = 31$.

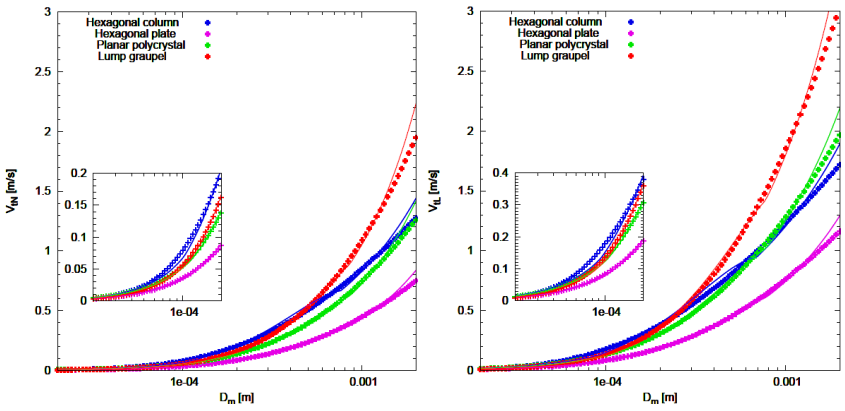

Figure 8.4: Dependencies of number weighted terminal velocity (v_{tN}) (left) and mass weighted terminal velocity (v_{tL}) (right) of ice particles on mean volume diameter (D_m). Abscissa is the mean volume diameter and vertical axis is the terminal velocity. Dots show the exact value calculated by Mitchell (1996) and solid lines show the fitting curves. Red, green, blue and purple denote lump graupels, assemblages of planar polycrystals, hexagonal columns and hexagonal plates respectively.

crophysics scheme. After their works, we modify the cloud nucleation process (Twomey 1959; and Lohmann 2002), the condensation process (Morrison et al. 2005), and the formulation of the terminal velocities (Mitchell, 1996) with expectation of the application to global cloud resolving simulations. We describe production and reduction terms of the mass concentration and the number concentration in the following sub-sections.

Phase change

Condensation/evaporation

Theoretical formulation of condensation or evaporation is basically derived by balance equation of vapor and thermal diffusion above the surface of a single particle (Rogers and Yau, 1989; Pruppacher and Klett, 1997). The growth rate of liquid droplet mass x_il is described as follows,

$$\begin{aligned} \frac{dx_{jl}}{d} &= 2\pi D(x_{jl}) G_{lv}(T,p) F_{vf}(x_(jl)) S_w, \ (jl = c, r) && (8.219) \\ G_{lv} &= \Big[\frac{R_v T}{p_{sw}(T) D_v} + \frac{L_{v0}}{K_T T}\big(\frac{L_{v0}}{R_v} T - 1\big)\Big]^{-1} && (8.220) \\ F_{vf}(x_r) &= a_{vf,r} + b_{vf,r} N_{S_c}^{1/3} N_{R_e}^{1/2} && (8.221) \end{aligned}$$

Here G_{lv} is a coefficient related with vapor and thermal diffusion, D_v is diffusivity of water vapor and K_T is thermal conductivity, and F_{vf} is the so-called ventilation coefficient. This is a correction factor for assumption that the water vapor field surrounding each droplet is spherically symmetrical. Formulation of Fvf was experimentally determined by Pruppacher and Klett (1997) and it depends on Schmidt number (N_{S_c}) and Reynolds number (N_{R_e}). This formulation for single droplets is transformed into that for moments following to Seifert and Beheng (2006). With assumption of DSD as a generalized Gamma distribution and neglecting the change of DSD caused by other process in a time step, we can derive the growth rate of moments,

$$\frac{\partial M_{jl}^k}{\partial t}\Big|_{cnd,evp} \cong \int_0^\infty f_{jl}(x) x^{k-1} \frac{\partial x}{\partial t}\Big|_{cnd,evp} dx \qquad (8.222)$$

we can consider eq.8.222 from a different view point as follows,

$$\begin{aligned} \frac{\partial M_{jl}^k}{\partial t}\Big|_{cnd,evp} &\cong \int_0^\infty f_{jl}(x) x^k \Big[\frac{1}{x}\frac{\partial x}{\partial t}\Big|_{cnd,evp}\Big] dx \\ &= \int_0^\infty \frac{f_{jl}(x) x^k}{\tau} dx, \ \tau \equiv \frac{x}{\frac{\partial x}{\partial t}\big|_{cnd,evp}} && (8.223) \end{aligned}$$

Here, we mention that the theoretical treatment of condensation or evaporation change droplet mass only. Then, we diagnose the growth rates of other moments by the change ratio of droplet mass with time scale τ. Thus, we can derive the growth equation for arbitrary moments,

$$\left.\frac{\partial M_{jl}^k}{\partial t}\right|_{cnd,evp} = 2\pi G_{lv} S_w \int_0^\infty D_{jl}(x) F_{vf,jl}(x) f_{jl}(x) x^{k-1} dx$$
$$= 2\pi G_{lv} S_w N_{jl} D_{jl}(\bar{x}_{jl}) \bar{F}_{vf,k,jl}(\bar{x}_{jl}) \bar{x}_{jl}^{k-1} \quad (8.224)$$

where $\bar{F}_{vf,k,il}$ is an averaged ventilation factor for the k-th moment of DSD. This formulation seems to be valid unless reduction of number concentration occurs. Because reduction of number concentration occurs only in the case of the smallest droplet being completely dissipated by evaporation, the formulation by change ratio is not suitable for complete dissipation. Therefore this formulation is incomplete to derive the reduction tendency of number concentration by evaporation (condensation never changes number concentration). Temporarily, we assumed that the number concentration of cloud droplets never reduces unless their mean mass of cloud ($\bar{x}_c$) falls below the lower limit $\bar{x}_{c,min}$. The treatment of rain droplets is discussed in the following section.

Evaporation of rain droplets

Only in the case of rain droplets, Seifert (2008) attempted to overcome the incompleteness for the reduction of number concentration in evaporation. He reformulated eq.8.224 as follows,

$$\left.\frac{\partial N_r}{\partial t}\right|_{evp} \equiv \gamma_{evp} \frac{N_r}{L_r} \frac{\partial L_r}{\partial t} = \frac{\gamma_{evp}}{\bar{x}} 2\pi G_{lv} S_w N_r D_r(\bar{x}_r) \bar{F}_{vf,l}(\bar{x}_r) \quad (8.225)$$

Here evaporation parameter γ_{evp} means the evaporation efficiency of number concentration towards to mean mass $\bar{x}_r$. According to Seifert (2008), γ_{evp} and $\mu_{m,r}$ are parameterized as follows,

$$\gamma_{evp} = \frac{D_{eq}}{D(\bar{x}_r)} exp(-0.2\mu_{m,r}) \quad (8.226)$$

$$\mu_{m,r} = \begin{cases} 6tauh[c_{evp,1}(D(\bar{x}_r) - D_{eq})^2] + 1 & (D(\bar{x}_r) \leq D_{eq}) \\ 30tauh[c_{evp,2}(D(\bar{x}_r) - D_{eq})^2] + 1 & (D(\bar{x}_r) \leq D_{eq}) \end{cases} \quad (8.227)$$

where $D_{eq} = 1.1 \times 10^{-3} m$ is the equilibrium diameter in breakup-coalescence processes and the $c_{evp,1}$ and $c_{evp,2}$ are set to 4000 m^{-1} and 1000 m^{-1}, respectively. In this study, we apply eq.8.224 for mass and eq.8.225 with $\gamma_{evp} = 1$ for number concentration as a default setting (refer to SB06-run).

Deposition/sublimation for solid water

Theoretical formulation of deposition or sublimation is the same as that of condensation or evaporation except for the definition of surface area. The shape of ice particles is not spherical and varies widely as is shown in section 2.1.2. Therefore, vapor and thermal transfer over the particle surface is expressed by the analogy between the diffusion equation and equations in electrostatics (Pruppacher and Klett, 1997). Replacing diameter D_{js} by capacitance $C_{js} \equiv Djs/c_{js}$, we can derive the growth equation of a single particle as follows,

$$\frac{dx_{js}}{dt}\Big|_{dep,sbl} = 4\pi C_{js} G_{sv}(T,p) F_{vf}(x_{js}) S_i, \quad (js = i,s,g) \tag{8.228}$$

$$G_{sv} = \Big[\frac{R_v T}{p_{si}(T) D_v} + \frac{L_{s,0}}{K_T T}\big(\frac{L_{s0}}{R_v T} - 1\big)\Big]^{-1} \tag{8.229}$$

Here $C_{js} = D_{js}/2$ for sphere, $C_{js} = D_{js}/\pi$ for circular plate, and capacitances of other typical shapes such as oblate spheroid crystals and columnar crystals are expressed by,

$$C_{js} = \frac{D_{js}\varepsilon}{2sin^{-1}\varepsilon}, \ \varepsilon \equiv \big(1 - \frac{b^2}{a^2}\big), \ (for\ spheroid) \tag{8.230}$$

$$C_{js} = \frac{A}{ln[(a+A)/b]}, \ A \equiv= (a^2 - b^2)^{1/2}, \ \ (for\ columnar) \tag{8.231}$$

where a is semi-major axis and b is semi-minor axis. For simplification, cloud, rain, snow and graupel are assumed as sphere and hexagonal plate ice is assumed as circular plate here. In the same manner as condensation (evaporation), we can derive the growth equation of arbitrary moments as follows,

$$\frac{\partial M_{js}^k}{\partial t}\Big|_{dep,sbl} = \frac{4\pi}{c_{js}} G_{sv} S_i N_{js} D_{js}(\bar{x}_{js}) \bar{F}_{vf,k}(\bar{x}_{js}) \bar{x}_{js}^{k-1} \tag{8.232}$$

Discussion concerning the reduction term of number concentration is the same as that for rain droplets. Therefore, we applied eq.8.232 for mass concentration of solid particles. For snow and graupel, the reduction rate of number concentration is as follows,

$$\begin{aligned} \frac{\partial N_{js}^k}{\partial t}\Big|_{sbl} &\equiv \frac{N_{js}}{L_{js}} \frac{\partial L_{js}}{\partial t}\Big|_{sbl} \\ &= \frac{1}{\bar{x}_{js}} \frac{4\pi}{c_{js}} G_{sv} S_i N_{js} D_{js}(\bar{x}_{js}) \bar{F}_{vf,1}(\bar{x}_{js}) (js = s,g) \end{aligned} \tag{8.233}$$

This formulation corresponds to $\gamma_{evp} = 1$ in the reduction term for rain droplets. That means sublimation occurs so as not to change the mean mass of DSD ($\bar{x}_{js}$). Number concentration of ice never reduces in sublimation unless the mean mass of ice ($\bar{x}_i$) falls below the lower limit. The formulations of the reduction rate for the number concentration of ice particles are somewhat temporary and will be improved by the insights drawn from the results of microphysics bin schemes and observations in future work.

Accurate integration method to solve condensation/evaporation and deposition/sublimation

The condensation/evaporation process for cloud droplets usually requires a smaller time step than rain droplets or other particles because of its timescale. When we apply the time integration with the first ordered Euler method, the accuracy of the condensation/evaporation and the deposition/sublimation processes are worse unless we resolve their timescale. We estimate the timescale

with the exact thermodynamic definition in NICAM initially and then formulate an accurate method to apply the condensation process and the evaporation process for cloud droplets similar to Khvorostyanov and Sassen (1998) and Morrison et al., (2005). Since the supersaturated condition is achieved by updraft of air mass, we consider a Lagrangian parcel model with constant updraft velocity and no mixing with external air mass. Basic formulation is based on the Lagrangian change rate of supersaturation ($\delta_{sw} = q_v - q_{sw}$) as follows,

$$\frac{d\delta_{sw}}{dt} = \Big(\frac{dq_v}{dt} - \frac{dq_{sw}}{dt}\Big) \tag{8.234}$$

Hereafter we consider the tendency of specific humidity and saturation specific humidity by dynamics, cloud microphysics and radiative heating.
At first, assuming an adiabatically ascending/descending parcel with no phase change ($q_v/dt = 0$), eq.(8.234) becomes

$$\frac{d\delta_{sw}}{dt} = -\big(\frac{\partial q_{sw}}{\partial T}\big)_p \frac{dT}{dt} - \big(\frac{\partial q_{sw}}{\partial p}\big)_T \frac{dp}{dt} \tag{8.235}$$

Here the tendencies of temperature and pressure are described as follows,

$$\frac{dT}{dt} = \frac{1}{\rho \bar{c}_p}\frac{dp}{dt}, \quad \frac{dp}{dt} \approx -\rho g w \tag{8.236}$$

where $\bar{c}_p \equiv q_d c_{pd} + q_v c_{pv} + q_{liq} c_l + q_{sol} c_i$ is the mean specific heat at constant pressure. We can derive the dynamic component of the tendency of δ_{sw} by substituting eq. 8.236 into eq.8.235 as follows

$$\frac{d\delta_{sw}}{dt}\Big|_{DYN} = wg\Big(\frac{1}{\bar{c}_p}\big(\frac{\partial q_{sw}}{\partial T}\big)_p + \rho\big(\frac{\partial q_{sw}}{\partial p}\big)_T\Big) \tag{8.237}$$

Assuming air parcel with only cooling/heating by latent heat release, eq. 8.234 becomes

$$\frac{d\delta_{sw}}{dt} = \frac{dq_v}{dt} - \big(\frac{\partial q_{sw}}{\partial T}\big)\frac{dT}{dt} \tag{8.238}$$

The tendency of temperature is caused by latent heat release with condensation/evaporation and deposition/sublimation

$$\begin{aligned}
\frac{dT}{dt} &= \frac{L_{v,00} + (c_{vv} - c_l)T}{\bar{c}_{va}}\frac{dq_{liq}}{dt} + \frac{L_{v,00} + L_{f,00} + (c_v - c_i)T}{\bar{c}_{va}}\frac{dq_{sol}}{dt} \\
&= \frac{L_{v,00} + (c_{vv} - c_l)T}{\bar{c}_{va}} \sum_{jl=1}^{jl_{max}} \frac{dq_{jl}}{dt}\Big|_{cnd,evp} \\
&+ \frac{L_{v,00} + L_{f,00} + (c_{vv} - c_i)T}{\bar{c}_{va}} \sum_{js=1}^{js_{max}} \frac{dq_{js}}{dt}\Big|_{dep,sbl}
\end{aligned} \tag{8.239}$$

The tendency of specific humidity is caused by condensation/evaporation and deposition/sublimation,

$$\frac{dq_v}{dt} = -\sum_{jl=1}^{jl_{max}} \frac{dq_{jl}}{dt}\Big|_{cnd,evp} - \sum_{js=1}^{js_{max}} \frac{dq_{js}}{dt}\Big|_{dep,sbl} \tag{8.240}$$

Then, we can derive the cloud microphysics component of the tendency of δ_{sw} by substituting eq.8.239 and eq.8.240 into eq.8.238,

$$\begin{aligned}\frac{d\delta_{sw}}{dt}\Big|_{MP} &= -\Big(1 + \frac{L_{v,00} + (c_{vv} - c_l)T}{\bar{c}_v}\big(\frac{\partial q_{sw}}{\partial T}\big)_p\Big) \sum_{jl=1}^{jl_{max}} \partial dq_{jl} dt\Big|_{cnd,evp} \\ &- \Big(1 + \frac{L_{v,00} + L_{f,00} + (c_{vv} - c_i)T}{\bar{c}_v}\big(\frac{\partial q_{sw}}{\partial T}\big)_p\Big) \sum_{js=1}^{js_{max}} \frac{dq_{js}}{dt}\Big|_{dep,sbl}\end{aligned} \tag{8.241}$$

By replacing the source term of the mixing ratio of hydrometeors in eq.8.241 with eq.8.224 and eq.8.232

$$\begin{aligned}\frac{dq_{jl}}{dt}\Big|_{cnd,evp} &= \frac{\delta_{sw}}{\tau_{cnd,jl}},\ or \\ \frac{dq_{jl}}{dt}\Big|_{cnd,evp} &= \frac{\delta_{si}}{\tau_{cnd,jl}} - \frac{q_{sw} - q_{si}}{\tau_{cnd,jl}},\ \ (jl = c, r) \qquad (8.242) \\ \frac{dq_{js}}{dt}\Big|_{de,sbl} &= \frac{\delta_{si}}{\tau_{dep,js}},\ or \\ \frac{dq_{js}}{dt}\Big|_{dep,sbl} &= \frac{\delta_{sw}}{\tau_{dep,js}} + \frac{q_{sw} - q_{si}}{\tau_{dep,js}},\ \ (js = i, s, g) \qquad (8.243) \\ \tau_{cnd,jl} &\equiv \Big(\frac{1}{\rho q_{sw}} 2\pi G_{lv} D_{jl}(\bar{x}_{jl}) N_{jl} \bar{F}_{vf,1}\Big)^{-1} \qquad (8.244) \\ \tau_{dep,js} &\equiv \Big(\frac{1}{\rho q_{si}} \frac{4\pi}{c_{js}} G_{sv} D_{js}(\bar{x}_{js}) N_{js} \bar{F}_{vf,1}\Big)^{-1} \qquad (8.245)\end{aligned}$$

We can rewrite eq.8.241 as a function of super saturation itself,

$$\begin{aligned}\frac{\partial \delta_{sw}}{\partial t}\Big|_{MP} = &- \big(\frac{a_{liq,liq}}{\tau_{cnd,c}} + \frac{a_{liq,liq}}{\tau_{cnd,r}} + \frac{a_{sol,liq}}{\tau_{dep}} + \frac{a_{sol,liq}}{\tau_{dep,s}} + \frac{a_{sol,liq}}{\tau_{dep,g}}\big)\delta_{sw} \\ &- \big(\frac{1}{\tau_{dep,i}} + \frac{1}{\tau_{dep,s}} + \frac{1}{\tau_{dep,g}}\big)(q_{sw} - q_{si}) \qquad (8.246) \\ a_{liq,liq} &\equiv 1 + \frac{L_{v00} + (c_{vv} - c_l)T}{\bar{c}_v}\big(\frac{\partial q_{sw}}{\partial T}\big)_p \qquad (8.247) \\ a_{sol,liq} &\equiv 1 + \frac{L_{v00} + L_{f00} + (c_{vv} - c_i)T}{\bar{c}_v}\big(\frac{\partial q_{sw}}{\partial T}\big)_p \qquad (8.248)\end{aligned}$$

Here, we can find that $\tau_{cnd,jl}$ and $\tau_{dep,js}$ in eq.8.246 are considered as the characteristic time scale to relax the super saturation condition by the condensation/evaporation and deposition/sublimation processes. The timescale of each hydrometeor is modified by coefficient $a_{liq,liq}$ or$a_{sol,liq}$, which means the effect of

latent heat release. The second term on the right hand side in eq.8.246 means the transfer of vapor from liquid droplets to solid particles. The Bergeron-Findeisen process is implicitly formulated by the difference of saturation vapor pressure between liquid and solid.
Finally assuming an air parcel with radiative heating (cooling), eq.8.234 becomes

$$\frac{d\delta_{sw}}{dt}\Big|_{RAD} = -\big(\frac{\partial q_{sw}}{\partial T}\big)_{\rho}\big(\frac{dT}{dt}\big)_{RAD} \tag{8.249}$$

All the components in the Lagrangian ascending/descending parcel model are described by eq.8.237, eq.8.246 and eq.8.249,

$$\begin{aligned}
\frac{d\delta_{sw}}{dt} &= A_{cnd} - \frac{\delta_{sw}}{\tau_{cnd}} && (8.250)\\
A_{cnd} &\equiv \frac{d\delta_{sw}}{dt}\Big|_{DYN} + \frac{d\delta_{sw}}{dt}\Big|_{RAD} \\
&- \big(\frac{1}{\tau_{dep,i}} + \frac{1}{\tau_{dep,s}} + \frac{1}{\tau_{dep,g}}\big)(q_{sw} - q_{si}) && (8.251)\\
\tau_{cnd} &\equiv \big(\frac{a_{liq,liq}}{\tau_{cnd,c}} + \frac{a_{liq,liq}}{\tau_{cnd,r}} + \frac{a_{sol,liq}}{\tau_{dep,i}} + \frac{a_{sol,liq}}{\tau_{dep,s}} + \frac{a_{sol,liq}}{\tau_{dep,g}}\big)^{-1} && (8.252)
\end{aligned}$$

Here, we can see that A_{cnd} is a production term of super saturation and cnd is a characteristic timescale of all the phase changes. From their formulation (eq.8.244 and eq.8.245), we can find that the timescale of each hydrometeor is in inverse proportion to its number concentration. The timescales under various conditions are shown in Fig.8.7.
Assuming that time variance of the production term and the timescale in a simulation time step dont vary much within a model timestep, we can analytically solve eq.8.250,

$$\delta_{sw}(t) = A_{cnd}\tau_{cnd} + (\delta_{sw}(t_0) - A_{cnd}\tau_{cnd})exp\big(-\frac{t}{\tau_{cnd}}\big) \tag{8.253}$$

where $t = t_0 + \Delta t$ and $t_0 = 0$. Then, the condensation (evaporation) rate of cloud and rain are reformulated by substituting eq.8.253 into eq.8.224 and integrating them,

$$\begin{aligned}
\frac{\Delta L_{jl}}{\Delta t}\Big|_{cnd,evp} &= \rho A_{cnd}\frac{\tau_{cnd}}{\tau_{cnd,jl}} \\
&- \rho\frac{(\delta_{sw}(t_0) - A_{cnd}\tau_{cnd})}{\Delta t}\frac{\tau_{cnd}}{\tau_{cnd,jl}}\Big[exp\big(-\frac{\Delta t}{\tau_{cnd}}\big) - 1\Big] && (8.254)
\end{aligned}$$

This semi-analytical formulation takes time variability of super saturation into condensation (evaporation) growth. Therefore, it is better than direct time integration with a first order Euler method.
In the same manner, we can also derive the semi-analytical formulation for deposition (sublimation) with super saturation for solid water (δ_{si}),

$$\delta_{si}(t) = A_{dep}\tau_{dep} + (\delta_{si}(t_0) - A_{dep}\tau_{dep})exp\big(-\frac{t}{\tau_{dep}}\big) \quad (8.255)$$

$$\frac{\Delta L_{js}}{\Delta t}\Big|_{dep,sbl} = \rho A_{dep}\frac{\tau_{dep}}{\tau_{dep,js}} - \rho\frac{(\delta_{si}(t_0) - A_{dep}\tau_{dep})}{\Delta t}\frac{\tau_{dep}}{\tau_{dep,js}}\Big[exp\big(-\frac{\Delta t}{\tau_{dep}}\big) - 1\Big] \quad (8.256)$$

where

$$A_{dep} \equiv \frac{d\delta_{si}}{dt}\Big|_{DYN} + \frac{d\delta_{si}}{dt}\Big|_{RAD} + \big(\frac{1}{\tau_{cnd,c}} + \frac{1}{\tau_{cnd,r}}\big)(q_{sw} - q_{si}) \quad (8.257)$$

$$\tau_{dep} \equiv \big(\frac{a_{liq,sol}}{\tau_{cnd,c}} + \frac{a_{liq,sol}}{\tau_{cnd,r}} + \frac{a_{sol,sol}}{\tau_{dep,i}} + \frac{a_{sol,sol}}{\tau_{dep,s}} + \frac{a_{sol,sol}}{\tau_{dep,g}}\big)^{-1} \quad (8.258)$$

$$a_{liq,sol} \equiv 1 + \frac{L_{v00} + (c_{vv} - c_l)T}{\bar{c}_v}\big(\frac{\partial q_{si}}{\partial T}\big)_p$$

$$a_{sol,sol} \equiv 1 + \frac{L_{v00} + L_{f00} + (c_{vv} - c_i)T}{\bar{c}_v}\big(\frac{\partial q_{si}}{\partial T}\big)_p$$

$$\frac{d\delta_{si}}{dt}\Big|_{DYN} = wg\Big(\frac{1}{\bar{c}_p}\big(\frac{\partial q_{si}}{\partial T}\big)_p + \rho\big(\frac{\partial q_{si}}{\partial p}\big)_T\Big)$$

$$\frac{d\delta_{si}}{dt}\Big|_{RAD} = -\big(\frac{\partial q_{si}}{\partial T}\big)_\rho\big(\frac{dT}{dt}\big)_{RAD}$$

Finally we applied eq.8.254 and eq.8.256 for the prediction of mass concentration and eq.8.225 and eq.8.233 for the prediction of number concentrations of rain, snow and graupel. Number concentrations of cloud and ice are assumed not to change by evaporation and sublimation.

Nucleation of cloud droplets

Seifert and Beheng (2006) applied traditional empirical formulation as an aerosol activation spectrum as follows,

$$N_c(S_{w,100}) = C_{ccn}S_{w,100}^{\kappa_{ccn}} \quad (8.259)$$

where super saturation ratio $S_{w,100}$ is in . They use $C_{ccn} = 1.26 \times 10^9 m^{-3}$ and $\kappa_{ccn} = 0.308$ in continental conditions and $C_{ccn} = 1.0 \times 10^8 m^{-3}$ and $\kappa_{ccn} = 0.462$ in maritime conditions. Further, Seifert and Beheng (2006) transformed eq.8.259 into a tendency formulation by time differentiation of the activation spectrum,

$$\frac{\partial N_c}{\partial t} = \begin{cases} C_{ccn}\kappa_{ccn}S_{w,100}^{\kappa_{ccn}-1}\frac{\partial S_{w,100}}{\partial z}w \\ (S_{w,100} > 0,\ w\frac{\partial S_{w,100}}{\partial z} > 0,\ and\ S_{w,100} < 1.1) \\ 0,\ \ (else) \end{cases}$$

$$\frac{\partial L_c}{\partial t}\Big|_{nuc} = x_{c,nuc}\frac{\partial N_c}{\partial t}\Big|_{nuc} \quad (8.260)$$

where $x_{c,nuc} = 10^{-12}kg$ is an arbitrary mass of nucleated droplets. Because the aerosol activity spectrum is a function of supersaturation and unbounded by the total aerosol number concentration, we chose an upper limit of activated aerosols as $1.5 \times C_{ccn}$, as similarly chosen by SB06: The maximum acticated aerosol number concentration is 1.5 times of the activated aerosol number concentration at ssw = 1 $^{o}/_{o}$. Here, we should mention that this formulation depends on the grid value of super saturation ratio, vertical velocity and vertical derivation of the super saturation ratio. Since super saturation significantly varies in tens of meters above cloud base (see Fig.8.9), accurate prediction of super saturation and its vertical derivation is quite difficult. In this study, we applied a traditional nucleation scheme (Twomey, 1959; Rogers and Yau, 1989) following Morrison et al. (2005),

$$N_{c,nuc}(w_{eff}) = 0.88 C_{ccn}^{2/(\kappa_{ccn}+2)} (0.07 w_{eff}^{3/2})^{\kappa_{ccn}/(\kappa_{ccn}+2)} \quad (8.261)$$

$$w_{eff} \equiv w + w_{TB} - \frac{\bar{c}_p}{g} \Big(\frac{dT}{dt}\Big)_{RAD} \quad (8.262)$$

where w_{eff} is effective vertical velocity for nucleation and w_{TB} is the sub-grid variability of terminal velocity. This is an analytical formulation of maximum number concentration around the cloud base for the Twomey equation with aerosol activated spectrum by eq.8.259 (see Fig.8.6). By using this scheme we do not have to resolve the vertical variability of super saturation around the cloud base. Furthermore, applying sub-grid turbulence effects on vertical velocity reduces under estimation of nucleated cloud number concentration caused by low horizontal resolution (Ghan, et al., 1997; Lohmann, 2002; Morrison and Pinto, 2005). In this study, implementation of the sub-grid turbulence effect follows Lohmann (2002),

$$w_{TB} = c_{TB} \Big(\frac{2}{3} TKE\Big)^{1/2} \quad (8.263)$$

$$\bar{N}_{c,nucl} = 0.1 \times N_{c,nuc}(w_{eff})^{1.27} \quad (8.264)$$

where $c_{TB} = 1$ is used in this study, $\bar{N}_{c,nuc}\ cm^{-3}$ is a grid averaged nucleated cloud number concentration and $N_{c,nuc}(w_{eff}) cm^{-3}$ is maximum cloud number concentration in turbulent air. By substituting eq.8.261, eq.8.262 and eq.8.263 into eq.8.264, the tendency of cloud number concentration is calculated by,

$$\frac{\partial N_c}{\partial t}\Big|_{nucl} = \begin{cases} \frac{N_{c,nu}(w_{eff}) - N_c}{\Delta t}, & (S_w > 0,\ \bar{N}_{c,nuc} > N_c \ and\ at\ cloud\ base) \\ 0, & (else) \end{cases} \quad (8.265)$$

$$\frac{\partial L_c}{\partial t}\Big|_{nuc} = min\Big(x_{c,min} \frac{\partial N_c}{\partial t}|_{nuc}, \frac{\delta_{sw}}{\Delta t}\Big) \quad (8.266)$$

Since nucleation is usually limited around the cloud base within several tens of meters (see Fig.8.9), we define cloud base layer (k_{cbase}) where the nucleation scheme works as follows,

$$1.5 \times C_{ccn} > \bar{N}_{c,nu}(k_{cbase}) > 0, \ \ and \ \ \bar{N}_{c,nu}(k_{cbase} - 1) < 10^6 \quad (8.267)$$

In addition, we prepare the option (NO-TB) to switch off the effect of turbulence by substituting eq.8.261, eq.8.262 with $w_{TB} = 0$ into eq.8.265. There remain some problems to be solved in future,
1.Definition of cloud base is empirical and arbitrary
2.Implementation of sub-grid scale is empirical and c_{TB} is a kind of tuning parameter. In particular, the TKE approach only considers isotropic eddies. Sub-grid should be expressed as sub-grid cloud dynamics.
3.Formulation of eq.8.264 does not converge with the NO-TB option when TKE = 0.
We need to investigate the above problems by using a large eddy simulation (LES) cloud model.

Nucleation of cloud ice

This study employed two simple ice nucleation schemes, which dont require the properties of ice nuclei. One is the depositional and condensational freezing nucleation scheme parameterized by Meyers et al. (1992),

$$N_{IN} = 10^3 exp(-0.639 + 12.96 S_{sol})$$

where N_{IN} is nucleated ice nuclei, and S_{sol} is supersaturation for solid water. While this scheme is widely used in CRMs (e.g., Walko et al. 1995; Khain et al., 2000; Seifert and Beheng, 2006), this scheme could not be acceptable for conditions at temperature below -20 degC or supersaturation over 0.25 where observational data were not available in their study. For simulating cirrus clouds around the tropopause, application of this scheme to CRMs may cause significant error. Phillips et al. (2007) proposed an alternative scheme to modify Meyerss scheme by fitting to observational data at temperature between -30 degC and -80 degC taken by Demott et al. (2003),

$$N_{IN} = 10^3 exp[0.3 \times 12.96(S_i - 0.1)] \tag{8.268}$$

In this study, the nucleation rate is formulated by the newly nucleated ice nuclei with the tendency of supersaturation in the same manner as Murakami (1990),

$$\frac{\Delta N_i}{\Delta t} = \begin{cases} \frac{\partial N_{IN}}{\partial S_{sol}} \frac{\partial S_{sol}}{\partial t}, & (S_{sol} > 0 \; and \; \frac{\partial S_{sol}}{\partial t} > 0) \\ 0, & (else) \end{cases} \tag{8.269}$$

$$\frac{\partial S_{sol}}{\partial t} \approx \Big[\frac{\partial S_{sol}}{\partial z} w + \big(\frac{\partial S_{sol}}{\partial T}\big)\big(\frac{\partial T}{\partial t}\big)_{RAD} \Big]$$

$$\frac{\Delta L_i}{\Delta t}\Big|_{nuc} = \frac{\Delta N_i}{\Delta t}\Big|_{nuc} x_{IN} \tag{8.270}$$

where $x_{IN} = 10^{-12} kg$ is an arbitrary parameter for a nucleated ice nuclei mass. Here, we assume the change of supersaturation comes from the vertical motion of airmass and the radiative cooling. Meyerss scheme produces the number concentration of cloud ice more than Phillipss scheme, and the departure becomes large as supersaturation increases. This difference would come from

the sampled air masses used in observational data that their schemes referred to, and also implicit dependencies of their schemes on temperature and aerosol species. It is expected that Phillipss scheme is appropriate for the simulation of mid-latitude cirrus clouds because Phillipss scheme is based on the air mass sampled in the free troposphere at the mid-latitude while Meyerss scheme is based on the air mass sampled in the atmospheric boundary layer where ice nuclei is rich.

Freezing

The freezing process consists of two types of mechanisms. One is the homogenous freezing which is freezing of supercooled water droplets for themselves without the other agents. Another is the heterogeneous freezing, which is freezing of supercooled water droplets with insoluble part of aerosols dissolved in cloud droplets. We apply the same parameterizations of both the homogeneous freezing and the heterogeneous freezing as Seifert and Beheng (2006a). Cotton and Field (2002) parameterized homogeneous freezing rate for a single droplet by a fitting to the theoretical estimation by Jeffery and Austin (1997). We apply their parameterization as Seifert and Beheng (2006a),

$$\frac{1}{f_c(x)}\frac{\partial f_c(x)}{\partial t}\Big|_{hom} = -xJ_{hom}(T_c) \tag{8.271}$$

where J_{hom} is a homogeneous freezing rate ($kg^{-1}s^{-1}$) and T_c is centigrade temperature. J_{hom} is formulated as a function of temperature as follows,

$$log_{10}(10^{-3}J_{hom}) = \begin{cases} 25.63 - 243.4 - 14.75T_c - 0.307T_c^2, & (-65^oC > T_c) \\ -0.00287T_c^3 - 0.0000102T_c^4, & (-65^oC \leq T_c < -30^oC) \\ -7.63 - 2.996(T_c + 30), & (-30^oC < T_c) \end{cases}$$

Based on the equation for a single droplet, we can derive the equation for moments by integrating eq.8.271 as follows

$$\frac{\partial N_c}{\partial t}\Big|_{hom} = -L_cJ_{hom} = -N_c\bar{x}_cJ_{hom} \tag{8.272}$$

$$\frac{\partial L_c}{\partial t}\Big|_{hom} = -Z_cJ_{hom} = -\frac{\Gamma\left(\frac{\nu_c+3}{\mu_c}\right)\Gamma\left(\frac{\nu_c+1}{\mu_c}\right)}{\Gamma\left(\frac{\nu_c+2}{\mu_c}\right)^2}L_c\bar{x}_cJ_{hom} \tag{8.273}$$

Here, we mention that eq.8.272 and eq.8.273 are expressed via filtered $\bar{x}_c$ in order to avoid artificial value of the prognostic variables. The homogeneous freezing for rain is not considered because it is negligible compared with the heterogeneous freezing due to their largeness. Although Cotton and Field (2002) considered also freezing point depression in freezing due to soluble aerosols, we dont consider the effect because Seiki and Nakajima (2014) is not yet coupled with aerosol transport models. Heterogeneous freezing is based on the empirical formulation by Biggs (1953) which is widely used in CRMs.

$$\frac{1}{f(x)}\frac{\partial f(x)}{\partial t} = -xJ_{het}(T_c) \tag{8.274}$$

where J_{het} is the heterogeneous freezing rate. J_{het} is formulated as a function of temperature as follows,

$$J_{het} = A_{het} exp(-B_{het} T_c - 1) \tag{8.275}$$

where $A_{het} = 0.2 kg^{-1} s^{-1}$ and $B_{het} = 0.65 K^{-1}$ are empirically determined parameters. Similar to the homogeneous freezing, we can derive the equation for moments as follows,

$$\frac{\partial N_{il}}{\partial t}\Big|_{het} = -N_{il} \bar{x}_{il} J_{het} \quad (il = c, r) sn126) \tag{8.276}$$

$$\frac{\partial L_{il}}{\partial t}\Big|_{het} = -\frac{\Gamma\left(\frac{\nu_{il}+3}{\mu_{il}}\right)\Gamma\left(\frac{\nu_{il}+1}{\mu_{il}}\right)}{\Gamma\left(\frac{\nu_{il}L2}{\mu_{il}}\right)^2} L_{il} \bar{x}_{il} J_{het} \quad (il = c, r) \tag{8.277}$$

Although the heterogeneous freezing should be also formulated as a function of aerosol concentration, here we apply simple formulation because our model is not yet coupled with an aerosol transport model.
Thus, these parameterizations dont include the information of aerosols and it is considered that they assume background aerosols. The validity of the parameterization was demonstrated by Khain et al. (2001). Nevertheless their model also applied the same simple freezing parameterizations, they could represented the observational features of supercooled liquid water by Rosenfeld and Woodley (2000). Both freezing rates are shown in Fig. 8.10. The heterogeneous freezing is dominated at temperature over -35 degrees Celsius. At the temperature, supercooled liquid water is mixed with ice particles. In contrast, the homogeneous freezing rate suddenly increase below -35 degrees Celsius. Liquid water droplets have been hardly observed below the temperature of -40 degrees Celsius (Rosenfeld and Woodley, 2000). The feature can be represented by using the parameterization.

Melting

Melting process is the same as Seifert and Beheng (2006a) based on Pruppacher and Klett (1997). Theoretical treatment of this process is similar to the condensation process. The differences are
1.Time scale of evaporation of a single particle is replaced by that of fusion of a single particle.
2.Vaporization of melted particle is considered in a balance equation of vapor and thermal diffusion.
As a result, the melting rate of a single ice particle is described as follows,

$$\begin{aligned} \frac{dx_{js}}{dt}\Big|_{mlt} = & -\frac{2\pi D_{js}}{L_{f0}}\Big[K_T(T - T_0)\frac{D_T}{D_v} F_{vf}(x_{js}) \\ & + \frac{D_v L_{v0}}{R_v}\Big(\frac{p_v}{T} - \frac{p_{sw}(T_0)}{T}\Big) F_{vf}(x_{js})\Big] \quad (js = i, s, g) \end{aligned} \tag{8.278}$$

where D_T is diffusivity of heat, and $T_0 = 273.15K$ is melting point. The growth rate of moments can be formulated by using a melting time scale τ_{mlt} defined as follows,

$$\tau_{mlt} \equiv \frac{x_{js}}{\left(\frac{dx_{js}}{dt}\right)_{mlt}} \tag{8.279}$$

$$\begin{aligned}\left.\frac{\partial M_{js}^k}{\partial t}\right|_{mlt} &= -\int_0^\infty \frac{x^k f_{js}(x)}{\tau_{mlt}} dx \\ &= -\frac{2\pi}{L_{f0}}\Big[\frac{K_T D_T}{D_v}(T-T_0) + \frac{D_v L_{v0}}{R_v}\Big(\frac{p_v}{T} - \frac{p_{sw}(T_0)}{T_0}\Big)\Big] \\ &\times N_{js} D_{js}(\bar{x}_{js}) x_{js}^{n-1} \bar{F}_{vf,js}\end{aligned} \tag{8.280}$$

We mention that this scheme allows the existence of ice particles over the melting point ($T > 273.15K$) since the melting time scale of large particles can be longer than a simulation time step. Actually, ice particles are transitionally converted into liquid droplets and the type of hydrometeor is not changed in the transition. However, here we assume that ice water mass is converted into liquid water mass in a certain melting time scale and the part of liquid water mass is categorized as the other hydrometeors. Here, graupel and snow is converted into rain, and ice is converted into cloud. This formulation has a possibility to cause an artificial production of cloud or rain in melting. Validation experiments and impact assessment are necessary in future.

Collection process

The collection processes are the same as Seifert and Beheng (2001), Seifert and Beheng (2006a) and Seifert (2008). The collection processes among hydrometeors are summarized in Table 8.5. In this section, the formulations of the collection processes, auto-conversion, accretion, aggregation, riming, and their related processes are described.

Table 8.5: Hydrometeors that result from binary collision. Collecting hydrometeors are written in the 1st row and collected hydrometeors are written in the 1st column.

	cloud water	rain	cloud ice	snow	graupel
cloud water	rain	-	-	-	-
rain	rain	rain	rain($T > 273K$), graupel($T < 273K$)	rain($T > 273K$), graupel($T < 273K$)	rain($T > 273K$)
cloud ice	cloud ice	-	snow	-	-
snow	snow	-	-	snow	-
graupel	graupel	graupel($T < 273K$)	graupel	graupel	-

Self-collection, auto-conversion, and accretion

With a few assumptions and a little algebra, Seifert and Beheng (2001) derived the analytical formulations of the self-collection, auto-conversion, and accretion processes as follows,

$$\frac{\partial N_c}{\partial t}\Big|_{aut+sle} = -k_{cc}\frac{(\nu_c+2)}{(\nu_c+1)}\frac{\rho_0}{\rho}L_c^2 \tag{8.281}$$

$$\frac{\partial L_c}{\partial t}\Big|_{aut} = -\frac{k_{cc}}{20x^*}\frac{(\nu_c+2)(\nu_c+4)}{(\nu_c+1)^2}\frac{\rho_0}{\rho}L_c^2x_c^2 \tag{8.282}$$

$$\frac{\partial N_c}{\partial t}\Big|_{aut} = \frac{2}{x^*}\frac{\partial L_c}{\partial t}\Big|_{aut} \tag{8.283}$$

$$\frac{\partial N_r}{\partial t}\Big|_{aut} = -\frac{1}{2}\frac{\partial N_c}{\partial t}\Big|_{aut} = -\frac{1}{x^*}\frac{\partial L_c}{\partial t}\Big|_{aut} \tag{8.284}$$

$$\frac{\partial N_c}{\partial t}\Big|_{acc} = -k_{cr}N_cL_r\big(\frac{\rho_0}{\rho}\big)^{1/2} \tag{8.285}$$

$$\frac{\partial L_c}{\partial t}\Big|_{acc} = -k_{cr}L_cL_r\big(\frac{\rho_0}{\rho}\big)^{1/2} \tag{8.286}$$

$$\frac{\partial N_r}{\partial t}\Big|_{slc} = -k_{rr}L_rL_r\big(\frac{\rho_0}{\rho}\big)^{1/2} \tag{8.287}$$

with $k_{rr} = 4.33m^3kg^{-1}s^{-1}$, and where density factors are introduced by Seifert and Beheng (2006a) in order to correct the effect of terminal velocity on the collision efficiency. In addition to the analytical derivation, Seifert and Beheng (2001) made corrections depending on the development stage by using the dimensionless internal time scale. Since moment bulk methods cannot represented complicated changes of high-order moments, the corrections are necessary as DSD undergoes evolution by the collection processes. Firstly, the auto-conversion rate is represented by τ by substituting eq.**??** to eq.8.282,

$$\frac{\partial \tau}{\partial t}\Big|_{aut} = \frac{k_{cc}}{20x^*}\frac{(\nu_c+2)(\nu_c+4)}{(\nu_c+1)^2}\frac{\rho_0}{\rho}x_c^2L(1-\tau^2) \tag{8.288}$$

The assumptions used in the derivation of eq.8.288 are valid for the initial stage of collisional growth. Therefore, the additional collection by a universal function ϕ_{aut} was introduced by Seifert and Beheng (2001) as follows,

$$\frac{\partial \tau}{\partial t}\Big|_{aut} = \frac{k_{cc}}{20x^*}\frac{(\nu_c+2)(\nu_c+4)}{(\nu_c+1)^2}\frac{\rho_0}{\rho}x_c^2L_c^2x_c^2\big[(1-\tau^2)+\phi_{aut}(\tau)\big] \tag{8.289}$$

Similarly, the correction for the accretion rate is also made by a universal function ϕ_{acc},

$$\frac{\partial \tau}{\partial t}\Big|_{acc} = k_{cr}L\big(\frac{\rho_0}{\rho}\big)^{1/2}(1-\tau)\tau\phi_{acc}(\tau) \tag{8.290}$$

In contrast to the correction for the auto-conversion rate, the assumptions used in the derivation of the accretion rate is valid for the mature stage of the collisional growth. Therefore a correction function is multiplied so that ϕ_{aut} becomes zero for the beginning of the collisional growth and one for the mature stage of the collisional growth. Here, it is recognized that the growth rate of the dimensional internal time scale is proportional to LWC in eq.8.289 and eq.8.290. Therefore, the parameterizations developed by Seifert and Beheng (2001) satisfy the similarity included in the SCE. Finally, the universal functions are derived

by fitting to the results by a bin cloud microphysics model,

$$\phi_{aut}(\tau) = 400\tau^{0.7}(1-\tau^{0.7})^3 \quad (8.291)$$

$$\phi_{acc}(\tau) = \Big(\frac{\tau}{\tau+5\times10^{-5}}\Big)^4 \quad (8.292)$$

These functions are shown in Fig.8.9.
Here, we mention that the fitting curves of the universal functions highly depend on the calculation by a bin cloud microphysics model. In fact, the functions proposed by Seifert and Beheng (2006a) were modified from the original functions by Seifert and Beheng (2001) with the progresses in the estimation of the collection kernel. We have to update the parameterizations when more sophisticated collection kernel will be estimated than the one used by Seifert and Beheng (2006a)

Break-up

Large rain droplets are not always stable in the collision process. It was observed that large rain droplets could break up into many small droplets after the collision (Low and Lists, 1982). Collisional break-up sustain mean droplet size so as not to grow extremely larger and cause strong precipitation. As discussed by Hu and Srivastava (1995), the system of collision, coalescence and break-up reaches the equilibrium condition between coalescence and break-up after the sufficient long time. Consequently the form of the DSD of rain is led to the self-similar equilibrium DSD with the equilibrium mean diameter $\bar{D}_{eq}$. Seifert and Beheng (2006a) simply parameterized the break-up process as a relaxation of the DSD with the mean diameter more than $\bar{D}_{eq}$ to the self-similar equilibrium DSD.

$$\frac{\partial N_r}{\partial t}\Big|_{brk} = -\big[\phi_{brk}(\Delta\bar{D}_r)+1\big]\frac{\partial N_r}{\partial t}\Big|_{slc} \quad (8.293)$$

where ϕ_{brk} is a universal function of break-up, and $\Delta\bar{D}_r \equiv \bar{D}_r - \bar{D}_{eq}$, $\bar{D}_r$ is the mean volume diameter of rain, with $\bar{D}_{eq} = 1.1mm$ according to Seifert (2008). The universal function was derived by a fitting to the results by a bin cloud microphysics model based on (Seifert et al. 2005), and formulated as follows,

$$\phi_{brk}(\Delta\bar{D}_r) = \begin{cases} 2exp(\kappa_{brk}\Delta\bar{D}_r)-1, & (\bar{D}_r > \bar{D}_{eq}) \\ \kappa_{brk}\Delta\bar{D}_r+1, & (\bar{D}_{eq} \geq \bar{D}_r > 0.35\times10^{-3}m) \\ -1, & (0.35\times10^{-3} > \bar{D}_r) \end{cases} \quad (8.294)$$

with $\kappa_{brk} = 2.3\times10^3 m^{-1}$, and $k_{brk} = 1000m^{-1}$. For the mean volume diameter less than $0.35\times10^{-3}m$, break-up is neglected.

Mixed-phase collection

In the previous sections, the collection processes are limited for warm cloud. In this section, the collection processes among mixed phase clouds are described. In contrast to warm cloud, there exist many kinds of particles in cold cloud as

discussed in section 2.1. Since the variety of the shape and their coexistence condition differs case by case, there are no systematized theory, observation, and experiments for the mixed phase collection processes. Therefore, Seifert and Beheng (2006a) proposed a general formulation of the collisional interactions among hydrometeors starting from the simplification of the SCE. Due to the variety of the types of hydrometeors, the patterns of the interaction are categorized into following five cases.
1.A particle of hydrometeor a collects b and then the collecting particle a grow. This pattern is corresponding to the collision between ice and cloud (ic), snow and cloud (sc), graupel and cloud (gc), snow and ice (si), graupel and rain (gr), and graupel and snow (gs).
2.A particle of hydrometeor a collects b and then the other particle c is produced. This pattern is corresponding to the collision between rain and ice (ri), and rain and snow (rs).
3.A particle of hydrometeor a collects a and then the other particle b is produced. This pattern is corresponding to the collision between ice and ice (ii).
4.A particle of hydrometeor a collects a and then the collecting particle a grows. This pattern is corresponding to the collision between snow and snow (ss).
In the following sections, we introduce the derivation of the mixed phase collection corresponding to the five cases.

The collision case 1: a+b $\rightarrow$ a

In contrast to the SCE for warm cloud, the production term and reduction term are slightly different in the binary collision between two types of hydrometeors. The reduction term of the hydrometeor b and the production term of the hydrometeor a are described as follows,

$$\frac{\partial f_b(y)}{\partial t}\Big|_{col,ab} = -\int_0^\infty f_b(y) f_a(x) K_{ab}(x,y) dx \tag{8.295}$$

$$\begin{aligned}\frac{\partial f_b(y)}{\partial t}\Big|_{col.ab} &= \int_0^\infty f_a(x-y) f_b(x) K_{ab}(x-y,y) dx \\ &- \int_0^\infty f_a(x) f_b(y) K_{ab}(x,y) dy\end{aligned} \tag{8.296}$$

Here, the formulation of the collection kernel is often described by the swept volume of large particle as follows,

$$K_{ab}(x,y) \equiv E_{ab}(x,y)\frac{\pi}{4}\big[D_a(x) + D_b(y)\big]^2\big[v_{t,a}(x) - v_{t,b}(y)\big] \tag{8.297}$$

where E_{ab} is the collection efficiency, D_i and $v_{t,i}$ are diameter and terminal velocity respectively. We can derive the growth rate of the kth moments by integrating eq.8.295 and eq.8.296,

$$\left.\frac{\partial M_b^k}{\partial t}\right|_{col,ab} = \frac{\pi}{4}\int_0^\infty\int_0^\infty f_b(y)f_a(x)\left[D_a(x)+D_b(y)\right]^2 \times \left|v_{t,a}(x)-v_{t,b}(y)\right|E_{ab}(x,y)y^k dxdy \quad (8.298)$$

$$\left.\frac{\partial M_a^k}{\partial t}\right|_{col,ab} = \frac{\pi}{4}\int_0^\infty\int_0^\infty f_a(x)f_b(y)\left[D_a(x)+D_b(y)\right]^2 \times \left|v_{t,a}(x)-v_{t,b}(y)\right|E_{ab}(x,y)\left[(x+y)^k-x^k\right]dxdy \quad (8.299)$$

Here, the difference of the terminal velocities, and the collection efficiency in the integrand make the analytical integration of eq.8.298 and eq.8.299 impossible. In the past, many researchers have made effort to express the integration by approximation. Seifert and Beheng (2006a) achieved the integration by using the approximation proposed by Wisner et al. (1972) with some improvements. Hereafter, we only demonstrate the equations for the 0th moment N and the 1st moment L.

$$\left.\frac{\partial L_b}{\partial t}\right|_{col,ab} \cong -\frac{\pi}{4}\bar{E}_{ab}\bar{\Delta v_{t,ab}^1} \times \int_0^\infty\int_0^\infty f_a(x)f_b(y)\left[D_a(x)+D_b(y)\right]^2 y dxdy \quad (8.300)$$

$$\left.\frac{\partial L_a}{\partial t}\right|_{col,ab} \cong \frac{\pi}{4}\bar{E}_{ab}\bar{\Delta v_{t,ab}^1}\int_0^\infty\int_0^\infty f_a(x)f_b(y)\left[D_a(x)+D_b(y)\right]^2 y dxdy = -\frac{\partial L_b}{\partial t} \quad (8.301)$$

$$\left.\frac{\partial N_b}{\partial t}\right|_{col,ab} \cong -\frac{\pi}{4}\bar{E}_{ab}\bar{\Delta v_{t,ab}^0}\int_0^\infty \times \int_0^\infty f_a(x)f_b(y)\left[D_a(x)+D_b(y)\right]^2 dxdy \quad (8.302)$$

$$\left.\frac{\partial N_a}{\partial t}\right|_{col,ab} = 0 \quad (8.303)$$

where $\bar{E}_{ab}$ is the mean collection efficiency, and $\bar{\Delta v_{t,ab}^k}$ is a characteristic velocity difference. Thus, the integrand are transformed so as to be integrated analytically and the problems result in the evaluation of $\bar{E}_{ab}$ and $\bar{\Delta v_{t,ab}^k}$. Some cloud microphysics schemes evaluate $\bar{\Delta v_{t,ab}^k}$ as the approximation proposed by Wisner (1972),

$$\bar{\Delta v_{t,ab}^k} = \left|\bar{v}_{M_a^k}(\bar{x}_a) - \bar{v}_{M_b^k}(\bar{y}_b)\right| \quad (8.304)$$

The characteristic velocity difference is simply approximated by the difference between the mass weighted mean terminal velocity of the hydrometeors. This is equivalent to the physical assumption that all the particles are falling with the same terminal velocity equal to the mass weighted mean terminal velocity. However, as pointed out by Seifert and Beheng (2006a), the formulation underestimates the term for the similar mass weighted mean terminal velocities even though larger particles preferentially collect smaller particles due to

their differences of the terminal velocities. Seifert and Beheng (2006a) applied an alternate approximation in order to avoid the abovementioned problem as follows,

$$\Delta\bar{v}_{t,ab}^{k} = \Big[\frac{\int_0^\infty \int_0^\infty v_{t,a}(x) - v_{t,b}(y)^2 D_a^2 D_b^2 f_a(x) f_b(y) y^k dx dy}{\int_0^\infty \int_0^\infty D_a^2 D_b^2 f_a(x) f_b(y) y^k dx dy}\Big]^{1/2} \tag{8.305}$$

The integrand can be integrated straightforwardly assuming the diameter and the terminal velocity follow power laws as given in section 2.1. Here, we apply the equivalent projected area diameter in contrast to the maximum dimension applied by Seifert and Beheng (2006a),

$$\begin{aligned} D &= D_C(x) = \big(\frac{4}{\pi}A\big)^{1/2} = a_C x^{b_C} \\ a_C &= \big(\frac{4}{\pi}a_{ax}\big)^{1/2}, \;\; b_C = \frac{b_{ax}}{2} \end{aligned} \tag{8.306}$$

Since the diameter is used in the calculation of collisional cross section, maximum dimension overestimates collisional cross section for needle or column like crystals. Firstly, the denominator in eq.8.305 is transformed as follows,

$$\begin{aligned} & \int_0^\infty \int_0^\infty D_{C,a}^2 D_{C,b}^2 f_a(x) f_b(y) y^k dx dy \\ = \;& a_{C_a}^2 a_{C_b}^2 M_a^{2b_{C,a}} M_b^{2b_{C,b}+k} \\ = \;& D_{C,a}^2(\bar{x}) D_{C,b}^2(\bar{y}) \bar{y}^k \\ \times \;& \frac{\Gamma\big(\frac{2b_{C,a}+\nu_a+1}{\mu_a}\big)}{\Gamma\big(\frac{\nu_a+1}{\mu_a}\big)} \frac{\Gamma\big(\frac{2b_{C,b}+k+\nu_a+1}{\mu_a}\big)}{\Gamma\big(\frac{\nu_a+1}{\mu_a}\big)} \\ \times \;& \Big[\frac{\Gamma\big(\frac{\nu_a+1}{\mu_a}\big)}{\Gamma\big(\frac{\nu_a+1}{\mu_a}\big)}\Big]^{2b_{C,a}} \Big[\frac{\Gamma\big(\frac{\nu_b+1}{\mu_b}\big)}{\Gamma\big(\frac{\nu_b+1}{\mu_b}\big)}\Big]^{2b_{C,b}+k} \end{aligned} \tag{8.307}$$

Secondly, the numerator in eq.8.305 is transformed as follows,

$$
\begin{aligned}
&\int_0^\infty \int_0^\infty \left[v_{t,a}(x) - v_{t,b}(y)\right]^2 D_{C,b}^2 D_{C,b}^2 f_a(x) f_b(y) y^k dx dy \\
= \;& a_{C_a}^2 a_{C_b}^2 \left[a_{v,a}^2 M_a^{2b_{C,a}+2b_{v,a}}\right. \\
+ \;& \left. M_b^{2b_{C,b}+k} - 2a_{v,a}a_{v,b} M_a^{2b_{C,a}+b_{v,a}} M_b^{2b_{C,b}+b_{v,b}+k} + a_{v,b}^2 M_a^{2b_{C,a}} M_b^{2b_{C,b}+2b_{v,b}+k}\right] \\
= \;& D_{C,a}^2(\bar{x}) D_{C,b}^2(\bar{y}) \bar{y}^k \\
+ \;& v_{t,a}^2(\bar{x}) \frac{\Gamma\left(\frac{2b_{C,a}+2b_{v,a}+v_a+1}{\mu_a}\right)}{\Gamma\left(\frac{v_a+1}{\mu_a}\right)} \frac{\Gamma\left(\frac{2b_{C,b}+k+v_a+1}{\mu_a}\right)}{\Gamma\left(\frac{v_a+1}{\mu_a}\right)} \left[\frac{\Gamma\left(\frac{v_a+1}{\mu_a}\right)}{\Gamma\left(\frac{v_a+2}{\mu_a}\right)}\right]^{2b_{C,a}+2b_{v,a}} \left[\frac{\Gamma\left(\frac{v_b+1}{\mu_b}\right)}{\Gamma\left(\frac{v_b+2}{\mu_b}\right)}\right]^{2b_{C,a}+k} \\
= \;& 2v_{t,a}(\bar{x}) v_{t,b}(\bar{y}) \frac{\Gamma\left(\frac{2b_{C,a}+b_{v,a}+v_a+1}{\mu_a}\right)}{\Gamma\left(\frac{v_a+1}{\mu_a}\right)} \frac{\Gamma\left(\frac{2b_{C,b}+b_{v,a}+k+v_a+1}{\mu_a}\right)}{\Gamma\left(\frac{v_a+1}{\mu_a}\right)} \\
\times \;& \left[\frac{\Gamma\left(\frac{v_a+1}{\mu_a}\right)}{\Gamma\left(\frac{v_a+2}{\mu_a}\right)}\right]^{2b_{C,a}+b_{v,a}} \left[\frac{\Gamma\left(\frac{v_b+1}{\mu_b}\right)}{\Gamma\left(\frac{v_b+2}{\mu_b}\right)}\right]^{2b_{C,a}+b_{v,b}+k} \\
+ \;& v_{t,b}^2(\bar{y}) \frac{\Gamma\left(\frac{2b_{C,a}+v_a+1}{\mu_a}\right)}{\Gamma\left(\frac{v_a+1}{\mu_a}\right)} \frac{\Gamma\left(\frac{2b_{C,b}+2b_{v,a}+k+v_a+1}{\mu_a}\right)}{\Gamma\left(\frac{v_a+1}{\mu_a}\right)} \left[\frac{\Gamma\left(\frac{v_a+1}{\mu_a}\right)}{\Gamma\left(\frac{v_a+2}{\mu_a}\right)}\right]^{2b_{C,a}} \\
\times \;& \left[\frac{\Gamma\left(\frac{v_b+1}{\mu_b}\right)}{\Gamma\left(\frac{v_b+2}{\mu_b}\right)}\right]^{2b_{C,a}+2b_{v,b}+k}
\end{aligned} \tag{8.308}
$$

Finally, the characteristic velocity difference are derived by substituting eq.8.307 and eq.8.308 into 8.305,

$$
\Delta \bar{v}_{t,ab}^k = \left[\theta_a^0 v_{t,a}^2(\bar{x}) - \theta_{ab}^k v_{t,a}(\bar{x}) v_{t,b}(\bar{y}) + \theta_b^k v_{t,b}^2\right]^{1/2} \tag{8.309}
$$

$$
\theta_a^k = \frac{\Gamma\left(\frac{2b_{C,a}+2b_{v,a}+k+v_a+1}{\mu_a}\right)}{\Gamma\left(\frac{2b_{C,a}+k+v_a+1}{\mu_a}\right)} \left[\frac{\Gamma\left(\frac{v_a+1}{\mu_a}\right)}{\Gamma\left(\frac{v_b+2}{\mu_b}\right)}\right] \{2b_{v,a+k} \tag{8.310}
$$

$$
\begin{aligned}
\theta_{ab}^k = \;& 2\frac{\Gamma\left(\frac{2b_{C,a}+b_{v,a}+v_a+1}{\mu_a}\right)}{\Gamma\left(\frac{2b_{C,a}+v_a+1}{\mu_a}\right)} \frac{\Gamma\left(\frac{2b_{C,b}+b_{v,b}+k+v_b+1}{\mu_b}\right)}{\Gamma\left(\frac{2b_{C,b}+k+v_b+1}{\mu_b}\right)} \\
\times \;& \left[\frac{\Gamma\left(\frac{v_a+1}{\mu_a}\right)}{\Gamma\left(\frac{v_a+2}{\mu_a}\right)}\right]^{b_{v,a}} \left[\frac{\Gamma\left(\frac{v_b+1}{\mu_b}\right)}{\Gamma\left(\frac{v_b+2}{\mu_b}\right)}\right]^{b_{v,b}}
\end{aligned} \tag{8.311}
$$

Here, it is noticed that the notation ab in θ_{ab}^k is not symmetric because θ_{ab}^k is weighted by the mass of collected particle to the power of k. Integrations in eq.8.300 and eq.8.302 are similarly calculated as follows,

$$
\begin{aligned}
& \int_0^\infty \int_0^\infty f_a(x) f_b(y) D_a(x) + D_b(y)^2 y^k dx \\
= \;& a_{C_a}^2 M_a^{2b_{C,a}} M_b^k + 2a_{C_a} a_{C_b} M_a^{b_{C,a}} M_b^{b_{C,b}+k} + a_{C_b}^2 M_a^0 M_b^{2b_{C,b}+k} \\
= \;& \delta_a^0 D_{C,a}^2(\bar{x}) N_a M_b^k + \delta_{ab}^k D_{C,a}(\bar{x}) D_{C,b}(\bar{y}) N_a N_b \bar{y}^k \\
+ \;& \delta_b^k D_{C,b}^2(\bar{y}) N_a N_b \bar{y^k} \qquad (8.312)
\end{aligned}
$$

$$
\delta_a^k = \frac{\Gamma\left(\frac{2b_{C,b}+k+v_a+1}{\mu_a}\right)}{\Gamma\left(\frac{\mu_a+1}{\mu_a}\right)} \left[\frac{\Gamma\left(\frac{v_a+1}{\mu_a}\right)}{\Gamma\left(\frac{v_a+2}{\mu_a}\right)}\right]^{2b_{C,a}+k} \qquad (8.313)
$$

$$
\delta_{ab}^k = 2\frac{\Gamma\left(\frac{b_{C,a}+v_a+1}{\mu_a}\right)}{\Gamma\left(\frac{v_a+1}{\mu_a}\right)} \frac{\Gamma\left(\frac{b_{C,b}+k+v_b+1}{\mu_b}\right)}{\Gamma\left(\frac{v_b+1}{\mu_b}\right)} \left[\frac{\Gamma\left(\frac{v_a+1}{\mu_a}\right)}{\Gamma\left(\frac{v_a+2}{\mu_a}\right)}\right]^{b_{C,a}} \left[\frac{\Gamma\left(\frac{v_b+1}{\mu_b}\right)}{\Gamma\left(\frac{v_b+2}{\mu_b}\right)}\right]^{b_{C,b}+k} \qquad (8.314)
$$

Here, δ_{ab}^k is also asymmetry in ab as θ_{ab}^k. Finally, the growth rates of the prognostic moments are represented as follows,

$$
\begin{aligned}
\left.\frac{\partial L_a}{\partial}\right|_{col,ab} &= \frac{\pi}{4} \bar{E}_{ab} N_a L_b \delta_a^0 D_{C,a}^2(\bar{x}_a) + \delta_{ab}^1 D_{C,a}(\bar{x}_a) D_{C,b}(\bar{x}_b) + \delta_b^1 D_{C,b}^2(\bar{x}_b) \\
&\times \left[\theta_a^0 v_{t,a}^2(\bar{x}_a) - \theta_{ab}^1 v_{t,a}(\bar{x}_a) v_{t,b}(\bar{x}_b) + \theta_b^1 v_{t,b}^2(\bar{x}_b) + \sigma_a + \sigma_b\right]^{1/2} \qquad (8.315) \\
\left.\frac{\partial L_b}{\partial t}\right|_{col,ab} &= -\left.\frac{\partial L_a}{\partial t}\right|_{col,ab} \qquad (8.316) \\
\left.\frac{\partial N_b}{\partial}\right|_{col,ab} &= \frac{\pi}{4} \bar{E}_{ab} N_a N_b \delta_a^0 D_{C,a}^2(\bar{x}_a) + \delta_{ab}^0 D_{C,a}(\bar{x}_a) D_{C,b}(\bar{x}_b) + \delta_b^0 D_{C,b}^2(\bar{x}_b) \\
&\times \left[\theta_a^0 v_{t,a}^2(\bar{x}_a) - \theta_{ab}^0 v_{t,a}(\bar{x}_a) v_{t,b}(\bar{x}_b) + \theta_b^0 v_{t,b}^2(\bar{x}_b) + \sigma_a + \sigma_b\right]^{1/2} \qquad (8.317) \\
\left.\frac{\partial N_b}{\partial t}\right|_{col,ab} &= 0 \qquad (8.318)
\end{aligned}
$$

where σ_a and σ_b are constant variances due to the probabilities of the terminal velocity of particles. Seifert and Beheng (2006a) proposed the concept to mimic an introduction of the effect of turbulence to the collection kernel with the use of the constant variances. The constant variances are only applied to ice and snow with $\sigma_i = \sigma_s = 0.2ms^{-1}$ while no variances are assumed for the other particles.

The collection efficiencies of ice particles

The collection efficiencies of ice particles are poorly understood due to their varieties and the lack of the systematic observations. In addition, the efficiencies cannot be approximated by power laws. Therefore, Seifert and Beheng (2006a) described them in a simple way. The collection efficiency E_{ab} can be decomposed into two part of efficiencies, the collision efficiency E_{col} and the sticking efficiency E_{stick}. This means that two particles stochastically collide each other with E_{col}, and then they stick each other with E_{stick}. It is considered that the mean possibility of collection $\bar{E}_{ab}$ is parameterized by the multiplying $\bar{E}_{col}$ by $\bar{E}_{stick}$.

$$
\bar{E}_{ab} = \bar{E}_{col,ab} \times \bar{E}_{stick,ab} \qquad (8.319)
$$

The mean collision efficiencies of each gydrometeor are given as follows,

$$\bar{E}_{col,ab} = \bar{E}_{col,a} \times \bar{E}_{colk,b} \tag{8.320}$$

$$\bar{E}_{col,c} = \begin{cases} 0, & (\bar{D}_c < \bar{D}_{c,0}) \\ \frac{\bar{D}_c - \bar{D}_{c,0}}{\bar{D}_{c,1} - \bar{D}_{c,0}}, & (\bar{D}_{c,0} \leq \bar{D}_c \leq \bar{D}_{c,1}) \\ 1, & (\bar{D}_{c,1} < \bar{D}_c) \end{cases} \tag{8.321}$$

$$\bar{E}_{col,r} = 1 \tag{8.322}$$

$$\bar{E}_{col,js} = \begin{cases} 0, & (\bar{D}_{js} < 150nm) \\ \bar{E}_{col,max,js}, & (\bar{D}_{js} > 150nm), \quad (js = i, s, g) \end{cases} \tag{8.323}$$

with $\bar{D}_{c,0} = 15\mu m$, $\bar{D}_{c,1} = 40\mu m$, $\bar{E}_{col,max,i} = \bar{E}_{col,max,s} = 0.8$, and $\bar{E}_{col,max,g} = 1.0$. Furthermore, the mean collision efficiency of one is assumed in the collision between rain droplets and ice particles, and the collision between ice particles. These values are so empirical that further investigations and assessments are required.
The sticking efficiency is considered only in the case of the collision between ice particles. Otherwise, the efficiency is assumed as one. It is known that the stick efficiency depends on the enviromental condition around ice particles and the shape of ice particle (Pruppacher and Klett, 1997). Ice crystals with many branches are likely to stick each other. In addition, the ice particles under wet conditions are also likely to coalescence because of the surface condition of ice particles. Since these dependencies of the stick efficiency are poorly understood, some simple formulations were proposed by past researchers. Lin et al. (1983) proposed the following formulation,

$$\bar{E}_{stick}(T) = \begin{cases} exp[0.09 \times T_c], & (T_c \leq 0^o C) \\ 1, & (T_c > 0^o C) \end{cases} \tag{8.324}$$

In contrast to their formulation, Cotton et al. (1986), proposed an alternative formulation based on observations (Hallgren and Hosler, 1960) as follows,

$$\bar{E}_{stick}(T_p) = min(10^{0.035(T_p - 273.15) - 0.7}, 0.2) \tag{8.325}$$

where T_p is particle surface temperature. They also diagnosed the departure of particle surface temperature from the enviroment due to phase change in the calculation. In addition, their formulation has a upper limit to reduce the efficiency as observations showed. In a similar way, Khain and Sednev (1996) proposed a formulation based on other observations (Hosler et al., 1957; Rogers et al., 1974). Their formulation also depends on vapor pressure as follows,

$$\bar{E}_{stick} = min\big(\delta E \frac{p_v}{p_{si}}, 1\big) \tag{8.326}$$

$$\delta E = max(a_\delta + b_\delta T_c + c_\delta T_c^2 + d_\delta T_c^3, 0) \tag{8.327}$$

with $a_\delta = 0.883$, $b_\delta = 0.093$, $c_\delta = 0.00348$, and $d_\delta = 4.5185 \times 10^{-5}$. In this study, the formulation proposed by Lin et al. (1983) is applied following Seifert

and Beheng (2006a). These efficiencies are shown in Fig.8.10 with the various obeservation data from Pruppacher and Klett (1997). The further investigations and assessments are necessary to determine which one is better than others although there are less information for making a decision.

The collision case 2: a+b → c

The case is the same as the case 1 except for the growing particles.

$$\frac{\partial f_b(y)}{\partial t}\Big|_{col,abs} = -\int_0^\infty f_b(y) f_a(x) K_{ab}(x,y) dx \tag{8.328}$$

$$\frac{\partial f_a(x)}{\partial t}\Big|_{col,abs} = -\int_0^\infty f_a(x) f_b(y) K_{ab}(x,y) dy \tag{8.329}$$

Similarly, the growth rates of the prognostic moments are derived as follows,

$$\begin{aligned}
\frac{\partial L_a}{\partial t}\Big|_{col,ab} &= -\frac{\pi}{4}\bar{E}_{ab}\Delta\bar{v}^1_{t,ab} \\
&\times \int_0^\infty\int_0^\infty f_a(x) f_b(y)[D_a(x)+D_b(y)]^2 x dx dy \qquad (8.330) \\
\frac{\partial L_b}{\partial t}\Big|_{col,ab} &= -\frac{\pi}{4}\bar{E}_{ab}\Delta\bar{v}^1_{t,ab} \\
&\times \int_0^\infty\int_0^\infty f_a(x) f_b(y)[D_a(x)+D_b(y)]^2 y dx dy \qquad (8.331) \\
\frac{\partial N_a}{\partial t}\Big|_{col,ab} &= \frac{\partial N_b}{\partial t}\Big|_{col,ab} = -\frac{\pi}{4}\bar{E}_{ab}\Delta\bar{v}^0_{t,ab} \\
&\times \int_0^\infty\int_0^\infty f_a(x) f_b(y)[D_a(x)+D_b(y)]^2 dx dy \qquad (8.332) \\
\frac{\partial N_c}{\partial t}\Big|_{col,ab} &= -\frac{\partial N_a}{\partial t}\Big|_{col,ab} \qquad (8.333)
\end{aligned}$$

Finally, the equations are transformed by using the approximations as follows,

$$
\begin{aligned}
\frac{\partial L_b}{\partial t}\Big|_{col,ab} &= -\frac{\pi}{4}\bar{E}_{ab}N_a L_b \\
&\times [\delta_a^0 D_{C,a}^2(\bar{x}_a) + \delta_{ab}^1 D_{C,a}(\bar{x}_a)D_{C,b}(\bar{x}_b) + \delta_b^1 D_{C,b}^2(\bar{x}_b)] \qquad (8.334)\\
&\times [\theta_a^0 v_{t,a}^2(\bar{x}_a) - \theta_{ab}^1 v_{t,a}(\bar{x}_a)v_{t,b}(\bar{x}_b) + \theta_b^1 v_{t,b}^2(\bar{x}_b) + \sigma_a + \sigma_b]^{1/2} \\
\frac{\partial L_a}{\partial t}\Big|_{col,ab} &= -\frac{\pi}{4}\bar{E}_{ab}N_b L_a \\
&\times [\delta_b^0 D_{C,b}^2(\bar{x}_b) + \delta_{ab}^1 D_{C,a}(\bar{x}_a)D_{C,b}(\bar{x}_b) + \delta_a^1 D_{C,a}^2(\bar{x}_b)] \qquad (8.335)\\
&\times [\theta_b^0 v_{t,b}^2(\bar{x}_b) - \theta_{ba}^1 v_{t,a}(\bar{x}_a)v_{t,b}(\bar{x}_b) + \theta_a^1 v_{t,a}^2(\bar{x}_b) + \sigma_a + \sigma_b]^{1/2} \\
\frac{\partial N_b}{\partial t}\Big|_{col,ab} &= -\frac{\pi}{4}\bar{E}_{ab}N_a N_b \\
&\times [\delta_a^0 D_{C,a}^2(\bar{x}_a) + \delta_{ab}^0 D_{C,a}(\bar{x}_a)D_{C,b}(\bar{x}_b) + \delta_b^0 D_{C,a}^2(\bar{x}_b)] \qquad (8.336)\\
&\times [\theta_a^0 v_{t,a}^2(\bar{x}_a) - \theta_{ab}^0 v_{t,a}(\bar{x}_a)v_{t,b}(\bar{x}_b) + \theta_b^0 v_{t,a}^2(\bar{x}_b) + \sigma_a + \sigma_b]^{1/2} \\
\frac{\partial N_a}{\partial t}\Big|_{col,ab} &= -\frac{\pi}{4}\bar{E}_{ab}N_a N_b \\
&\times [\delta_a^0 D_{C,a}^2(\bar{x}_a) + \delta_{ab}^0 D_{C,b}(\bar{x}_a)D_{C,b}(\bar{x}_b) + \delta_b^0 D_{C,b}^2(\bar{x}_b)] \qquad (8.337)\\
&\times [\theta_a^0 v_{t,a}^2(\bar{x}_a) - \theta_{ba}^0 v_{t,b}(\bar{x}_a)v_{t,b}(\bar{x}_b) + \theta_b^0 v_{t,b}^2(\bar{x}_b) + \sigma_a + \sigma_b]^{1/2}
\end{aligned}
$$

The collision case3: a+a → b

In the case, binary collision between particles in the same hydrometeor is considered. All the pairs in the collision turn into the other hydormeteor as follows,

$$
\frac{\partial f_a(x)}{\partial t}\Big|_{col,aa} = -\int_0^\infty f_a(x)f_a(y)K_{aa}(x,y)dy \qquad (8.338)
$$

The growth rate of the prognostic moments is as follows,

$$
\begin{aligned}
\frac{\partial L_a}{\partial t}\Big|_{col,aa} &= -\frac{\pi}{4}\bar{E}_{aa}N_a L_a \\
&\times \delta_a^0 D_{C,a}^2(\bar{x}_a) + \delta_{aa}^1 D_{C,a}^2(\bar{x}_a) \\
&\times \theta_a^0 v_{t,a}^2(\bar{x}_a) - \theta_{aa}^1 v_{t,a}^2(\bar{x}_a) + 2\sigma_a \qquad (8.339)\\
\frac{\partial N_a}{\partial t}\Big|_{col,aa} &= -\frac{\pi}{4}\bar{E}_{aa}N_a N_a \\
&\times 2\delta_a^0 D_{C,a}^2(\bar{x}_a) + \delta_{aa}^0 D_{C,a}^2(\bar{x}_a) \\
&\times 2\theta_a^0 v_{t,a}^2(\bar{x}_a) - \theta_{aa}^0 v_{t,a}^2(\bar{x}_a) + 2\sigma_a \qquad (8.340)\\
\frac{\partial L_b}{\partial t}\Big|_{col,aa} &= -\frac{\partial L_a}{\partial t}\Big|_{col,aa} \qquad (8.341)\\
\frac{\partial N_b}{\partial t}\Big|_{col,aa} &= -\frac{1}{2}\frac{\partial N_a}{\partial t}\Big|_{col,aa} \qquad (8.342)
\end{aligned}
$$

The collision case 4: a+a → a

In the case, self aggregational growth is considered. In the aggregation, the number concentration of the hydrometeor a decreases under the conservation of

the mass concentration. The basic equation is the same as the case 3 except for the absence of the other hydrometeor.

$$\begin{aligned}\frac{\partial N_a}{\partial t} &= -\frac{1}{2}\frac{\pi}{4}\bar{E}_{aa}N_aN_a \\ &\times \quad 2\delta_a^0 D_{C,a}^2(\bar{x}_a) + \delta_{aa}^0 D_{C,a}^2(\bar{x}_a) \\ &\times \quad 2\theta_a^0 v_{t,a}^2(\bar{x}_a) + \theta_{aa}^0 v_{t,a}^2(\bar{x}_a) + 2\sigma_a{}^{1/2}\end{aligned} \tag{8.343}$$

The secondary processes

There are several secondary processes associated with the mixed phase collection. Here, we briefly describe them following Seifert and Beheng (2006a).

Enhanced melting

We assume that the particle temperature is the same as the enviromental temperature. However, the melting process allows the existence of ice particles under the warmer condition than the melting point. In the riming process under the condition, coalescence of a liquid droplet uniformizes the temperature of colliding two particles. Subsequently, the temperature difference between a ice particle and a liquid droplet are compensated by the latent heat relase of the ice particle. In our model framework, since the category of wet ice particle is not considered, the melting part of a riming particle is accounted as the production of a liquid droplet. The melting rate by the riming process is formulated following Rutledge and Hobbs (1984),

$$\frac{\partial L_{js}}{\partial t}\Big|_{eml} = -\frac{c_1 T_c}{L_{f0}}\frac{\partial L_{js}}{\partial t}\Big|_{col} \quad (T_c > 0^o C),\ (js = i, s, g) \tag{8.344}$$

Here, the reduction rate of number conentration is treated similarly to the melting process,

$$\frac{\partial N_{js}}{\partial t}\Big|_{eml} = \frac{1}{\bar{x}_{js}}\frac{\partial L_{js}}{\partial t}\Big|_{col} \tag{8.345}$$

Partial convesrion

According to Seifert and Beheng (2006a), a riming particle becomes a densely rimed spherical particle as soon as the collected liquid droplet fills up the envelop of the collecting ice particle. The produced densely rimed spherical particle is categorized as graupel. Here, we consider that the volume difference between a ice crystal or a spongy ice particle and its enveloping sphere is filled by the collected liquid droplet. The critical liquid droplet mass $\bar{x}_{crit,pcon}$ is estimated by the geometry of ice as follows,

$$\bar{x}_{crit,pcon,js} = \alpha_{fill,js}\rho_w\Big(\frac{\pi}{6}\bar{D}_{js}^3 - \frac{\bar{x}_{js}}{\rho_\varepsilon}, \quad (js = i, s) \tag{8.346}$$

where α_{fill} is the so-called filling coefficient, $\rho_\varepsilon = 900kgm^{-3}$ is density of ice. The filling coefficient is the criterion to categorize a ice particle as graupel by its dense. Tentatively, α_{fill}, $i = 0.68$ and α_{fill}, $s = 0.01$ are set by Seifert and Beheng (2006a). This means that snow is categorized as almost unrimed ice particles. The characteristic conversion time scale pcon is estimated by the growth rate of mean particle mass by the riming process as follows,

$$\tau_{pcon,js} = \frac{\bar{x}_{crit,pcon,js}}{\frac{1}{N_{js}}\frac{\partial L_{js}}{\partial t}\Big|_{rime}} \tag{8.347}$$

Finally, the conversion rates of riming particles into graupel are derived by using the characteristic time scale.

$$\frac{\partial L_g}{\partial t}\Big|_{pcon} = \frac{L_{js}}{\tau_{pcon,js}} = min\Big(\frac{\bar{x}_{js}}{\bar{x}_{crit,pcon,js}}, 1\Big)\frac{\partial L_{js}}{\partial t}\Big|_{rime} \tag{8.348}$$

$$\frac{\bar{x}_{js}}{\bar{x}_{crit,pcon,js}} = \Big[\alpha_{fill,js}\frac{\rho_w}{\rho_\varepsilon}\Big(\frac{\pi}{6}D_i^3\rho_i\frac{1}{\bar{x_{js}}} - 1\Big)\Big]^{-1} \tag{8.349}$$

The conversion rate of number concentration is as follows,

$$\frac{\partial N_g}{\partial t}\Big|_{pcon} = \frac{1}{\bar{x}_{js}}\frac{\partial L_g}{\partial t}\Big|_{pcon} \tag{8.350}$$

The conversion coefficient of riming particle $\bar{x}/\bar{x}_{crit,pconv}$ is shown in Fig.8.11. In this formulation, small ice particles are likely to convert into graupel in riming because small ice particles have simple geometry and are almost sphere. In order to suppress the conversion of small ice particles, partial conversion are limited to ice particles with the mean diameter of more than 500 μm.

Ice multiplication

It has been observed that the number concentration of ice particles can be up to several orders of magnitude larger than ice nuclei in atmospheric cloud (Pruppacher and Klett, 1997). Among the possible mechanisms to explain the fact, the Hallet-Mossop mechanism has been received in many literatures and widely applied in cloud microphysics schemes. The Hallet-Mossop mechanism is based on the fact that ice splintering occurs when many liquid droplets are collected by graupel. Cotton et al. (1986) applied the formulations based on the observations by Hallet and Mossop (1974), and Mossop (1976). Hallet and Mossop (1974) reported that approximately 350 ice splinters were produced for every $10^{-3}g$ of rime accreted by a graupel at -5 degC. The parameterization is formulated with the temperature correction f1 in the units of mks as follows,

$$\frac{\partial N_i}{\partial t}\Big|_{spl1,js} = 350 \times 10^6 \times f_1(T) \times \frac{\partial L_{js}}{\partial t}\Big|_{rime,js}, \quad (js = i, s, g) \tag{8.351}$$

$$f_1(T) = \begin{cases} 0, & (T >< 270.16K) \\ \frac{T-268.16}{3}, & (270.16K \geq T \geq 268.16K) \\ \frac{T-268.16}{3}, & (268.16K > T \geq 265.16K) \\ 0, & (265.16K > T) \end{cases} \tag{8.352}$$

The splintering mass concentration is assumed as follows

$$\frac{\partial L_i}{\partial t}\Big|_{spl1} = \bar{x}_i \frac{\partial N_i}{\partial t}\Big|_{spl1} \tag{8.353}$$

On the other hand, Mossop (1976) reported that approximately one ice crystal was produced per 250 drops larger than 12 μm radius accreted onto a graupel at -5 degC. Here, since it is difficult to calculate the number concentration of riming cloud droplets larger than 12 μm ($N_{rime,c}$), we assume simple relationship following Cotton et al. (1986) as follows,

$$\frac{N_{rime,c}}{N_{rime,c}} \approx \frac{N_c}{N_c} = Q\big(\frac{\nu_c + 1}{\mu_c}, x_{12}\big) \tag{8.354}$$

where Q is the complement of the incomplete gamma function, and x_{12} is the droplet mass with the radius of $12\mu m$. With the above relation, the parameterization is formulated with the same temperature correction function in the units of mks as follows,

$$\frac{\partial N_i}{\partial t}\Big|_{spl2,js} = \frac{1}{250} \times f_1 \times Q \times \big(\frac{N_c}{L_c}\frac{\partial L_{js}}{\partial t}\Big|_{rime,js}\big), \quad (js = i, s, g) \tag{8.355}$$

In contrast to Cotton et al. (1986), we evaluate the incomplete gamma function with an accurate approximation by Press et al. (2007). The splintering rates of mass concentration is assumed as follows,

$$\frac{\partial L_i}{\partial t}\Big|_{spl2} = \bar{x}_i \frac{\partial N_i}{\partial t}\Big|_{spl2} \tag{8.356}$$

Here, it should be noticed that we may double count the ice multiplication process due to the Hallet-Mossop mechanism by using the two formulations. Those two formulations may be two independent processes or the interpretations of the same process in different two development stages. Since the process is poorly understood by the lack of observation, the assessment of the process by a set of sensitivity studies is necessary in the future.

Appendix of Seiki and Nakajima (2014)

The k-th moment of generalized Gamma distribution

The kth moment of the DSD frequently appear in the equations of cloud microphysics. In this section, derivation of the kth moment of the generalized Gamma distribution is described. The generalized Gamma distribution is defined as $f(x) = \alpha x \nu exp(-\lambda x \mu)$. There are four parameters in this generalized Gamma distribution but only two prognostic moments in a CRM; the number concentration N and mass concentration L. Hence μ and ν are set constant parameters so that the other coefficients α and λ can be related to N and L as follows.

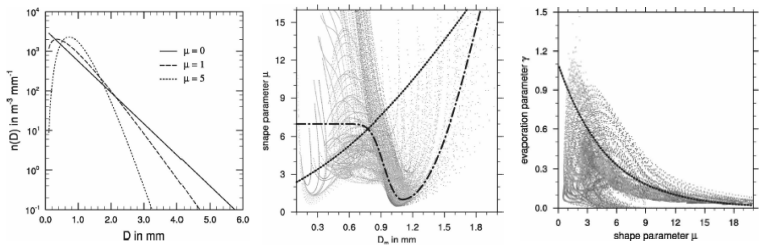

Figure 8.5: Left figure shows the modified Gamma distribution for various shape parameters m. Center figure shows the scatter plot of shape parameter and mean volume diameter for various initial conditions. Gray dots are from cloud model, dotted line is parameterization of Milbrandt and Yau (2005) and dashed-dotted line is that of Seifert (2008). Right figure shows the scatter plot of evaporation parameter and shape parameter. These are from Seifert (2008).

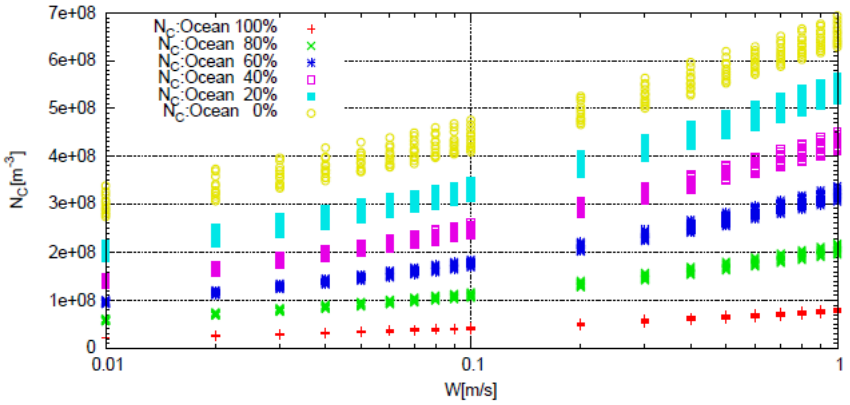

Figure 8.6: Dependency of maximum number concentration on updraft velocity in ascending air parcel. These are based on a Twomey equation with various CCN conditions. Aerosol activation spectrum refers to eq.8.259.

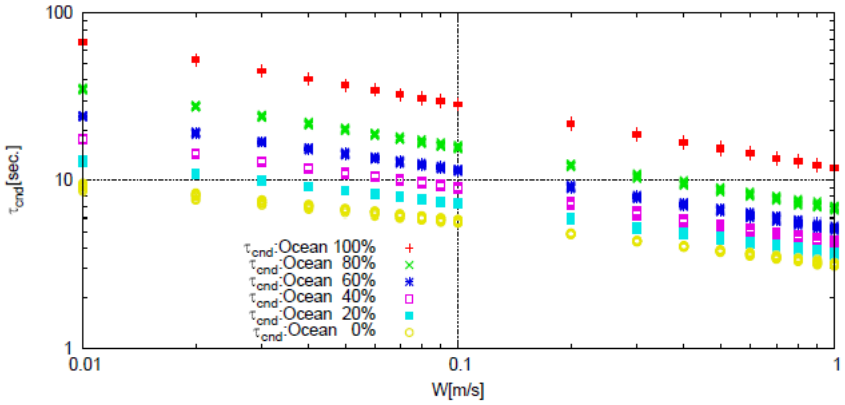

Figure 8.7: Timescale of condensation for cloud droplets at maximum number concentration in ascending air parcel. Experimental design is the same as Fig.8.6.

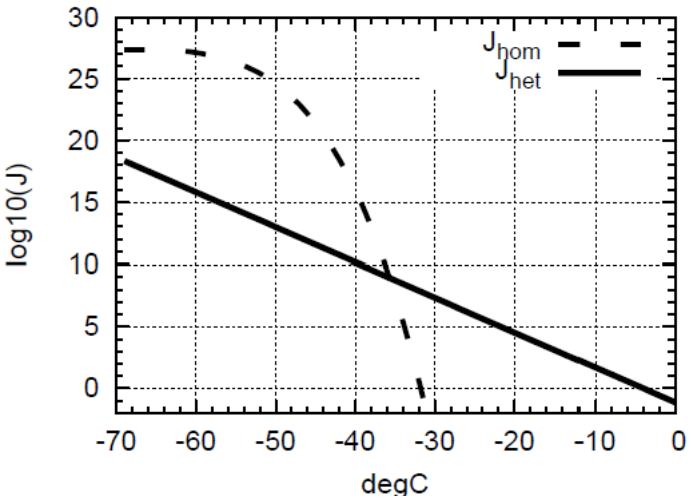

Figure 8.8: The dependencies of the homogeneous freezing rate (dashed line) and the heterogeneous freezing rate (solid line) on centigrade temperature. The freezing rates are in common logarithmic scale.

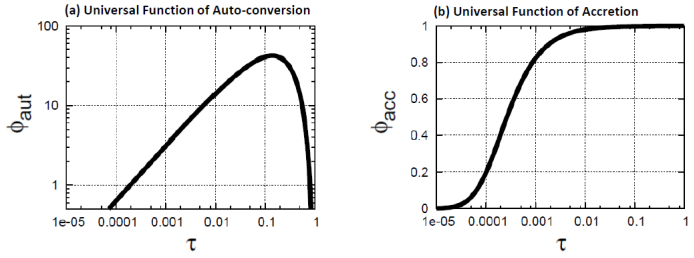

Figure 8.9: The universal functions of (a) auto-conversion and (b) accretion as a function of the dimensionless internal time scale.

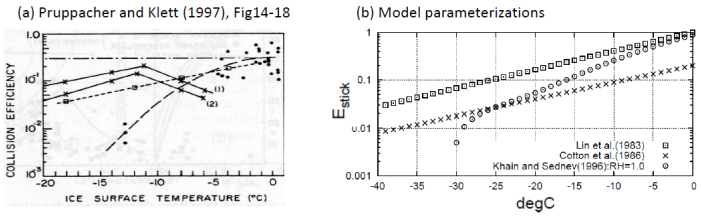

Figure 8.10: The dependency of stick efficiencies on centigrade temperature. The stick efficiencies by (a) the various observations from Pruppacher and Klett (1997) and (b) model parameterizations.

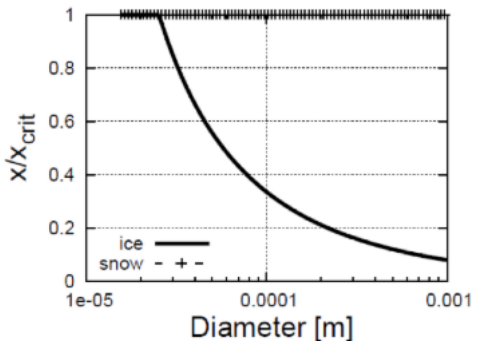

Figure 8.11: The coefficients of partial conversion. Solid line shows the coefficient of ice, and the line with symbol shows the coefficient of snow.

$$
\begin{aligned}
M^0 = N &= \alpha \int_0^\infty x^\nu exp(\lambda x^\mu) dx \\
&= \frac{\alpha}{\lambda^{(\nu+1)/\mu}\mu} \int_0^\infty y^{(\nu+1)/\mu - 1} exp(-y) dy, \ (y \equiv \lambda x^\mu) \\
&= \frac{\alpha}{\lambda^{(\nu+2)/\mu}\mu} \Gamma\big(\frac{\nu+1}{\mu}\big) \qquad (8.357) \\
M^1 = L &= \frac{\alpha}{\lambda^{(\nu+2)/\mu}\mu} \Gamma\big(\frac{\nu+1}{\mu}\big)
\end{aligned}
$$

Then α is expressed as,

$$
\alpha = \frac{N\mu\lambda^{(\nu+1)/\mu}}{\Gamma\big(\frac{\nu+1}{\mu}\big)} = \frac{L\mu\lambda^{(\nu+2)/\mu}}{\Gamma\big(\frac{\nu+2}{\mu}\big)}
$$

and then we can derivev λ and α,

$$
\lambda = \Big[\frac{\Gamma\big(\frac{\nu+1}{\mu}\big)}{\Gamma\big(\frac{\nu+2}{\mu}\big)}\Big]^{-\mu} \bar{x}^{-\mu} \ \ and \ \ \alpha = \frac{\nu N}{\Gamma\big(\frac{\nu+1}{\mu}\big)} \lambda^{(\nu+1)/\mu} \qquad (8.358)
$$

where $\bar{x} = L/N$ define the mean particle mass. Here we can rewrite the generalized Gamma distribution by using N and L in following form,

$$
f(x) = \frac{N}{\bar{x}} \big(\frac{x}{\bar{x}}\big)^\nu \frac{\mu}{\Gamma\big(\frac{nu+1}{\mu}\big)} \Big[\frac{\Gamma\big(\frac{\nu+2}{\mu}\big)}{\Gamma\big(\frac{\nu+1}{\mu}\big)}\Big]^{\nu+1} \exp\Big[-\big[\frac{\Gamma((\nu+2)/\mu)}{\Gamma((\nu+1)/\mu)} \frac{x}{\bar{x}}\big]^\mu\Big] \qquad (8.359)
$$

The kth moment of DSD is now given by the expansion of eq.8.357 and by using eq.8.358,

$$
M^k = \frac{\Gamma\big(\frac{k+\nu+1}{\mu}\big)}{\Gamma\big(\frac{\nu+1}{\mu}\big)} \Big[\frac{\Gamma\big(\frac{\nu+1}{\mu}\big)}{\Gamma\big(\frac{\nu+2}{\mu}\big)}\Big]^k N\bar{x}^k, \ \ (k \in R) \qquad (8.360)
$$

8.3.3 Spectral Bin Model(SBM)Kentaroh et al. (2010)

The Spectral Bin Model (SBM) was developed by Suzuki et al. (2010)Kentaroh et al. (2010). The model forecasts Size Distribution Function(SDF) of 7 types hydrometeors (liquid, plate-ice, columner-ice, dendrite-ice, snow, graupel, and hail).

The SBM calculates mass density of the 7 types of hydrometeor and 1 type of aerosol as their SDFs. The SDF of aerosol can be changed by advection and acvitvaiton (i.e. nucleation from aerosol to cloud) process. The SDF of hydrometeors can be changed by several growth processes (i.e. activation from aerosol to cloud, condensation/evaporation, collision/coaguration, freezing/melting, ice nucleation, riming, aggregation, advection, and gravitational falling).

The time evolution of SDF (number density) of aerosol ($f_a(m,t)$) and SDF (number density) of hydrometeor ($f_c(m,t)$) are shown as equations:

$$\frac{\partial f_c^{(\mu)}(m,t)}{\partial t} = Adv\big[f_c^{(\mu)}(m,t)\big] + Grav\big[f_c^{(\mu)}(m,t)\big] + \Big[\frac{\partial f_c^{(\mu)}(m,t)}{\partial t}\Big]_{cloud\ microphysics} \quad (8.361)$$

$$\frac{\partial f_a(m_a,t)}{\partial t} = Adv\big[f_a(m_a,t)\big] + Grav\big[f_a(m_a,t)\big] + \Big[\frac{\partial f_a(m_a,t)}{\partial t}\Big]_{cloud\ microphysics} \quad (8.362)$$

where μ shows type of hydrometeor (the 7 types), $Adv[]$, $Grav[]$) shows change of SDF by the advection and the gravitational falling. $\Big[\Big]_{cloud\ microphycis}$ shows changes of SDF by the cloud microphysical processes.
The time evolution of $f_c^{(\mu)}(m,t)$ and $f_a(m,t)$ are shown as:

$$\begin{aligned}
\Big[\frac{\partial f_c^{(\mu)}(m,t)}{\partial t}\Big]_{cloud\ microphysics} &= \Big[\frac{\partial f_c^{(\mu)}(m,t)}{\partial t}\Big]_{activation} + \Big[\frac{\partial f_c^{(\mu)}(m,t)}{\partial t}\Big]_{cond/evap} \\
&+ \Big[\frac{\partial f_c^{(\mu)}(m,t)}{\partial t}\Big]_{coll/coag/rim/agg} \\
&+ \Big[\frac{\partial f_c^{(\mu)}(m,t)}{\partial t}\Big]_{frz} + \Big[\frac{\partial f_c^{(\mu)}(m,t)}{\partial t}\Big]_{melt} \\
\Big[\frac{\partial f_a(m_a,t)}{\partial t}\Big]_{cloud\ microphysics} &= \Big[\frac{\partial f_a(m_a,t)}{\partial t}\Big]_{activation}
\end{aligned}$$

where $\Big[\ \Big]_{***}$ show change of SDF by each cloud growth processes. The detail of these processes will be shown later.
The change of SDFs by advection and gravitational falling (i.e. first and second term of eq. 8.361, and 8.362) are calculated by dynamical core of SCALE-RM shown in section 3.

Discretization of Size Distribution Function(SDF)

The SDF of aerosol and cloud is predict as mass density of each particle size ($g_a(m_a)$, $g_c^{(\mu)}(m)$). However most of equations are given as equations of number density of cloud/aerosol ($f_c^{(\mu)}(m,t)$, $f_a(m_a,t)$), the mass density of cloud/aerosol are transferred to number density of cloud/aerosol ($g_a(m_a,t) = m_a g_a(m_a,t)$, $g_c^{(\mu)}(m,t) = m^{(\mu)} f_c^{(\mu)}(m,t)$).
To cover wide size range (i.e. $2\ \mu m \sim 3\ mm$), logarithmically uniform grid system ($log(m) \equiv \eta$, $log(m_a) \equiv \eta_a$) is used. In this system, the relationship, $\frac{m_{i+1}}{m_i} = const.$ is satisfied.

Activation from aerosol to cloud particles (Nucleation process)

The change of SDFs by activation from aerosol to cloud particles are calculated based on Kohler theory (Kohler 1936). Through this process, aerosols whose radii are larger than critical radius of aerosol ($r_{a,crit}$) are activated to clouds. The critical radius is given as

$$r_{a,crit} = \Big(\frac{4}{27}\frac{A^3}{B}\frac{1}{S_w}\Big)^{1/3}, \quad A = \frac{2\sigma}{R_v \rho_L T}, \quad B = i_v \frac{M_v}{M_s}\frac{\rho_s}{\rho_L}. \quad (8.363)$$

where S_w, σ, R_v, ρ_L, T, i_v, M_v, M_s, ρ_s show supersaturation of water, surface tention of water, gas constant of vapor, temperature, van't Hoff factor (= 2), moleculer weight of water, moleculer weight of aerosol, and density of aerosol, respectively.
At each time step, $r_{a,crit}$ are calculated by using temperature, and mass of aerosols whose radii are larger than $r_{a,crit}$ remove from SDF of aerosol and they are transferred to SDF of cloud as newly generated cloud particles.
The radii of newly generated clouds are corresponding to those of aerosols, but if the radii of aeorol are smaller than the lower limit of cloud SDF, the radii of newly generated clouds are set to smallest size of cloud SDF ($\sim 2\mu m$).
The change of aerosol's SDF and hydrometeor's SDF are shown as:

$$\Big[\frac{\partial f_a}{\partial t}\Big]_{activation} = -\int_{m_{a,crit}}^{\infty} f_a(m_a,t)dm_a \tag{8.364}$$

$$\Big[\frac{\partial f_c^{(\mu)}}{\partial t}\Big]_{activation} = -\Big[\frac{\partial f_a}{\partial t}\Big]_{activarion} \tag{8.365}$$

where $m_{a,crit} = \big(= \frac{4\pi}{3} r_a^3 \rho_a$ is mass of aerosol particles whose radii are the same as critical radii, $r_{a,crit}$. When there are not enough vapor to activate all aerosol particles whose radii are larger than the critical radius, i.e.

$$\int_{m_{a,crit}}^{\infty} m_a f_a(m_a,t)dm_a > q_v\rho, \tag{8.366}$$

only the aerosol particles whose radii are larger than $r_{a0,crit}$, which are given as:

$$\int_{m_{a0,crit}}^{\infty} m_a f_a(m_a,t)dm_a = q_v\rho, \tag{8.367}$$

are transferred to cloud paricles as:

$$\Big[\frac{\partial f_a}{\partial t}\Big]_{activation} = -\int_{m_{a0,crit}}^{\infty} f_a(m_a,t)dm_a, \tag{8.368}$$

$$\Big[\frac{\partial f_c^{(\mu)}}{\partial t}\Big]_{activation} = -\Big[\frac{\partial f_a}{\partial t}\Big]_{activarion}. \tag{8.369}$$

where q_v and ρ is mixing ratio of water vapor and density.

Condensation/Evaporation

Calculation of condensation and evaporation process are based on a equation. The mass change by these two process are given by an equation (e.g. Rogers and Yau, 1989Rogers and Yau (1989)):

$$
\begin{aligned}
\frac{dm}{dt} &= C^{(\mu)}(m)G^{(\mu)}(T)S^{(\mu)} \qquad (8.370)\\
G^{(\mu)}(T) &= \begin{cases} G_w(T) & (\mu:\ liquid) \\ G_i(T) & (\mu:\ ice) \end{cases} \\
G_w(T) &= \frac{4\pi}{\frac{R_vT}{e_w(T)D_v} + \frac{L_w}{KT}\Big(\frac{L_w}{R_vT} - 1\Big)} \\
G_i(T) &= \frac{4\pi}{\frac{R_vT}{e_i(T)D_v} + \frac{L_i}{KT}\Big(\frac{L_i}{R_vT} - 1\Big)} \\
S^{(\mu)} &= \begin{cases} S_w & (\mu : liquid) \\ S_i & (\mu : ice) \end{cases}
\end{aligned}
$$

where $C^{(\mu)}(m)$ is capasitance, which depends on shape of each types of hydrometeor, S_w, S_i are super saturation of water and ice, L_w, L_i is sensible heat of evaporation, sublimation, D_v is diffusion constant of vapor, K is conductivity of air, and e_w, e_i is saturation vapor pressure and saturation ice pressure, respectively. Condensation (evaporation) occur when $S^{(\mu)}$ is positive (negative). To calculate change of SDF by condensation/evaporation, mass flux ($F^{(\mu)}_{cond/evap}$) on each bin is given by using number density ($f_c^{(\mu)}$) and $\frac{dm}{dt}$ as:

$$
F^{(\mu)}_{cond/evap} = f^{(\mu)}(m)\frac{dm}{dt} = f^{(\mu)}(m)C^{(\mu)}G^{(\mu)}(T)S^{(\mu)}. \qquad (8.371)
$$

Using this equation, time evolution of SDF ($f^{(\mu)}$) is given as

$$
\begin{aligned}
\Big[\frac{\partial f^{(\mu)}(m,t)}{\partial t}\Big]_{cond/evap} &= -\frac{\partial}{\partial m}F^{(\mu)}_{cond/evap}(m) \\
&= -\frac{\partial}{\partial m}\big(f^{(\mu)}(m)C^{(\mu)}\big)G^{(\mu)}(T)S^{(\mu)}. \qquad (8.372)
\end{aligned}
$$

By using the $\eta(=\log(m))$, the eq.8.372 is transferred to advection equation :

$$
\begin{aligned}
\frac{\partial f^{(\mu)}(\eta)}{\partial t} &= -\frac{\partial}{\partial \eta}\big(f^{(\mu)}(\eta)U^{(\mu)}(\eta)\big) \qquad (8.373)\\
U^{(\mu)}(\eta) &= \frac{C^{(\mu)}(\eta)}{\exp(\eta)}G^{(\eta)}(T)S^{(\eta)}.
\end{aligned}
$$

To solve the eq. 8.373, a scheme developed by Bott (1989)Bott (1989) is used. The number density of i-th bin after Δt ($f_i(t+\Delta t)$) is given as follow:

$$
\begin{aligned}
f_i(t+\Delta t) &= f_i(t) - \frac{\Delta t}{\Delta \eta}\Big[F_{cond/evap,i+1/2} - F_{cond/evap,i-1/2}\Big]. \\
F_{cond/evap,i+1/2} &= \frac{\Delta \eta}{\Delta t}\Big[\frac{i^+_{l,i+1/2}}{i_{l,j}} f_i(t) - \frac{i^-_{l,i+1/2}}{i_{l,i+1}} f_{i+1}(t)\Big] \\
i^+_{l,i+1/2} &= max\big(0, I^+_l(c_{i+1/2})\big) \\
i^-_{l,i+1/2} &= max\big(0, I^-_l(c_{i+1/2})\big) \\
i^+_{l,i} &= max\big(I_{l,i}, i^+_{l,i+1/2} + i^-_{l,i+1/2})\big) \\
I^+_l(c_{i+1/2}) &= \sum_{k=0}^{2} \frac{a_{i,k}}{(k+1)2^{k+1}}\big[1 - (1-2c^+_j)^{k+1}\big] \\
I^-_l(c_{i+1/2}) &= \sum_{k=0}^{2} \frac{a_{i+1,k}}{(k+1)2^{k+1}}(-1)^k\big[1 - (1-2c^-_j)^{k+1}\big] \\
a_{i,0} &= -\frac{1}{24}\big(f_{i+1}(t) - 26 f_i(t) + f_{i-1}(t)\big) \\
a_{i,1} &= \frac{1}{2}\big(f_{i+1}(t) - f_{i-1}(t)\big) \\
a_{i,2} &= \frac{1}{2}\big(f_{i+1}(t) - 2f_i(t) + f_{i-1}(t)\big) \\
c^{\pm}_i &= \pm\big(c^n_{i+1/2} \pm |c^n_{i+1/2}|\big)/2 \\
c^n_{i+1/2} &= U^n_{i+1/2}\frac{\Delta t}{\Delta \eta}
\end{aligned}
\tag{8.374}
$$

Since the super saturation ($S^{(\mu)}$) can change during time step (Δt), we apply a method shown below to reflect the change of supersaturation during Δt. Time evolution of supersaturation can be given by equations:

$$
\begin{aligned}
\frac{d}{dt}\begin{pmatrix} S_w \\ S_i \end{pmatrix} &= \begin{pmatrix} a_{c/e} & b_{c/e} \\ c_{c/e} & d_{c/e} \end{pmatrix}\begin{pmatrix} S_w \\ S_i \end{pmatrix} = A\begin{pmatrix} S_w \\ S_i \end{pmatrix} \\
a_{c/e} &= -(S_w+1)\Big(\frac{1}{q_v} + \frac{L_w}{R_v T^2}\frac{L_w}{C_p}\Big)\int f^{(w)}(m)C^{(w)}(m)dmG_w(t) \\
b_{c/e} &= -(S_w+1)\Big(\frac{1}{q_v} + \frac{L_w}{R_v T^2}\frac{L_i}{C_p}\Big)\sum_{\mu\in ice}\int f^{(\mu)}(m)C^{(\mu)}(m)dmG_i(t) \\
c_{c/e} &= -(S_i+1)\Big(\frac{1}{q_v} + \frac{L_i}{R_v T^2}\frac{L_w}{C_p}\Big)\int f^{(w)}(m)C^{(w)}(m)dmG_w(t) \\
d_{c/e} &= -(S_i+1)\Big(\frac{1}{q_v} + \frac{L_i}{R_v T^2}\frac{L_i}{C_p}\Big)\sum_{\mu\in ice}\int f^{(\mu)}(m)C^{(^m u)}(m)dmG_i(t)
\end{aligned}
\tag{8.375}
$$

where q_v is mixing ration of vapor.
Using eigen value of A (Λ_+, Λ_- ($\Lambda_+ > \Lambda_-$)), and assuming $a_{c/e}$, $b_{c/e}$, $c_{c/e}$, $d_{c/e}$ is constant during Δt, average value of super saturation ($\bar{S}_{w,i}(t)$) during Δt is given as:

$$
\begin{aligned}
\bar{S}_w(t) = \frac{1}{\Delta t}\int_t^{t+\Delta t} S_w(\tau)d\tau &= b\frac{e^{\Lambda_+\Delta t}-1}{\Lambda_+\Delta t}S_+(t) + b\frac{e^{\Lambda_-\Delta t}-1}{\Lambda_-\Delta t}S_-(t) \\
\bar{S}_i(t) = \frac{1}{\Delta t}\int_t^{t+\Delta t} S_i(\tau)d\tau &= (\Lambda_+ - a)\frac{e^{\Lambda_+\Delta t}-1}{\Lambda_+\Delta t}S_+(t) + (\Lambda_- - a)\frac{e^{\Lambda_-\Delta t}-1}{\Lambda_-\Delta t}S_-(t) \\
S_+(t) &= \frac{(\Lambda_- - a)S_w(t) - bS_i(t)}{b(\Lambda_- - \Lambda_+)} \\
S_+(t) &= \frac{(a - \Lambda_+)S_w(t) + bS_i(t)}{b(\Lambda_- - \Lambda_+)}
\end{aligned}
$$

The averaged super saturation ($\bar{S}_{w,i}(t)$) is used to solve the eq. 8.375.

Collision/Coagulation/Riming/Aggregation

Collision/Coagulation process are calculated by solving Stochastic Collision Equation (e.g. Pruppecher and Klett, 1997)Pruppacher and Klett (1997):

$$
\begin{aligned}
\frac{\partial f(m)}{\partial t} &= \int_0^{m/2} f(m')f(m-m')K(m', m-m')dm' \\
&- f(m)\int_0^{\infty} f(m'')K(m, m'')dm''
\end{aligned} \tag{8.376}
$$

where $K(m, m')$ is collection kernel function. Three types of the kernel function, i.e. Long type kernel (Long, 1974Long (1974)), Golovin type kernel (Golovin, 1963Golovin (1963)) and Hydro-dynamic dynamic kernel as shown eq. 8.377 are implemented into the SCALE-RM.

$$
K(m, m') = \pi(r(m) - r(m'))\,|V(m) - V(m')|\,E_{col}(m, m')E_{coag}(m, m') \tag{8.377}
$$

where $r(m)$ is radius of hydrometeros whose mass is m, and $V(m)$ is terminal velocity of hydrometeors. The terminal velocity of each species of hydrometeor and each size are shown in Figure 8.12 E_{col}, and E_{coag} is collision effieiency and coagulation efficiansy, respectively.

Although the stochastic collision equation can be apply for collision/coagulation of one type of hydrometeros (i.e. liquid water), the SCALE-RM predicts 7 types of hydrometeors, and interactions of these types hydrometeors (i.e. riming/aggregation) must be calculated. To calculate the interaction of all 7 types of hydrometeors, the extented stochastic collision equation:

$$
\begin{aligned}
\left[\frac{\partial f^{(\mu)}(m)}{\partial t}\right]_{coll/coag/rim/agg} &= \\
\sum_\lambda \sum_\nu \int_0^{m/2} f^{(\lambda)} &(\quad m')f^{(\nu)}(m-m')K_{\lambda\nu}(m', m-m')dm' \\
-f^{(\mu)}(m)\sum_\kappa \int_0^{\infty} f^{(\kappa)} &(\quad m'')K_{\kappa\mu}(m, m'')dm''
\end{aligned} \tag{8.378}
$$

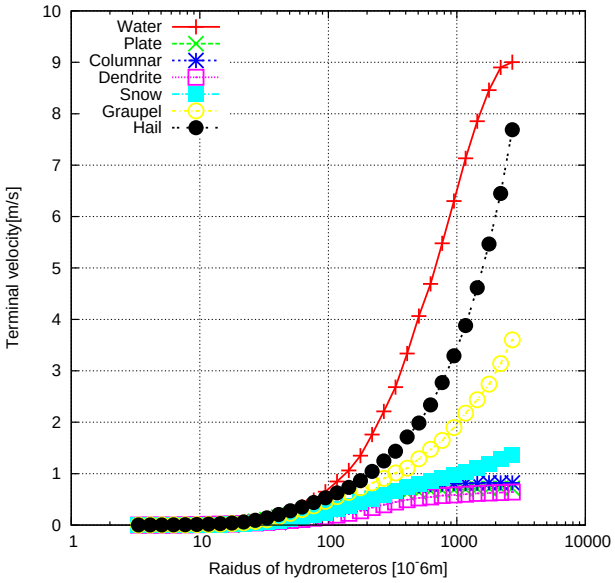

Figure 8.12: Terminal velocity of Water (Plus), Plate-type ice (Cross), Columnar-type ice (Asterisk), Dendrite-type ice(Open square), Snow(Closed square), Graupel(Open circle), and Hail(Closed circle)

is applied (where μ, ν, λ, κ represent species of hydrometeor). The convinations of μ, ν, λ are shown in table 8.6.

Table 8.6: Catalog of interaction between 7 species. W, I, S, G, H shows water, ice, snow, graupel, and hail, respectively. G/H shows graupel(hail) generates when T is lower(higher) than 270.15

	W	I	S	G	H
W	W	G/H	G/H	G/H	G/H
I	I	S	S	I	I
S	S	S	S	S	S
G	G/H	G/H	G	G	G/H
H	G/H	G/H	G/H	G/H	H

To solve the stochastic collision equation, a scheme developed by Bott (1998)Bott (1998) was implemented into SCLAE-RM.
The Bott (1998)Bott (1998) scheme calculate evolution of mass density distribution ($g(\eta) = mf(\eta)$, $\eta = \log(m)$). The stochastic collision equation can be transferred to

$$\frac{\partial g(\eta)}{\partial t} = \int_{\eta_0}^{\eta_1} \frac{m^2}{(m-m')^2 m'} g(\eta-\eta')K(\eta-\eta',\eta')g(\eta')d\eta' - \int_{\eta_0}^{\infty} g(\eta)\frac{K(\eta,\eta')}{m'}g(\eta')d\eta'. \quad (8.379)$$

where $\eta_1 = \log(m/2)$. Decreases of mass of i-th bin and j-th bin are given by

$$\frac{\partial g_i^{(\mu)}}{\partial t} = -\Delta g_i^{(\mu)} K_{\mu\nu}(i,j)\frac{g_j^{(\nu)}}{m_j}\Delta\eta \quad (8.380)$$

and

$$\frac{\partial g_j^{(\mu)}}{\partial t} = -\Delta g_j^{(\nu)} K_{\mu\nu}(i,j)\frac{g_i^{(\mu)}}{m_i}\Delta\eta \quad (8.381)$$

respectively. The terms corresponds to the second term of right-hand side of eq.8.379. The eq. 8.380 and eq. 8.381 can transfer to

$$\Delta g_i^{(\mu)} = g_i^{(\mu)}\Big[1-\exp\big(-K_{\mu\nu}(i,j)\frac{g_j^{(\nu)}}{m_j}\Delta\eta\Delta t\big)\Big] \quad (8.382)$$

$$\Delta g_j^{(\nu)} = g_j^{(\nu)}\Big[1-\exp\big(-K_{\mu\nu}(i,j)\frac{g_i^{(\mu)}}{m_i}\Delta\eta\Delta t\big)\Big]. \quad (8.383)$$

The sum of $\Delta g_i^{(\mu)}$ and $\Delta g_j^{(\nu)}$ corresponds to newley generated mass by collision of hydrometeor whose mass is m_i and m_j. The newly generated mass ($g' = \Delta g_i^{(\mu)} + \Delta g_j^{(\nu)}$, which is coresponding to first term of right-hand side of eq.8.379) added k-th bin ($m_k = m_i + m_j$). Since m_k is not always bin center, newly generated mass is devided to k-th and k+1-th bin as follow.
The production of k-th and k+1-th bin is represened:

$$\Delta g_k^{(\lambda)} = g_k^{\lambda} + g' - \zeta \quad (8.384)$$

$$\Delta g_{k+1}^{(\lambda)} = g_{k+1}^{\lambda} + \zeta \quad (8.385)$$

$$\zeta = \frac{g'}{g_k^{(\lambda)} + g'}\sum_{s=0}^{2}\frac{a_{k,s}}{(s+1)2^{k+1}}[1-(1-2c_k)^{k+1}]$$

$$c_k = \frac{m'-m_k}{m_{k+1}-m_k}$$

$$a_{k,0} = -\frac{1}{24}(g_{k+1}^{(\lambda)} - 26g_k^{(\lambda)} + g_{k-1}^{(\lambda)})$$

$$a_{k,1} = -\frac{1}{2}(g_{k+1}^{(\lambda)} - g_{k-1}^{(\lambda)})$$

$$a_{k,2} = -\frac{1}{2}(g_{k+1}^{(\lambda)} - 2g_k^{(\lambda)} + g_{k-1}^{(\lambda)})$$

These procedure is applied for all bin of all types of hydrometeors.
In addition, to calculate this process fastly, a scheme of Sato et al. (2009)Sato et al. (2009) are also implemented into SCALE-RM.

Freezing

The calculation of freezing process is based on a parameterization of Bigg (1953)Bigg (1953). The parameterization is calculated number density of water ($f_c^{(w)}$), wchich can be freezed:

$$\begin{aligned} \frac{\partial}{\partial t} f^{(w)}(m) &= -\frac{f^{(w)}(m)}{\tau_{fr}} \\ \tau_{fr} &= \frac{\exp\left[b_{fr}(T_0 - T)\right]}{a_{fr} m} \end{aligned} \tag{8.386}$$

where $a_{fr} = 10^{-4} s^{-1}$, and $b_{fr} = 0.66^o C^{-1}$ are emperical parameters, and T_0 is 273.15 K.
The eq. 8.386 can transfer to

$$\begin{aligned} \frac{\partial g^{(w)(m)}}{\partial t} &= -\frac{g^{(w)}(m)}{\tau_{fr}(m)} \\ \tau_{fr,i} &= \frac{\exp\left(b_{fr}(T_0 - T)\right)}{a_{fr} m} \end{aligned} \tag{8.387}$$

From this equation, The mass change of i-th bin during Δt is given as

$$g_i^{(w)}(t + \Delta t) = g_i^{(w)} - Frz_i \tag{8.388}$$

$$\begin{cases} g_i^{(plate)}(t + \Delta t) = g_i^{(plate)} + Frz_i & (r_w < 200\mu m) \\ g_i^{(hail)}(t + \Delta t) = g_i^{(hail)} + Frz_i & (r_w > 200\mu m) \end{cases} \tag{8.389}$$

$$Frz_i = g_i^{(w)}(t)\Big[1 - \exp\big(-\frac{\Delta t}{\tau_{fr,i}}\big)\Big]$$

As shown in eq. 8.389, the mass of liuid is transfer from to plate type ice ($r_w < 200\mu m$) or hail ($r_w > 200\mu m$).

Melting

The calculation of melting process is too simple way, that is, all ice particles (i.e. plate, columner, dendrite, snow, graupel and hail) melt immediately when the temperature is larger than $T_0 = 273.15$ K. This is too simply to represent ice phase process, and we will modify this method near future.

8.4 Radiation

TBD

8.5 Surface flux

Corresponding author : Seiya Nishizawa

8.5.1 Monin-Obukhov similarity

The first of the all, we assume that in the boundary layer 1. fluxes are constant, and 2. variables are horizontally uniform.

Relations between flux and vertical gradient are

$$\frac{kz}{u_*}\frac{\partial u}{\partial z} = \phi_m\left(\frac{z}{L}\right), \tag{8.390}$$

$$\frac{kz}{\theta_*}\frac{\partial \theta}{\partial z} = \phi_h\left(\frac{z}{L}\right), \tag{8.391}$$

$$\frac{kz}{q_*}\frac{\partial q}{\partial z} = \phi_q\left(\frac{z}{L}\right), \tag{8.392}$$

where k is the Von Karman constant. L is the Monin-Obukhov scale height, which is

$$L = \frac{\theta u_*^2}{kg\theta_*}, \tag{8.393}$$

where g is the gravity. The scaling velocity, u_*, temperature, θ_*, and water vapor, q_*, are defined from the vertical eddy fluxes of momentum, sensible heat and water vapor:

$$\overline{u'w'} = -u_*u_*, \tag{8.394}$$

$$\overline{w'\theta'} = -u_*\theta_*, \tag{8.395}$$

$$\overline{w'q'} = -u_*q_*. \tag{8.396}$$

The integration between the roughness length z_0 to the height z of the lowest model level, eqs. (8.390) and (8.391) become

$$u(z) = \frac{u_*}{k}\left\{\ln(z/z_0) - \Phi_m(z/L) + \Phi_m(z_0/L)\right\}, \tag{8.397}$$

$$\Delta\theta = R\frac{\theta_*}{k}\left\{\ln(z/z_0) - \Phi_h(z/L) + \Phi_h(z_0/L)\right\}, \tag{8.398}$$

where $\Delta\theta = \theta - \theta_0$, and

$$\Phi_m(z) = \int^z \frac{1-\phi_m(z')}{z'}dz', \tag{8.399}$$

$$\Phi_h(z) = \int^z \frac{R-\phi_h(z')}{Rz'}dz'. \tag{8.400}$$

8.5.2 Louis (1979) Model

Louis (1979) introduced a parametric model of vertical eddy fluxes.

The L becomes

$$L = \frac{\theta u^2}{g\Delta\theta}\frac{\ln(z/z_0) - \Phi_h(z/L) + \Phi_h(z_0/L)}{\left\{\ln(z/z_0) - \Phi_m(z/L) + \Phi_m(z/L)\right\}^2}. \tag{8.401}$$

The bulk Richardson number for the layer Ri_B is

$$Ri_B = \frac{gz\Delta\theta}{\theta u^2}, \tag{8.402}$$

and its form implies relationship with the Monin-Obukhov scale height L. Then the fluxes could be written as

$$u_*^2 = a^2 u^2 F_m \left(\frac{z}{z_0}, Ri_B \right), \tag{8.403}$$

$$u_* \theta_* = \frac{a^2}{R} u \Delta\theta F_h \left(\frac{z}{z_0}, Ri_B \right), \tag{8.404}$$

where R is ratio of the drag coefficients for momentum and heat in the neutral limit, (the turbulent Prandtl number), and

$$a^2 = \frac{k^2}{\{\ln(z/z_0)\}^2} \tag{8.405}$$

is the drag coefficient in neutral conditions.

For the unstable condition ($Ri_B < 0$), F_is ($i = m, h$) could be

$$F_i = 1 - \frac{bRi_B}{1 + c_i\sqrt{|Ri_B|}}, \tag{8.406}$$

under the consideration that F_i must behave as $1/u$ (i.e. $\sqrt{|Ri_B|}$) in the free convection limit ($u \to 0$), and becomes 1 in neutral conditions ($Ri_B \to 0$). In the stable conditions (Ri_b), on the other hand, Louis (1979) adopted the following form for F_i:

$$F_i = \frac{1}{(1 + b' Ri_B)^2}. \tag{8.407}$$

The constants are estimated as $R = 0.74$ by Businger et al. (1971), and $b = 2b' = 9.4$ by Louis (1979). By the dimensional analysis,

$$c_i = C_i^* a^2 b \sqrt{\frac{z}{z_0}}, \tag{8.408}$$

and $C_m^* = 7.4, C_h^* = 5.3$, which result best fit curves.

8.5.3 Uno et al. (1995) Model

Uno et al. (1995) extended the Louis Model, which considers difference of the roughness length between for momentum, z_0, and temperature, z_t.

The potential temperature difference between $z = z$ and $z = z_t$, $\Delta\theta_t$, is

$$\begin{aligned}
\Delta\theta_t &= R\frac{\theta_*}{k}\{\ln(z_0/z_t) - \Phi_h(z_0/L) + \Phi_h(z_t/L)\} + \Delta\theta_0, \\
&= R\frac{\theta_*}{k}\ln(z_0/z_t) + \Delta\theta_0, \\
&= \Delta\theta_0 \left\{ \frac{R\ln(z_0/z_t)}{\Psi_h} + 1 \right\},
\end{aligned} \tag{8.409}$$

where $\Delta\theta_0 = \theta_z - \theta_{z_0} (= \Delta\theta)$,

$$\Psi_h = \int_{z_0}^{z} \frac{\phi_h}{z'} dz', \tag{8.410}$$

and ϕ_h is assumed to be R in the range $z_t < z < z_0$. Thus

$$\Delta\theta_0 = \Delta\theta_t \left\{ \frac{R \ln(z_0/z_t)}{\Psi_h} + 1 \right\}^{-1}, \tag{8.411}$$

or equivalently,

$$Ri_{B0} = Ri_{Bt} \left\{ \frac{R \ln(z_0/z_t)}{\Psi_h} + 1 \right\}^{-1}. \tag{8.412}$$

From the eqs. (8.403) and (8.404),

$$\Delta\theta_0 = \frac{R\theta_*}{k} \ln\left(\frac{z}{z_0}\right) \frac{\sqrt{F_m}}{F_h}, \tag{8.413}$$

while

$$\Delta\theta_0 = \frac{\theta_*}{k} \Psi_h, \tag{8.414}$$

from eqs. (8.391) and (8.410). Therefore

$$\Psi_h = R \ln\left(\frac{z}{z_0}\right) \frac{\sqrt{F_m}}{F_h}. \tag{8.415}$$

Because Ψ_h depends on Ri_{B0}, Ri_{B0} cannot be calculated from Ri_{Bt} with eq. (8.412) directly, so numerical iteration is required to obtain Ri_{B0} [3]. Starting from Ri_{Bt} as the first estimation of Ri_{B0}, the second estimate by the Newton-Raphson iteration becomes

$$\hat{R}i_{B0} = Ri_{Bt} - \frac{Ri_{Bt} R \ln(z_0/z_t)}{\ln(z_0/z_t) + \hat{\Psi}_h}, \tag{8.416}$$

where $\hat{\Psi}_h$ is the estimate of Ψ_h using Ri_{Bt} instead of Ri_{B0}. Approximate values for F_m, F_h, and Ψ_h are re-calculated based on the $\hat{R}i_{B0}$, and then $\Delta\theta_0$, and the surface fluxes u_*^2 and $u_*\theta_*$ are calculated from eqs. (8.411), (8.403), and (8.404), respectively.

R

8.5.4 Roughness length

Miller et al. (1992) provides the roughness length over the tropical ocean, based on the numerical calculations by combining the smooth surface values with the Charnock relation for the aerodynamic roughness length and the constant values for heat and moisture in accordance with Smith (1988,1989) suggestions:

$$z_0 = 0.11u/\nu_* + 0.018u_*^2/g, \tag{8.417}$$

$$z_t = 0.40u/\nu_* + 1.4 \times 10^{-5}, \tag{8.418}$$

$$z_q = 0.62u/\nu_* + 1.3 \times 10^{-4}, \tag{8.419}$$

where ν_* is the kinematic viscosity of air ($\sim 1.5 \times 10^{-5}$), and z_0, z_t, and z_q are the roughness length for the momentum, heat, and vapor, respectively.

[3] In the stable case, it can be solved analytically with eq. (8.407), but the solution is too complicated.

8.5.5 Discretization

All the fluxes are calculated based on the velocity at the first full-level (k=1) ($z = \Delta z/2$). The absolute velocities U are

$$U^2_{i+\frac{1}{2},j,1} = \left\{ \frac{2(\rho u)_{i+\frac{1}{2},j,1}}{\rho_{i,j,1} + \rho_{i+1,j,1}} \right\}^2 + \left\{ \frac{(\rho v)_{i,j-\frac{1}{2},1} + (\rho v)_{i,j+\frac{1}{2},1} + (\rho v)_{i+1,j-\frac{1}{2},1} + (\rho v)_{i+1,j+\frac{1}{2},1}}{2(\rho_{i,j,1} + \rho_{i+1,j,1})} \right\}^2 + \left\{ \frac{(\rho w)_{i,j,1+\frac{1}{2}} + (\rho w)_{i+1,j,1+\frac{1}{2}}}{2(\rho_{i,j,1} + \rho_{i+1,j,1})} \right\}^2, \tag{8.420}$$

$$U^2_{i,j+\frac{1}{2},1} = \left\{ \frac{(\rho u)_{i-\frac{1}{2},j,1} + (\rho u)_{i+\frac{1}{2},j,1} + (\rho u)_{i-\frac{1}{2},j+1,1} + (\rho u)_{i+\frac{1}{2},j+1,1}}{2(\rho_{i,j,1} + \rho_{i,j+1,1})} \right\}^2 + \left\{ \frac{2(\rho v)_{i,j+\frac{1}{2},1}}{\rho_{i,j,1} + \rho_{i,j+1,1}} \right\}^2 + \left\{ \frac{(\rho w)_{i,j,1+\frac{1}{2}} + (\rho w)_{i,j+1,1+\frac{1}{2}}}{2(\rho_{i,j,1} + \rho_{i,j+1,1})} \right\}^2, \tag{8.421}$$

$$U^2_{i,j,1} = \left\{ \frac{(\rho u)_{i-\frac{1}{2},j,1} + (\rho u)_{i+\frac{1}{2},j,1}}{2\rho_{i,j,1}} \right\}^2 + \left\{ \frac{(\rho v)_{i,j-\frac{1}{2},1} + (\rho v)_{i,j+\frac{1}{2},1}}{2\rho_{i,j,1}} \right\}^2 + \left\{ \frac{(\rho w)_{i,j,1+\frac{1}{2}}}{2\rho_{i,j,1}} \right\}^2, \tag{8.422}$$

here it is note that $(\rho w)_{i,j,\frac{1}{2}} = 0$. The potential temperatures θ are

$$\theta_{i,j,1} = \frac{(\rho\theta)_{i,j,1}}{\rho_{i,j,1}}, \tag{8.423}$$

$$\bar{\theta}_{i+\frac{1}{2},j,1} = \frac{\theta_{i,j,1} + \theta_{i+1,j,1}}{2}, \tag{8.424}$$

$$\bar{\theta}_{i,j+\frac{1}{2},1} = \frac{\theta_{i,j,1} + \theta_{i,j+1,1}}{2}. \tag{8.425}$$

The roughness lengthes, z_0, z_t, and z_q are caluclated from the eqs. (8.417), (8.418), and (8.419), in which the friction verociy u_* is estimated as

$$u_* = \sqrt{C_{m0}}U, \tag{8.426}$$

where C_{m0} is a constant bulk coefficient, and we use 1.0×10^{-3} as its value.

From eq. (8.412) The Ri_{Bt}, which is the first guess of the Ri_{B0}, is

$$Ri_{Bt} = \frac{gz_1(\theta_1 - \theta_{sfc})}{\bar{\Theta}U^2}, \tag{8.427}$$

with the assumption that $\theta_{z_t} = \theta_{sfc}$. The estimation of the $\hat{\Psi}_h$ is calculated with Ri_{Bt} from the eqs. (8.415), (8.406), and (8.407). The final estimation of Ri_{B0} is obtained from the eq. (8.416), and the final estimation of Ψ_h is obtaind with the Ri_{B0}.

Now we can calculate the bulk coefficients, C_m, C_h, and C_e for the moments,

heat, and vapor:

$$C_m = \frac{k^2}{\ln(z_1/z_0)} F_m(Ri_{B0}), \tag{8.428}$$

$$C_h = \frac{k^2}{R\ln(z_1/z_0)} F_h(Ri_{B0}) \left\{ \frac{R\ln(z_0/z_t)}{\Psi_h} + 1 \right\}^{-1}, \tag{8.429}$$

$$C_e = \frac{k^2}{R\ln(z_1/z_0)} F_h(Ri_{B0}) \left\{ \frac{R\ln(z_0/z_e)}{\Psi_h} + 1 \right\}^{-1}. \tag{8.430}$$

The fluxes are

$$\overline{\rho u' w'} = -C_m U \rho u, \tag{8.431}$$

$$\overline{\rho v' w'} = -C_m U \rho v, \tag{8.432}$$

$$\overline{\rho w' w'} = -C_m U \rho w, \tag{8.433}$$

$$\overline{\rho \theta' w'} = -C_h U \{\rho\theta - \rho\theta_{sfc}\}, \tag{8.434}$$

$$\overline{\rho q' w'} = -C_e U \rho (q - q_{evap}), \tag{8.435}$$

where q_{evap} is the saturation value at surface.

8.6 Aerosol

Chapter 9

Aerosol

Corresponding author : Mizuo Kajino

9.1 Large scale sinking

Corresponding author : Seiya Nishizawa

In the DYCOMS01 experiment, the large scale sinking is added to express large scale downward motion corresponding to the Haddley circulation. The motion converges virtually and results mass escape to out of the system.

The density loss rate is constant L:

$$L = -\frac{\partial \rho w_L}{\partial z}, \tag{9.1}$$

where w_l is vertical velocity corresponding to the large scale sinking. Then vertical momentum with the sinking is

$$\rho w_L = -Lz. \tag{9.2}$$

Continuous equation is now

$$\frac{\partial \rho}{\partial z} + \frac{\partial \rho u}{\partial x} + \frac{\partial \rho v}{\partial y} + \frac{\partial \rho (w + w_L)}{\partial z} = -L. \tag{9.3}$$

Lagrangian conservation equation for scalar quantities are

$$\rho \frac{\partial \phi}{\partial t} + \rho u \frac{\partial \phi}{\partial x} + \rho v \frac{\partial \phi}{\partial y} + \rho (w + w_L) \frac{\partial \phi}{\partial z} = 0, \tag{9.4}$$

and becomes with eq. (9.3)

$$\frac{\partial \rho \phi}{\partial t} + \frac{\partial \rho u \phi}{\partial x} + \frac{\partial \rho v \phi}{\partial y} + \frac{\partial \rho (w + w_L) \phi}{\partial z} = -L\phi. \tag{9.5}$$

The equations for mixing ratio is

$$\frac{\partial \rho Q}{\partial t} + \frac{\partial \rho Q u}{\partial x} + \frac{\partial \rho Q v}{\partial y} + \frac{\partial \rho Q (w + w_L)}{\partial z} = -LQ. \tag{9.6}$$

Note that this is identical to that of scalar quantities.

The w_L at the top boundary is not zero while w is zero. The vertical flux $\rho w_L \phi$ at the top layer interface could be determined as that convergence of the flux is canceled with $L\phi$.

Bibliography

E. K. Bigg. The formation of atmospheric ice crystals by the freezing of droplets. *Quarterly Journal of the Royal Meteorological Society*, 79:510–519, 1953.

A. Bott. A positive definite advection scheme obtained by nonlinear renormalization of the advective fluxes. *Monthly Weather Review*, 117:833–853, 1989.

A. Bott. A flux method for the numerical solution of the stochastic collection equation. *Journal of the Atmospheric Sciences*, 55:2284–2293, 1998.

A. R. Brown, S. H. Derbyshire, and P. J. Mason. Large-eddy simulation of stable atmospheric boundary layers with a revised stochastic subgrid model. *Quarterly Journal of the Royal Meteorological Society*, 120:1485–1512, 1994.

J. W. Deardorff. Stratocumulus-capped mixed layers derived from a three-dimensional model. *Boundary-Layer Meteorology*, 18:495–527, 1980.

A. Favre. Turbulence: Spacetime statistical properties and behavior in supersonic flows. *Physics of Fluids*, 26:2851–2863, 1983.

A. M. Golovin. The solution of the coagulation equation for cloud droplets in arising air current. *Bull. Acad. Sci., USSR, Geophys. Ser. X*, 5:833–853, 1963.

S. Kentaroh, T. Nakajima, T. Y. Nakajima, and A. P. Khain. Aerosol effects of the condensation process on a convective cloud simulation. *Journal of the Atmospheric Sciences*, 67:1126–1141, 2010.

A. Long. Solutions to the droplet collection equation for polynomial kernels. *Journal of the Atmospheric Sciences*, 31:1041–1052, 1974.

C.-H. Moeng and J. C. Wyngaard. Spectral analysis of large-eddy simulation of the convective boundary layer. *Journal of the Atmospheric Sciences*, 45: 3573–3587, 1988.

H. R. Pruppacher and J. D. Klett. *Microphysics of Clouds and Precipitation, 2nd edition.* Lkuwer Academic Publishers, 1997.

R. R. Rogers and M. K. Yau. *Short Course in Cloud Physics, 3rd edition.* Butterworth-Heinemann, Elsevier, Unitate States, 1989.

Y. Sato, T. Nakajima, K. Suzuki, and T. Iguchi. Application of a monte carlo integration method to collision and coagulation growth processes of hydrometeors in a bin-type model. *Journal of Geophysical Research*, 114:D09215, doi:10.1029/2008JD011247, 2009.

A. Scotti, C. Meneveau, and D. K. Lilly. Generalized smagorinsky model for anisotropic grids. *Physics of Fluids A*, 5:2306–2308, 1993.

T. Seiki and T. Nakajima. Aerosol effects of the condensation process on a convective cloud simulation. *Journal of the Atmospheric Sciences*, 71:833–853, 2014.

L. J. Wicker and W. C. Skamarock. Time-splitting methods for elastic models using forward time schemes. *Mon. Wea. Rev.*, 130:2088–2098, 2002.

Appendix A

The detal numerics

A.1 4th order central differnce

The 4th order central difference is given by

$$\frac{\partial \phi}{\partial x} = \frac{-\phi_{i+2} + 8\phi_{i+1} - 8\phi_{i-1} + \phi_{i+2}}{12\Delta x} = 0 \tag{A.1}$$

where

$$\phi_{i+2} = \phi_i + 2\Delta x \left(\frac{\partial \phi}{\partial x}\right)_i + 2\Delta x^2 \left(\frac{\partial^2 \phi}{\partial x^2}\right)_i + \frac{4\Delta x^3}{3} \left(\frac{\partial^3 \phi}{\partial x^3}\right)_i + \frac{2\Delta x^4}{3} \left(\frac{\partial^3 \phi}{\partial x^4}\right)_i + O(\Delta x^5) \tag{A.2}$$

$$\phi_{i+1} = \phi_i + \Delta x \left(\frac{\partial \phi}{\partial x}\right)_i + \frac{\Delta x^2}{2} \left(\frac{\partial^2 \phi}{\partial x^2}\right)_i + \frac{\Delta x^3}{6} \left(\frac{\partial^3 \phi}{\partial x^3}\right)_i + \frac{\Delta x^4}{24} \left(\frac{\partial^3 \phi}{\partial x^4}\right)_i + O(\Delta x^5) \tag{A.3}$$

$$\phi_i = \phi_i \tag{A.4}$$

$$\phi_{i-1} = \phi_i - \Delta x \left(\frac{\partial \phi}{\partial x}\right)_i + \frac{\Delta x^2}{2} \left(\frac{\partial^2 \phi}{\partial x^2}\right)_i - \frac{\Delta x^3}{6} \left(\frac{\partial^3 \phi}{\partial x^3}\right)_i + \frac{\Delta x^4}{24} \left(\frac{\partial^3 \phi}{\partial x^4}\right)_i + O(\Delta x^5) \tag{A.5}$$

$$\phi_{i+2} = \phi_i - 2\Delta x \left(\frac{\partial \phi}{\partial x}\right)_i + 2\Delta x^2 \left(\frac{\partial^2 \phi}{\partial x^2}\right)_i - \frac{4\Delta x^3}{3} \left(\frac{\partial^3 \phi}{\partial x^3}\right)_i + \frac{2\Delta x^4}{3} \left(\frac{\partial^3 \phi}{\partial x^4}\right)_i + O(\Delta x^5) \tag{A.6}$$

Therefore,

$$\frac{-\phi_{i+2} + 8\phi_{i+1} - 8\phi_{i-1} + \phi_{i+2}}{12\Delta x} = \left(\frac{\partial \phi}{\partial x}\right)_i + O(\Delta x^4) \tag{A.7}$$

$$\frac{(-\phi_{i+2} + 7\phi_{i+1} + 7\phi_i - \phi_{i-1}) - (-\phi_{i+1} + 7\phi_i + 7\phi_{i-1} - \phi_{i-2})}{12\Delta x} = \left(\frac{\partial \phi}{\partial x}\right)_i + O(\Delta x^4) \tag{A.8}$$

A.2 Flux Corrected Transport scheme

Equation (3.106) can be written as

$$\begin{aligned}
(\rho q)^{n+1}_{i,j,k} &= (\rho q)^{n}_{i,j,k} - \frac{1}{\Delta x \Delta y \Delta z}\Big[\\
&+ \left[C_{i+\frac{1}{2},j,k} F^{high}_{i+\frac{1}{2},j,k} + \left(1 - C_{i+\frac{1}{2},j,k}\right) F^{low}_{i+\frac{1}{2},j,k}\right] \\
&- \left[C_{i-\frac{1}{2},j,k} F^{high}_{i-\frac{1}{2},j,k} + \left(1 - C_{i-\frac{1}{2},j,k}\right) F^{low}_{i-\frac{1}{2},j,k}\right] \\
&+ \left[C_{i,j+\frac{1}{2},k} F^{high}_{i,j+\frac{1}{2},k} + \left(1 - C_{i,j+\frac{1}{2},k}\right) F^{low}_{i,j+\frac{1}{2},k}\right] \\
&- \left[C_{i,j-\frac{1}{2},k} F^{high}_{i,j-\frac{1}{2},k} + \left(1 - C_{i,j-\frac{1}{2},k}\right) F^{low}_{i,j-\frac{1}{2},k}\right] \\
&+ \left[C_{i,j,k+\frac{1}{2}} F^{high}_{i,j,k+\frac{1}{2}} + \left(1 - C_{i,j,k+\frac{1}{2}}\right) F^{low}_{i,j,k+\frac{1}{2}}\right] \\
&- \left[C_{i,j,k-\frac{1}{2}} F^{high}_{i,j,k-\frac{1}{2}} + \left(1 - C_{i,j,k-\frac{1}{2}}\right) F^{low}_{i,j,k-\frac{1}{2}}\right] \\
\Big] &
\end{aligned} \tag{A.9}$$

where

$$F^{high,low}_{i+\frac{1}{2},j,k} = \Delta t \Delta y \Delta z (\rho u)_{i+\frac{1}{2},j,k} q^{high,low}_{i+\frac{1}{2},j,k} \tag{A.10}$$

$$F^{high,low}_{i,j+\frac{1}{2},k} = \Delta t \Delta z \Delta x (\rho u)_{i,j+\frac{1}{2},k} q^{high,low}_{i,j+\frac{1}{2},k} \tag{A.11}$$

$$F^{high,low}_{i,j,k+\frac{1}{2}} = \Delta t \Delta x \Delta y (\rho u)_{i,j,k+\frac{1}{2}} q^{high,low}_{i,j,k+\frac{1}{2}} \tag{A.12}$$

The anti-diffusive flux are defined as

$$A_{i+\frac{1}{2},j,k} = F^{high}_{i+\frac{1}{2},j,k} - F^{low}_{i+\frac{1}{2},j,k} \tag{A.13}$$

$$A_{i,j+\frac{1}{2},k} = F^{high}_{i,j+\frac{1}{2},k} - F^{low}_{i,j+\frac{1}{2},k} \tag{A.14}$$

$$A_{i,j,k+\frac{1}{2}} = F^{high}_{i,j,k+\frac{1}{2}} - F^{low}_{i,j,k+\frac{1}{2}} \tag{A.15}$$

Equation (A.9) can be rewritten as

$$\begin{aligned}
(\rho q)^{n+1}_{i,j,k} &= (\rho q)^{n}_{i,j,k} - \frac{1}{\Delta x \Delta y \Delta z}\Big[\\
&+ \left[F^{low}_{i+\frac{1}{2},j,k} + C_{i+\frac{1}{2},j,k} A_{i+\frac{1}{2},j,k}\right] \\
&- \left[F^{low}_{i-\frac{1}{2},j,k} + C_{i-\frac{1}{2},j,k} A_{i-\frac{1}{2},j,k}\right] \\
&+ \left[F^{low}_{i,j+\frac{1}{2},k} + C_{i,j+\frac{1}{2},k} A_{i,j+\frac{1}{2},k}\right] \\
&- \left[F^{low}_{i,j-\frac{1}{2},k} + C_{i,j-\frac{1}{2},k} A_{i,j-\frac{1}{2},k}\right] \\
&+ \left[F^{low}_{i,j,k+\frac{1}{2}} + C_{i,j,k+\frac{1}{2}} A_{i,j,k+\frac{1}{2}}\right] \\
&- \left[F^{low}_{i,j,k-\frac{1}{2}} + C_{i,j,k-\frac{1}{2}} A_{i,j,k-\frac{1}{2}}\right] \\
\Big] &
\end{aligned} \tag{A.16}$$

In practice, we calculate Eq.(A.16) by the following steps:

1. The tentative values are calculated by using the low order flux:

$$\begin{aligned}
(\rho q)^{\dagger}_{i,j,k} &= (\rho q)^{n}_{i,j,k} \\
&- \frac{1}{\Delta x \Delta y \Delta z}\left[+F^{low}_{i+\frac{1}{2},j,k} - F^{low}_{i-\frac{1}{2},j,k} + F^{low}_{i,j+\frac{1}{2},k} - F^{low}_{i,j-\frac{1}{2},k} + F^{low}_{i,j,k+\frac{1}{2}} - F^{low}_{i,j,k-\frac{1}{2}}\right]
\end{aligned} \tag{A.17}$$

2. Allowable maximum and minimum values are calculated:

$$
\begin{aligned}
(\rho q)^{\max}_{i,j,k} &= \max[\\
&\quad \max((\rho q)^{\dagger}_{i,j,k}, (\rho q)^{n}_{i,j,k}), \\
&\quad \max((\rho q)^{\dagger}_{i-1,j,k}, (\rho q)^{n}_{i-1,j,k}), \\
&\quad \max((\rho q)^{\dagger}_{i+1,j,k}, (\rho q)^{n}_{i+1,j,k}), \\
&\quad \max((\rho q)^{\dagger}_{i,j-1,k}, (\rho q)^{n}_{i,j-1,k}), \\
&\quad \max((\rho q)^{\dagger}_{i,j+1,k}, (\rho q)^{n}_{i,j+1,k}), \\
&\quad \max((\rho q)^{\dagger}_{i,j,k-1}, (\rho q)^{n}_{i,j,k-1}), \\
&\quad \max((\rho q)^{\dagger}_{i,j,k+1}, (\rho q)^{n}_{i,j,k+1}) \\
&\quad] \qquad \text{(A.18)} \\
(\rho q)^{\min}_{i,j,k} &= \min[\\
&\quad \min((\rho q)^{\dagger}_{i,j,k}, (\rho q)^{n}_{i,j,k}), \\
&\quad \min((\rho q)^{\dagger}_{i-1,j,k}, (\rho q)^{n}_{i-1,j,k}), \\
&\quad \min((\rho q)^{\dagger}_{i+1,j,k}, (\rho q)^{n}_{i+1,j,k}), \\
&\quad \min((\rho q)^{\dagger}_{i,j-1,k}, (\rho q)^{n}_{i,j-1,k}), \\
&\quad \min((\rho q)^{\dagger}_{i,j+1,k}, (\rho q)^{n}_{i,j+1,k}), \\
&\quad \min((\rho q)^{\dagger}_{i,j,k-1}, (\rho q)^{n}_{i,j,k-1}), \\
&\quad \min((\rho q)^{\dagger}_{i,j,k+1}, (\rho q)^{n}_{i,j,k+1}) \\
&\quad] \qquad \text{(A.19)}
\end{aligned}
$$

3. Several values for the flux limiter are calculated:

$$
\begin{aligned}
P^{+}_{i,j,k} &= -\min(0, A_{i+\frac{1}{2},j,k}) + \max(0, A_{i-\frac{1}{2},j,k}) \\
&\quad -\min(0, A_{i,j+\frac{1}{2},k}) + \max(0, A_{i,j-\frac{1}{2},k}) \\
&\quad -\min(0, A_{i,j,k+\frac{1}{2}}) + \max(0, A_{i,j,k-\frac{1}{2}}) \qquad \text{(A.20)} \\
P^{-}_{i,j,k} &= -\max(0, A_{i+\frac{1}{2},j,k}) + \min(0, A_{i-\frac{1}{2},j,k}) \\
&\quad -\max(0, A_{i,j+\frac{1}{2},k}) + \min(0, A_{i,j-\frac{1}{2},k}) \\
&\quad -\max(0, A_{i,j,k+\frac{1}{2}}) + \min(0, A_{i,j,k-\frac{1}{2}}) \qquad \text{(A.21)} \\
& \qquad \text{(A.22)}
\end{aligned}
$$

$$
Q^{+}_{i,j,k} = \left[(\rho q)^{\max}_{i,j,k} - (\rho q)^{\dagger}_{i,j,k}\right] \Delta x \Delta y \Delta z \qquad \text{(A.23)}
$$

$$
Q^{-}_{i,j,k} = \left[(\rho q)^{\dagger}_{i,j,k} - (\rho q)^{\min}_{i,j,k}\right] \Delta x \Delta y \Delta z \qquad \text{(A.24)}
$$

$$
R^{+}_{i,j,k} = \begin{cases} \min(1, Q^{+}_{i,j,k}/P^{+}_{i,j,k}) & \text{if } P^{+}_{i,j,k} > 0 \\ 0 & \text{if } P^{+}_{i,j,k} = 0 \end{cases} \qquad \text{(A.25)}
$$

$$
R^{-}_{i,j,k} = \begin{cases} \min(1, Q^{-}_{i,j,k}/P^{-}_{i,j,k}) & \text{if } P^{-}_{i,j,k} > 0 \\ 0 & \text{if } P^{-}_{i,j,k} = 0 \end{cases} \qquad \text{(A.26)}
$$

4. The flux limters at the cell wall are calculated:

$$C_{i+\frac{1}{2},j,k} = \begin{cases} \min(R^+_{i+1,j,k}, R^-_{i,j,k}) & \text{if } A^-_{i+\frac{1}{2},j,k} \geq 0 \\ \min(R^+_{i,j,k}, R^-_{i+1,j,k}) & \text{if } A^-_{i+\frac{1}{2},j,k} < 0 \end{cases} \tag{A.27}$$

$$C_{i,j+\frac{1}{2},k} = \begin{cases} \min(R^+_{i,j+1,k}, R^-_{i,j,k}) & \text{if } A^-_{i,j+\frac{1}{2},k} \geq 0 \\ \min(R^+_{i,j,k}, R^-_{i,j+1,k}) & \text{if } A^-_{i,j+\frac{1}{2},k} < 0 \end{cases} \tag{A.28}$$

$$C_{i,j,k+\frac{1}{2}} = \begin{cases} \min(R^+_{i,j,k+1}, R^-_{i,j,k}) & \text{if } A^-_{i,j,k+\frac{1}{2}} \geq 0 \\ \min(R^+_{i,j,k}, R^-_{i,j,k+1}) & \text{if } A^-_{i,j,k+\frac{1}{2}} < 0 \end{cases} \tag{A.29}$$

Appendix B

Notation

Table B.1: Notation of symbols

ρ	total density	kg/m^3
q_d	mass concentration of dry air	$-$
q_v	mass concentration of water vapor	$-$
q_l	mass concentration of liquid water	$-$
q_s	mass concentration of solid water	$-$
t	time	s
$\mathbf{u}$	velocity of air flow	m/s
w_l	relative velocity of liquid water to the gas	m/s
w_s	relative velocity of solid water to the gas	m/s
DIFF $[x]$	Diffusion term by turbulene	$kg/m^3\,[x]\,/s$
S_v	source term of water vapor	$kg/m^3/s$
S_l	source term of liquid water	$kg/m^3/s$
S_s	source term of solid water	$kg/m^3/s$
p	pressure	N/m^2
g	gravitational acceraration	9.8 m/s^2
f_l	drag force due to water loading by liquid water	$kg/m^2/s^2$
f_s	drag force due to water loading by solid water	$kg/m^2/s^2$
$\mathbf{e_z}$	vertical unit vector (upward)	$-$
R_d	gas constant for dry air for uint mass	J/kg
R_v	gas constant for water vapor for uint mass	J/kg
T	temperature	K
Q_d	diabatic heating due to physical processes for dry air	$J/m^3/s$
Q_v	diabatic heating due to physical processes for water vapor	$J/m^3/s$
Q_l	diabatic heating due to physical processes for liquid water	$J/m^3/s$
Q_s	diabatic heating due to physical processes for solid water	$J/m^3/s$
e_d	internal energy for dry air	J/kg
e_v	internal energy for water vapor	J/kg
e_l	internal energy for liquid water	J/kg
e_s	internal energy for solid water	J/kg
e	total internal energy	J/kg
c_{vd}	specific heat at constant volume for dry air	$J/kg/K$
c_{vv}	specific heat at constant volume for water vapor	$J/kg/K$
c_{pd}	specific heat at constant pressure for dry air	$J/kg/K$
c_{pv}	specific heat at constant pressure for water vapor	$J/kg/K$
c_l	specific heat for liquid water	$J/kg/K$
c_s	specific heat for solid water	$J/kg/K$
p_{00}	standard pressure	1000.0 Pa
θ_d	potential temperature for dry air	K
θ	total potential temperature	K

Appendix C

Variables in the source code

Table C.1: Variables in atmos/mod_atmos_dyn_fent_fct.f90.

DENS(k,i,j)	$\rho_{i,j,k}$
MOMZ(k,i,j)	$(\rho w)_{i,j,k+\frac{1}{2}}$
MOMX(k,i,j)	$(\rho u)_{i+\frac{1}{2},j,k}$
MOMY(k,i,j)	$(\rho v)_{i,j+\frac{1}{2},k}$
RHOT(k,i,j)	$(\rho\theta)_{i,j,k}$
QTRC(k,i,j,iq)	$q_{i,j,k}$
PRES(k,i,j)	$p_{i,j,k}$
VELZ(k,i,j)	$\bar{w}_{i,j,k+\frac{1}{2}}$
VELX(k,i,j)	$\bar{u}_{i+\frac{1}{2},j,k}$
VELY(k,i,j)	$\bar{v}_{i,j+\frac{1}{2},k}$
POTT(k,i,j)	$\theta_{i,j,k}$
QDRY(k,i,j)	q_d
Rtot(k,i,j)	R^*
num_diff(k,i,j)	$F_{i+\frac{1}{2}}$
qflx_hi(k,i,j)	$\bar{q}^{high}$
qflx_lo(k,i,j)	$\bar{q}^{low}$
qjpls(k,i,j)	$Q^+_{i,j,k}$
qjmns(k,i,j)	$Q^-_{i,j,k}$
pjpls(k,i,j)	$P^+_{i,j,k}$
pjmns(k,i,j)	$P^-_{i,j,k}$
rjpls(k,i,j)	$R^+_{i,j,k}$
rjmns(k,i,j)	$R^-_{i,j,k}$

Table C.2: Variables in atmos/mod_atmos_phy_tb_smg.f90.

tke(k,i,j)	TKE
nu(k,i,j), nu_*(k,i,j)	ν_{SGS}
Ri(k,i,j)	Ri
Pr(k,i,j)	Pr
S33_*(k,i,j)	S_{33}
S11_*(k,i,j)	S_{11}
S22_*(k,i,j)	S_{22}
S31_*(k,i,j)	S_{31}
S12_*(k,i,j)	S_{12}
S23_*(k,i,j)	S_{23}
qflx_sgs(k,i,j)	$\bar{\rho}\tau_{ij}$, $\bar{\rho}\tau^*_{ij}$